



Published in final edited form as:

Chem Soc Rev. 2014 October 7; 43(19): 6765–6813. doi:10.1039/c3cs60460h.

BACE1 (β -Secretase) Inhibitors for the Treatment of Alzheimer's Disease

Arun K. Ghosh and Heather L. Osswald

Department of Chemistry and Department of Medicinal Chemistry, Purdue University, West Lafayette, IN 47907

Abstract

BACE1 (β -secretase, memapsin 2, Asp2) has emerged as a promising target for the treatment of Alzheimer's Disease. BACE1 is an aspartic protease which functions in the first step of the pathway leading to the production and deposition of amyloid- β peptide ($A\beta$). Its gene deletion showed only mild phenotypes. BACE1 inhibition has direct implications in the Alzheimer's Disease pathology without largely affecting viability. However, inhibiting BACE1 selectively *in vivo* has presented many challenges to medicinal chemists. Since its identification in 2000, inhibitors covering many different structural classes have been designed and developed. These inhibitors can be largely classified as either peptidomimetic or non-peptidic inhibitors. Progress in these fields resulted in inhibitors that contain many targeted drug-like characteristics. In this review, we describe structure-based design strategies and evolution of a wide range of BACE1 inhibitors including compounds that have been shown to reduce brain $A\beta$, rescue the cognitive decline in transgenic AD mice and inhibitor drug candidates that are currently in clinical trials.

1. Introduction

Alzheimer's disease (AD) is a devastating neurodegenerative disorder that alters the mental capacity of patients suffering from the disease. It is the most common cause of senile dementia and is characterized by loss of memory, disorientation, difficulty speaking or writing, loss of reasoning skills, and delusions, among other symptoms.¹ While it seems both genetic and environmental factors may play a role in the progression of the disease, direct causes are not entirely clear. Current therapies are aimed at management of symptoms, yet no disease altering treatment exists for Alzheimer's patients. β -Secretase, also known as beta-site amyloid precursor protein cleaving enzyme 1 (BACE1), or, membrane-associated aspartic protease 2 (memapsin 2) or, aspartyl protease 2 (Asp2), is an important enzyme found early in the cascade of biological events leading to disease progression.² BACE1 has become an interesting therapeutic target for small molecule inhibitors that could alter the course of Alzheimer's disease.

2. Biological Implications of Alzheimer's Disease

Pathologically, AD arises mainly due to the formation of two types of lesions in the brain, neuritic plaques and neurofibrillary tangles. Neurofibrillary tangles are insoluble bundles of fibers that locate in the perinuclear cytoplasm and are generally composed of phosphorylated tau protein. These tangles can also be found in other neurodegenerative disorders such as Kuf's disease and subacute sclerosing panencephalitis.¹ What is lacking in these alternate forms of neurodegeneration, however, is the formation of neuritic plaques. While neurofibrillary tangles and neuritic plaques can arise independently,³ neuritic plaques seem to be the primary lesion in AD⁴ and it has been suggested that the appearance of tangles in the AD brain could be due to neuronal responses to the formation of plaques.^{1, 5}

Neuritic plaques are spherical lesions that contain extracellular aggregates of amyloid- β protein ($A\beta$).⁶ Surrounding these plaques are an array of abnormal dendrites and axons.⁷ $A\beta$ comes from the processing of β -amyloid precursor protein (APP) via a pair of proteases, β -secretase (BACE1) and γ -secretase. Two main species of $A\beta$ are produced, $A\beta_{40}$, which ends at residue 40 of the preceding APP, and $A\beta_{42}$, which ends at residue 42 of the preceding APP. $A\beta_{42}$ seems to favor aggregation more so than $A\beta_{40}$, however both species have been found in senile plaques. Increases in both $A\beta_{40}$ and $A\beta_{42}$ are seen early on in AD and overall levels of $A\beta$ in the brain have been shown to correlate to the degree of dementia in AD patients.⁸ The less aggregative $A\beta_{40}$ is much more abundantly produced in normal cells and accounts for about 90% of the $A\beta$ produced in normal cells.³ Once these plaques are formed they are quite stable.^{9, 10} $A\beta$ has been shown to be neurotoxic and lead to neuron death.¹¹

In contrast to the insoluble deposition of neuritic $A\beta$ plaques, diffuse plaques of $A\beta$, lacking the compact nature of neuritic plaques, have also been found. Diffuse plaques are generally more amorphous and granular, made almost entirely of $A\beta_{42}$, and contain few amyloidogenic filaments and fibers that are found in neuritic plaques.^{3, 7} These plaques are usually found in areas of the brain that do not have any implications in the symptoms of AD. This, in addition to the appearance of diffuse plaques in identical areas of the brains of healthy patients, leads to the assumption that diffuse plaques do not play a significant role in the progression of AD.¹

The production of $A\beta_{40}$ and $A\beta_{42}$ comes from the processing of a much larger peptide, APP. APP is a 695-770 residue peptide that is expressed in many tissues throughout the body, with higher concentrations being found in the kidneys and brain.¹² Cellularly, it is found mostly in the late endosomes, however some cycling from the cell surface through the endocytic system does occur.¹³ The main form expressed in neuronal cells is APP₆₉₅, which lacks a 56-amino acid sequence similar to the Kunitz serine protease inhibitors that is present in the longer isoforms of APP, APP₇₅₁, and APP₇₇₀.¹ While the exact physiological function of APP is not entirely clear, APP and its derivatives have broad functions in cell-cell¹⁴ or cell-matrix interaction and synapse localization and metabolism.¹⁵ Further functions include roles in serine protease inhibition, in the case of APP₇₅₁ or APP₇₇₀, as well as cell adhesion,^{16, 17} growth promotion, neuroprotection via regulation of intracellular calcium levels,^{1, 7} and synapse formation and maintenance.¹⁷

(a) Proteolytic processing of APP by α -secretase, β -secretase, and γ -secretase

APP is a type I transmembrane protein consisting of an N-terminal 17 residue signaling peptide, a large ectodomain, a 23 residue hydrophobic transmembrane domain, and a 47 residue cytoplasmic domain.^{6, 7} The A β region accounts for only a small portion of APP, 28 residues in the luminal domain plus the first 12-14 residues of the transmembrane domain. The signal peptide translocates APP to the endoplasmic reticulum (ER) where it is bound to the membrane via the 23 residue hydrophobic stretch. It is then posttranslationally modified via N- and O-glycosylation, sulfation, and phosphorylation⁷ as it is moved through the secretory pathway by way of the Golgi apparatus and endosomes. Along the way, APP is subjected to different proteolytic events that can release a variety of soluble and membrane bound fragments. Only fully modified and glycosylated APP undergoes proteolytic processing.¹⁵ These proteolytic cleavages are performed by enzymes initially called α -secretase, β -secretase (BACE1), and γ -secretase.

α -Secretase acts on full length APP. (Figure 1) It cleaves in the luminal region of APP releasing a soluble ectodomain fragment (sAPP α) and a membrane bound, 83 residue C-terminal fragment (C83). Interestingly, α -secretase cleavage takes place between residues 16 and 17 of the A β region. Therefore, the proteolytic cleavage performed by α -secretase precludes the formation of A β , thus eliminating the possibility of the formation aggregates and plaques and causing α -secretase activity to be considered nonamyloidogenic.^{7, 18} Further, sAPP α has been suggested to have some neuroprotective properties.¹⁹ It seems that the specificity of α -secretase does not come from the identity of the amino acids adjacent to the scissile bond, as α -secretase has shown activity on a variety of peptidic bonds. Specificity seems to arise from the proximity of the enzyme to the membrane, as it has been demonstrated that α -secretase consistently cleaves 12-13 residues N-terminal to the membrane.⁷

BACE1 also cleaves full length APP (Figure 1). It cleaves at the N-terminus of A β ,²⁰ 16 residues down from the α -secretase cleavage site, which results in a smaller soluble ectodomain fragment (sAPP β), but a larger C-terminal fragment (C99).¹ C99 starts at residue 1 of A β , whereas C83 from α -secretase cleavage starts at residue 17 of A β . BACE1 cleavage between methionine 671 and aspartic acid 672 is common in neuronal cells, but is observed far less in peripheral cells such as HEK-293 cells.¹⁸

Further processing of both C-terminal fragments, C83 and C99, takes place via γ -secretase activity. γ -Secretase cleaves at the C-terminus of the A β region in both C83 and C99. In the case of C83, γ -secretase activity releases a peptide fragment called p3. In the case of C99, γ -secretase activity releases A β . The cleavage to release both A β and p3 occurs within the transmembrane region of APP indicating that this cleavage must occur within the membrane rather than the luminal cleavage of both α - and β -secretase.⁶ This sequential proteolytic cleavage of APP by β -secretase and γ -secretase accounts for the formation of A β in the brain.

(b) Amyloid hypothesis of Alzheimer's disease

While many Alzheimer's patients seem to have no genetic predisposition to the disease, called sporadic AD, many genetic mutations, can lead to forms of familial AD. Phenotypically, these forms of AD are very similar or identical, however familial AD often occurs as early-onset AD.¹ Missense mutations in both APP and the presenilins, with presenilin mutations being more common, lead to these familial cases of AD.¹

There are multiple known mutations in the APP sequence that lead to the onset of familial AD. (Figure 1) The mutation of the two residues near the N-terminus of the A β sequence of APP, K670N and M671L, is known as the Swedish mutation.^{21, 22} Located near the β -secretase site, these mutations make APP a better substrate for β -secretase, thus generating more C99 to be further processed into increased levels of A β ,⁷ about three to six times higher than normal APP.²⁰ Swedish A β production is thought to occur only in the secretory vesicles, as Swedish A β is found to be excreted from the apical surface as opposed to wild-type A β which is excreted from the basolateral surface.²⁰ As A β is a normal outcome of cellular metabolism, people carrying the Swedish mutation will have elevated levels of A β throughout their entire life, even before AD symptoms are present.²² There are five different mutation sites that may appear just after the γ -secretase cleavage site, T714I (Austrian type)²³, V715M (French type)²⁴, I716V (Florida type)²⁵, V717I/G/F/L (London type and Indiana type)²⁶⁻²⁹, and L723P (Australian type).³⁰ These each affect the cleavage by γ -secretase slightly differently, however the overall effect is that more A β ₄₂ is produced. The last two mutations occur within the A β sequence. While they do not affect the cleavage activity of either β - or γ -secretase, they seem to have an effect on the aggregative properties of A β . E693Q is associated with Dutch type hereditary cerebral hemorrhage with amyloidosis (HCHWA-D)³¹, which shows A β aggregation in the meningeal and cerebral microvessels, while A692G (Flemish type)³² affects both microvascular β -amyloidosis similar to HCHWA-D and neuritic plaque formation.^{1, 7} As knowledge of this disease increases, more and more APP mutations are being linked to familial AD.

Much more common are the presenilin mutations. There are as many as 75 missense mutations in presenilin 1 (PS1) and three in presenilin 2 (PS2) which lead to a much earlier onset of familial AD, with some cases showing clinical signs of AD as early as age 30.¹ These mutations lead to an increased level of A β ₄₂, as much as 3-fold, which subsequently leads to an increase in A β plaques.

Overproduction of A β is also seen in Down's syndrome. Since APP is encoded on chromosome 21,⁶ AD-type symptoms often appear in Down's syndrome patients due to the duplication of chromosome 21.¹ This is not caused by a mutation of the APP or presenilins, as discussed above, but by overexpression of normal APP. This results in an overproduction of A β , both A β ₄₀ and A β ₄₂, which can cause diffuse plaques to be seen in Down's syndrome patients as early as age 12.¹ This accumulation of A β starts from birth, with plaque formation and cognitive loss associated with AD found in patients in their 30s.

The discovery of these mutations, along with the formation of A β aggregates in sporadic AD, has led to the development of the amyloid hypothesis of the progression of Alzheimer's disease. (Figure 2) The amyloid hypothesis states that the formation of A β plaques begins a

cascade of events ultimately leading to dementia in AD patients.³³ It seems that the accumulation of A β may initially affect the efficiency and function of synapses, leading up to neuronal loss and dementia.³⁴ Many research groups have focused on the amyloid hypothesis and there are significant findings that support this hypothesis. However the subject is very complex and there are questions that remain to be answered.

It has been found that frontotemporal dementia with Parkinson's disease is caused by mutations in the gene for the tau protein, which in turn cause neurofibrillary tangles in the brain. The lack of AD-like plaques in the brains of these patients, even in the most severe cases, leads to the suggests that A β plaques are formed first and tangles in the brains of AD patients are perhaps a result of this.³³ Further, mice that overexpress mutated human APP and tau show increased formation of tangles, while plaques remain about the same, which suggests that the APP processing occurs prior to the tau tangle formation.³³

The genetic mutations of familial AD seem to be a strong proponent for the amyloid hypothesis.⁴ However, the amyloid hypothesis does not adequately explain all observations. For instance, it has histologically been argued that the number of A β plaques in the brain does not correspond to the degree of dementia in AD patients. However, when investigated biochemically rather than histologically, A β count does correlate to the impaired cognitive state.³³ Some studies have shown that there is, in fact, a quantitative correlation between histologically visible plaques and the degree of cognitive decline.^{4, 8} However, since the exact effects of A β on neuronal toxicity are not known *in vivo*, the amyloid hypothesis is drawn into question.³³ Still, the amyloid hypothesis seems a broadly accepted general scheme of the pathophysiological events in AD.

(c) Role of β -secretase in A β production

The proteolytic cleavage activities of APP were deemed α -, β -, and γ -secretase prior to the identity of any specific enzyme being known to have these functions. The ambiguity of these enzymes made some studies difficult to perform and conclusions difficult to draw. However, since the identity of the secretases responsible for APP processing have now been discovered, much knowledge has been obtained on the function of these enzymes in both AD and in other physiological functions.

Several proteins have been found to have α -secretase activity. They are all a part of the A disintegrin and metalloprotease (ADAM) family of enzymes. While some, like ADAM17 (tumor necrosis factor- α converting enzyme, TACE), are believed to have shown α -secretase activity,³⁵ ADAM10 is generally regarded as the α -secretase most active in the brain.³⁶ Overexpression of ADAM10 in HEK cells showed increased levels of sAPP α and C83 led to this conclusion.³⁶

It is speculated that γ -secretase activity, is carried out though a complex of proteins rather than being attributed to one enzyme. The presenilins (PSs) are thought to be a part of that complex, either by having γ -secretase activity themselves, or by modulating γ -secretase activity. PS1 has two transmembrane aspartates that are aligned with the transmembrane domain of APP making γ -secretase cleavage by this enzyme feasible.³⁷ Mutations in PS1 and PS2 that support the formation of A β ₄₂, the form of A β more susceptible to aggregation,

solidify the influence of PSs in γ -secretase activity.³⁸ It has also been found that PS1 knockout reduces A β formation, further supporting the role of PSs in γ -secretase activity.^{39, 40} Other proteins thought to be a part of the γ -secretase complex are nicastrin (Nct), anterior pharynx-defective phenotype (APH-1) and PS-enhancer (PEN-2). In fact, the expression of all of the above components together in *Saccharomyces cerevisiae*, which normally lacks any form of γ -secretase activity, results in fully active γ -secretase, suggesting that the above-mentioned four components account for full γ -secretase activity.³⁹

Many different enzymes have been proposed to be β -secretase throughout the years. Many, including cathepsin D,⁴¹⁻⁴⁴ a chymotrypsin-like protease (CLIP) isolated from the rat brain,⁴⁵ cathepsin G,⁴⁶ BACE2,⁴⁷ metalloendopeptidase MP78,⁴³ and metalloprotease MP100,⁴⁸ have been ruled out for various reasons. At about the same time, five independent groups correctly identified the protein responsible for β -secretase activity. It has been named Asp2,^{44, 49} β -site APP cleaving enzyme 1 (BACE1),⁵⁰ β -secretase,⁵¹ and memapsin2⁵² by the various groups that correctly identified this enzyme. Herein, β -secretase will primarily be referred to as BACE1.

BACE1 is formed in the endoplasmic reticulum as an immature, glycosylated propeptide, pro-BACE1.⁵³ Pro-BACE1 is then processed and cleaved into mature BACE1 in the Golgi apparatus.⁵⁴ The propeptide has two conformations, both an open and closed conformation. (Figure 3) When in the open conformation, pro-BACE1 can exhibit some enzymatic activity. However, when in the closed conformation, with the pro-domain covering the active site, the activity of pro-BACE1 is diminished which allows the pro-domain to serve as a weak inhibitor of BACE1 activity.⁵⁵ This pro-domain has also been shown to play a role in the folding of mature BACE1.⁵⁵ Cleavage of the pro-domain allows BACE1 to have full enzymatic activity by allowing the catalytic active site to be fully accessible to substrate.⁵⁶ BACE1 is a monomeric protein that is shuttled between the endosomes and the cell surface. It presents four potential *N*-glycosylation sites as well as six cysteine residues that form three disulfide bonds.⁵⁷ These disulfide bonds are important for proper folding and activity of the enzyme. In particular, Cys330/Cys380 is found inside the active site of BACE1 and is especially important for stability and activity.⁵⁸ As BACE1 is matured through the endoplasmic reticulum and Golgi apparatus, three of the four potential *N*-glycosylation sites are utilized. BACE1 is then trafficked through the endosomal system to the cell surface where it is then reinternalized and recycled. There is a dileucine motif in the cytoplasmic domain that aids in the localization of BACE1 to the endosomes.⁵⁷ While BACE1 is cycled from the endosomes to the cell surface, it has been shown that BACE1 is most active at a mildly acidic pH of about 5.5. This suggests that BACE1 acts in the endosomes on the way to the cell surface and not at the cell surface.^{57, 59}

Similarly to pro-BACE1, mature BACE1 also has two major conformations a flap open conformation and a flap closed conformation. (Figure 4) Free BACE1 is found in the flap open conformation. This conformation is energetically stable and is held by optimal hydrogen bonds.⁶⁰ However, when bound to substrate, BACE1 adopts a flap closed conformation. To make this conformational shift, there is breakage of hydrogen bonds between the oxygen of Tyr71 and the nitrogen of Gly74, the nitrogen of Lys75 and the oxygen of Glu77, and the Tyr71 hydroxyl with the Lys107 oxygen. This destabilization is

justified by the interaction of the enzyme with the substrate.⁶⁰ Also a new interaction of the Tyr71 side chain with the indole nitrogen of Trp76 is formed. While in the open conformation, substrates can enter through a cleft in the enzyme. However, due to a bottleneck being formed by Thr72, Arg235, Ser328, and Thr329, some flexibility in the substrate is needed.⁶⁰ It has been suggested that this bottleneck may serve as a specificity mechanism.

3. BACE1 as a therapeutic target for AD

Since the recognition of their central role of APP processing, secretases have been identified as a possible target for therapeutic intervention of AD. α -Secretase has not been targeted, as it cleaves APP in the A β region and does not lead to the formation of A β deposits. However, both β - and γ -secretases have been suggested as targets to inhibit A β formation and thereby, stop the progression of AD.^{61, 62}

PS1 and PS2 are the major enzymatic targets for γ -secretase inhibition for the treatment of AD.⁶³ PS1 and PS2 are integral membrane proteins found in the endoplasmic reticulum and Golgi apparatus. Apart from the apparent role in AD, they also control the Notch signaling pathway responsible for cell proliferation and differentiation during embryonic development.³⁷

Transgenic PS1 knockout mice do not survive past birth⁴⁰ and have underdeveloped subventricular areas and cortical dysplasia.³⁸ Other substrates of PSs have also been identified, suggesting a strong biological function of the PSs.³⁹ Thus, inhibition of γ -secretase is likely to cause unwanted side effects.

BACE1 has been identified as a significant target for AD intervention. Its inhibition would halt the formation of A β at the very beginning of APP processing. It is feasible to target later stages in the cascade, however it has been shown that generation of excess A β can be detrimental to cognitive function even before neuronal death by limiting synaptic function.⁶⁴ Thus, slowing the progression of AD by inhibiting A β formation at an early stage is ideal. While the true biological function of BACE1 is not entirely known, it is thought to have implications in myelin sheath formation and other biological processes, most associated with the processing of neuregulin-1.⁶⁵ BACE1 null mice have proven to be viable, with few to no phenotypical abnormalities, suggesting that inhibition of this enzyme could be clinically feasible with few mechanistic side effects.⁶⁶⁻⁶⁸ The therapeutic potential of BACE1 was further elaborated when the genetic inhibition of the enzyme was shown to rescue memory deficits in AD animals.⁶⁹

4. Design of mechanism-based BACE1 inhibitors, X-ray structures, and drug-design templates

The druggability of BACE1 was first demonstrated with the development of substrate inhibitor OM99-2 and the elucidation of the crystal structure of the BACE1 and OM99-2 complex (Figure 5).^{70, 71} This inhibitor was designed based upon a transition-state mimetic concept using non-hydrolyzable dipeptide isostere at the scissile site. It was noted that

BACE1 cleavage of the Swedish APP (SENΛ/DΛEFR) is 40x-faster than APP (SEVRM/DΛEFR). Also, initial specificity studies indicated that Ala is a preferred residue at P1'. Therefore, the design of a substrate-based inhibitor followed with the incorporation of a Leu-Ala hydroxyethylene isostere at the cleavage site. One of the inhibitors, OM99-2 showed very potent BACE1 inhibitory activity with a K_i of 1.6 nM.⁷⁰ Subsequently the X-ray structure of inhibitor-bound BACE1 was determined at 1.9 Å resolution.⁷¹ This structure gave much insight into the binding mode of inhibitors in the BACE1 active site. As can be seen, BACE1 adopts a bilobal structure with the inhibitor binding in the substrate binding pocket between the N-terminal and C-terminal lobes of the enzyme. Catalytic aspartates Asp32 and Asp228 are located in the center of this pocket and form part of an extensive hydrogen bonding network in the active site. In contrast, in apo-enzyme, the catalytic aspartic acid residues bind to a water molecule between them. For the complex with OM99-2, there are four hydrogen bonds between the catalytic aspartates and the transition state isostere hydroxyl and an additional ten hydrogen bonds between the active site and flap region of the enzyme. The flap region closes over the top of the cleft when bound to the inhibitor as discussed previously (Figure 4). Additionally, some characteristics of the subsites in the active site have been identified. For instance, the S2 and S4 subsites are mostly hydrophilic while S1 and S3 are generally hydrophobic.⁷¹ The P1 leucine and P3 valine of OM99-2 nicely fill the hydrophobic S1 and S3 sites of BACE1 with extensive hydrophobic contacts. P1 leucine interacts specifically with Tyr71 and Phe108 of the enzyme. P2 asparagine hydrogen bonds with the P4 glutamate of the inhibitor and Arg235 of the enzyme. Interestingly, OM99-2 abandons the extended conformation and turns at P2' to orient P3' and P4' towards the protein surface. This results in these parts of the inhibitor having little interaction with the protein.⁷¹

Further elaboration of substrate-based inhibitors led to the design of inhibitor **2**. The X-ray crystal structure of the BACE1 and OM00-3 complex was determined at 2.1 Å resolution. It showed a K_i of 0.3 nM for BACE1 compared to the K_i of 1.6 nM for inhibitor **1**.^{71, 72} Knowledge of the subsite specificity of BACE1 greatly aided the design of inhibitor **2** which showed a fivefold enhancement of inhibitory potency. It was determined that the BACE1 substrate cleft could accommodate eight substrate side chains, however none were particularly specific, with the S' side showing the most tolerance of different side chains. On the nonprime side, some subsites showed a greater affinity for some side chains over others. In particular, P4 favors glutamine over glutamate over aspartate, P3 favors isoleucine over valine, P2 favors aspartate or asparagine, and P1 favors leucine, phenylalanine, and methionine. P1 was found to be the most specific site.⁷³ Overall, acidic or polar residues are preferred at the P2 and P1' sites.⁷⁴ Utilizing this information, P2'-Val was introduced in inhibitor **2**. It retained the conformation of OM99-2 from P3 to P2', however stayed in the extended conformation past P2'.⁷² This extended conformation was stabilized by a hydrogen bond from the P3' backbone carbonyl to the side chain of Arg235 and a hydrogen bond between the P4' backbone and Tyr198.

The design of substrate-based pseudopeptide inhibitors and subsequent determination of inhibitor-bound X-ray structure provided important drug design templates as well as a wealth of information regarding the enzyme and inhibitor interactions in the BACE1 active

site. While druggability of these BACE1 inhibitors is limited due to their large molecular size, the presence of numerous peptide bonds, and peptidic features, the structural insight of these inhibitors has been a very important first step in the evolution of the structure-based design of a variety of BACE1 inhibitors.

5. Potential issues and complexities of BACE1 inhibitors

In addition to peptidic features and molecular size, there are many barriers that must be overcome in order to bring a drug-like BACE1 inhibitor to clinical development. Selectivity over other aspartic proteases is especially important. With aspartic acid proteases being found in nearly all body tissues, off target activity is possible and likely if an inhibitor is not specific to BACE1. BACE2, pepsin, renin, cathepsin D, and cathepsin E, among others, all may also be inhibited by an unselective BACE1 inhibitor, causing off target side effects. The two catalytic aspartic acid residues are conserved across the class, however subsite specificity in each active site may differ slightly, making the full utilization of interactions in these subsites important to inhibitor specificity.

BACE2, also called Asp1 and memapsin1,⁵² is a homolog of BACE1. It is 64% identical to BACE1 and is a part of the same family of transmembrane aspartic proteases.⁴⁷ (Figure 6) Unlike BACE1, however, BACE2 is expressed only marginally in the brain and is found in higher concentrations in the colon, kidney, pancreas, placenta, prostate, stomach, and trachea.⁴⁷ It has been shown that BACE2 can cleave APP, however it does not cleave in a way that can form A β plaques. In fact, BACE2 cleaves more efficiently within the A β region and has been suggested to degrade C99 as well.⁷⁵ Ultimately, BACE2 has been ruled out as a player in β -secretase activity in Alzheimer's disease.⁷⁶ Still, selectivity of BACE1 inhibitors over BACE2 is important to the therapeutic utility of BACE1 inhibitors. The specificity of the BACE2 binding pocket is very similar to that of BACE1 with differences presenting themselves in the P3' and P4' areas. Utilization of non-native side chains will likely be the most helpful in specificity over BACE2.⁷⁷ Additionally, BACE1 has been shown to have S7-S5 subsites that are unique to BACE1, allowing a decameric inhibitor to span P7-P4'. Hydrophobic residues, more specifically tryptophan, are preferred at these sites.⁷⁸

Selectivity over cathepsin D (CatD) is very important as well. CatD has functions in protein degradation, apoptosis regulation, and hydrolysis of LDL cholesterol, among others.⁷⁹ Noninhibition of CatD is very important for viability. CatD null mice have shown tendency for seizures and blindness as well as neuronal ceroid lipofuscinosis.⁸⁰ CatD may also have a role as a modulator of the immune system of the skin, as it has been found in sweat and able to process the antimicrobial peptide dermidicin 1-L (DCD-1L).⁸¹

An additional challenge in the development of BACE1 inhibitors has been the large size of the substrate pocket. Initially, decreasing the size of a peptidic inhibitor resulted in a decrease in potency⁷⁴ however, such large inhibitors are not practical *in vivo*. As such, smaller inhibitors would not be able to fill the pocket as adequately as APP and thus were not good inhibitors. Some of this difficulty can be overcome by increasing the affinity of the inhibitor for the BACE1 active site through increasing interactions with the enzyme in the

active site. Further, the bottleneck of the cleft created by residues Thr72, Arg235, Ser328, and Thr329 creates an additional barrier for inhibitors. However, it has been suggested that conformationally bound inhibitors, locked into the conformation that will best access the active site, may be helpful for entrance to the active site and binding.⁸²

Cell membrane and blood-brain barrier permeability is also a prominent issue in the development of BACE1 inhibitors. The inhibitors must penetrate the blood brain barrier to exert their effect. Validation of the target and concept of BACE1 inhibition was gained when a carrier peptide known to cross the blood-brain barrier was linked to a very large inhibitor. In one intraperitoneal injection, A β levels decreased 64% and brain tissue extracts showed decreased levels of A β .⁸³ Sterol linkers have also been used to show cell membrane permeability as a limiting factor in BACE1 inhibition. Linking sterol to an inhibitor that was enzymatically potent, but greatly lost activity in cellular assays, allowed the inhibitor to permeate the cell membrane and reach the endosomes, where BACE1 is most active.⁸⁴ Another hurdle encountered is P-glycoprotein (Pgp) efflux, a mechanism which essentially removes the inhibitor from cells. BACE1 inhibitors showed a dose and concentration dependent lowering of A β levels in Pgp knockout mice, where no reduction was seen in wild type mice.⁸⁵ This shows that even when brain permeability is achieved, Pgp efflux is another limiting factor in the efficacy of BACE1 inhibitors.

Generally, BACE1 knockout mice show good viability. However, some studies have shown BACE1 knockout mice to have some phenotypical abnormalities. Hippocampal impairments leading to learning and memory disabilities have been shown in one study.⁸⁶ It has also been suggested that normal levels of A β may play a role in modulating synaptic function⁸⁶ and inhibition of BACE1 may impair the formation of synapses.^{87, 88} The necessity of BACE1 for myelination of nerves has also been suggested.⁶⁵ BACE1 knockout did not, however, completely prevent nerve myelination, but resulted in thinner myelin sheaths than controls.^{89, 90} Further studies have also shown that BACE1 knockout mice show a greater likelihood of displaying seizure activity than the wild type counterparts.^{90, 91, 92} BACE1 null mice have also displayed an increased risk of schizophrenic behavior.⁹³ Further influence of BACE1 has been suggested in axonal guidance⁹⁴ with BACE1 null mice showing roles in targeting the olfactory sensory neuron axons to the glomeruli of the olfactory bulb.^{95, 96} Vascularization issues have also been seen in BACE1 knockout mice, both cerebrovascular and retinal.^{97, 98} In addition to retinal vascularization issues, problems with retinal thinning and increases in age pigmentation were shown as well.⁹⁷ While the above potential complications with BACE1 inhibition are key, it is important to note that the above studies were performed under full BACE1 ablation in animal models. With the determination of a specific therapeutic window, it may be possible for BACE1 inhibitors to be clinically applicable for the treatment of AD patients with few mechanistic side effects.

As such, BACE1 has revealed itself to be a desirable target for inhibition with small molecule inhibitors for the potential treatment of AD. Many academic and industrial laboratories have focused research into finding potent, selective, and bioavailable inhibitors. To date, none have made it through clinical trials to FDA approval, however many have shown clinical potential. Inhibitors can be classified into two major categories, peptidomimetic and nonpeptidic inhibitors. Further subclassification can be made based on

the structure of the inhibitor. The remainder of this review serves to give an overview of the discoveries made in small molecule inhibition of BACE1 and the strides that are being made towards a drug for the treatment of AD.

6. Design of Peptidomimetic BACE1 Inhibitors

Peptidomimetic inhibitors are designed to emulate the natural substrate of an enzyme. This allows for subsite specificity, hydrogen bonding, and hydrophobic interactions to be conserved or enhanced via side chain choices. While this is desirable, the transition state isostere is what gives these molecules their inhibitory power. In free BACE1, a catalytic aspartic acid residue hydrogen bonds to a water molecule, holding it in place. When encountered with a substrate molecule, one of the aspartic acids assists nucleophilic attack of the water molecule at the carbonyl carbon, while the other activates the carbonyl of the peptide bond. This forms a tetrahedral intermediate. Reformation of the carbonyl breaks the amide bond, resulting in a new N- and C-terminus of two substrate fragments. (Figure 7) When BACE1 is encountered with an inhibitor, the hydroxyl group of the transition state isostere displaces the water molecule and forms tight hydrogen bonds to the catalytic aspartic acid residues, thus precluding catalytic activity. Further optimization of substrate-based inhibitors is usually focused towards the lowering of molecular weight, decreasing peptidic character while maintaining binding interactions, and optimizing pharmacokinetic properties

Peptidomimetic inhibitors can be classified based on their transition state isostere. The isosteres discussed here are not exhaustive of the field, but gives an overview of the most widely used isosteres (Figure 8).

(a) Statine- and Norstatine-based Inhibitors

Statines are utilized as transition state inhibitors due to the leucine side chain at the P1 position. This emulates the Swedish mutant APP which has shown to have higher affinity for BACE1 than wild type APP. The statine isostere has been widely investigated (Figure 9). Patents as early as 2000, show statine based inhibitors, such as compound **3**, which displayed IC₅₀ values lower than 10 μM.^{99,100} Compound **4** showed micromolar activity in BACE1 inhibitory assay.¹⁰¹ Molecular docking studies suggested that P3 isoleucine and P2 alanine fit nicely into the S3 and S2 subsites respectively. Similarly, the isobutyl P1 group is situated in the S1 pocket and the S1' pocket was left empty. Incorporation of nonnative side chains have been investigated, as shown in compound **5** with a cyclopropyl moiety in the P2 position.¹⁰² Difluorostatine derivatives have also been examined. A series of compounds, of which compound **6** is an example, were all found to have IC₅₀ values of less than 10 μM.^{103,104}

Phenylstatine-based inhibitors were investigated to place a larger, hydrophobic substituent at the P1 position. Inhibitors with benzyl substituents at this position were twenty times more potent than inhibitors with 2-methylbutyl substituents at this position. Compound **7** (Figure 10) showed a BACE1 IC₅₀ of 21 nM.¹⁰⁵ The incorporation of a *p*-aminomethylbenzoic acid moiety at the C-terminus helped contribute to an increase in potency over previous inhibitors. At the N-terminus, the N-acetyl-leucine motif seemed optimal as inhibitors with

larger or smaller side chains at this position displayed a significant loss of potency. A modeling study of compound **7** in the active site of BACE1 showed that the phenylstatine transition state isostere formed hydrogen bonds with the catalytic aspartic acid residues as expected. The benzyl group at the P1 position nicely filled in the S1 site. The N-terminal motif formed a hydrogen bond to Gln73 while the C-terminal benzoic acid formed a hydrogen bond with Lys224. Further examples of phenylstatine inhibitors include a series with IC₅₀ values less than 50 μM, exemplified by compound **8**.¹⁰⁶ (Figure 10)

Phenylnorstatine based inhibitors have also been investigated.¹⁰⁷ Octapeptide **9** (Figure 11) was developed with a phenylnorstatine hydroxymethyl carbonyl isostere. The leucine residue in the P2 position gave a favorable hydrophobic interaction in the S2 site, while the aspartic acid residue at the P1' position packed into the S1' subsite tightly, leading to an IC₅₀ of 413 nM.¹⁰⁸ In an attempt to decrease the number of peptidic bonds and molecular weight, removal of the nonprime side residues resulted in compounds with no enzymatic inhibitory activity. However, the residues in the prime side may be removed. A structure-activity relationship (SAR) study revealed that a peptide spanning P4 to P1' was necessary to maintain activity. This led to the design of compound **10** which displayed an enzyme IC₅₀ value of 3.4 nM and an IC₅₀ value of 0.20 μM in BACE1 transfected HEK-293 cells.¹⁰⁹ As seen in previous SAR studies, P2 leucine and P3 valine residues remained to be favored for these positions. At the P1' position, it was shown that phenylamide was more successful than benzylamide suggesting that a conformationally restricted moiety is preferred. The carboxylic acid moieties were incorporated to pick up hydrogen bonding opportunities in the active site and flap region. The P4 side chain was investigated as well. It was found that both the amino and carboxyl groups were favored and contributed to binding. Length of the side chain was investigated with the four-atom side chain being the most favorable. While still very peptidic in nature, it was assumed that **10** may be more metabolically stable due to the presence of unnatural amino acid derived residues.

Compound **10** contains a β-*N*-oxalyl-L-α-β-diaminopropionic acid group in the P4. This moiety thermally isomerizes to α-*N*-oxalyl-L-α-β-diaminopropionic acid, contributing to the instability of the inhibitor. In an attempt to create more stable derivatives, the oxalyl substituent was replaced with 1*H*-tetrazole-5-carbonyl, leading to compound **11**.¹¹⁰ This compound showed no isomerization at as many as 5 days and exhibited an IC₅₀ value of 3.9 nM. Modeling studies showed that the tetrazole ring hydrogen bonds to Arg235 and Arg307, thus maintaining the potency of **10**. Compound **11** was brought to further biological evaluation and was found to have a cellular IC₅₀ of 42.8 nM. When injected into the hippocampus of APP transgenic mice, compound **11** exhibited a 20% decrease of hippocampal sAPPβ 3 hours after a 2.5 nmol dose. When dosed in wild type mice, a reduction of Aβ₄₀ and Aβ₄₂ was seen at 42.9% and 39.8% respectively and soluble forms were reduced by 34.6% and 31.0% respectively following a 10 nmol dose hippocampal injection. When dosed with a 2.5 nmol hippocampal injection, wild type mice displayed a reduction of Aβ₄₀ and Aβ₄₂ of 38.1% and 31.5% respectively with soluble forms being reduced by 32% and 38% respectively.¹¹¹

Attention was then turned towards the issue of cell membrane and blood-brain barrier permeability. While previously discussed compounds have been shown to be potent, their

many acidic and polar moieties hinder their transport across cell membranes and the blood-brain barrier. Further optimization resulted in compound **12** with an IC_{50} of 1.2 nM.¹¹² Many other heterocycles were attempted at the P1' position as carboxylic acid isostere. Among the moieties investigated were 5-oxo-1,2,4-oxadiazole, 5-oxo-1,2,4-thiadiazole, 2-thioxo-1,3,4-oxadiazole, and 1H-tetrazole. Among these, 1H-tetrazole showed the most promising results. Modeling studies showed that the phenylnorstatine transition state isostere positions itself between the catalytic aspartates and hydrogen bonds to both Asp32 and Asp 228 (Figure 12). The amide backbone of the inhibitor made hydrogen bonds with Gly11, Thr232, Gly230, Gln73, and Thr72 while the P4 tetrazole formed hydrogen bonds with Arg307, Gly264, and Asn233.¹¹²

Further investigations of norstatine derivatives led to the design of compound **13** (Figure 13) with an IC_{50} of 5.6 nM.¹¹³ In this inhibitor, the P2-leucine was changed to a cyclohexylmethyl moiety. Further examination of the P4 moiety was performed in an attempt to gain selectivity over BACE2. It is thought that an acidic moiety in the P4 position may help inhibitors be selective for BACE1 over BACE2 due to interaction with Arg307 in BACE1 but absent in BACE2. The 5-fluoroorotyl group was shown to maintain potency in cells with 84% inhibition at 100 μ M concentrations.

Incorporation of a phenylthionorstatine transition state isostere in place of phenylnorstatine counterpart showed 99% inhibition at 2 μ M concentration.¹¹⁴ Modeling studies suggested the phenylthionorstatine hydrogen bonds to the catalytic aspartic acid residues similarly to phenylnorstatine derivatives. Modifications in the P4 region led to the formation of a new hydrogen bond between Ser325 and the 3-amino group on the side chain. Efforts were focused on replacing acidic moieties at the P1' position with nonacidic and low molecular weight functional groups. Optimization efforts led to compounds **14** and **15** (Figure 13).¹¹⁵ Increasing lipophilicity via the addition of a dichlorobenzene moiety in the P1' position resulted in **14** which showed 99% BACE1 inhibition at 2 μ M and 84% BACE1 inhibition at 0.2 μ M.¹¹⁵ Modeling studies showed that Thr72 was located near to the P1' benzene ring suggesting that the addition of a hydrogen bond acceptor will aid in the binding of these molecules. This insight led to the replacement of the dichlorobenzene moiety with a trifluoromethyl sulfonyl moiety, **15**.¹¹⁵ Modeling studies with this compound suggested that the P1' moiety can act as a bridge between the flap region and the active site via interactions with Thr72.

Inhibitors containing 4-amino-3-hydroxy-5-difluoro-phenylpentanoic acid as a statine mimic gave inhibitors in the micromolar range with inhibitor **16** (Figure 14) showing the highest potency in BACE1 assay and HEK-293 cells.¹¹⁶ Other statine side chain mimics, such as 3,5-difluorophenylloxymethyl **17** have been attempted. Compound **17** exhibited a BACE1 IC_{50} of 0.037 μ M with 21-fold selectivity over cathepsin D.¹¹⁷ The X-ray crystal structure of the inhibitor **17** and BACE1 complex showed extensive hydrogen bonding of the nonprime backbone of the inhibitor with the active site (Figure 15). The P3 amide NH hydrogen bonds with the carbonyl of Gly230, while the two P2 carbonyls interact with the side chain of Thr232 and the backbone of Gln73 in the flap of the protein. Additionally, the amide NH of the P1 position hydrogen bonds to the carbonyl of Gly230. The P3 phenyl group was stacked between Thr232 and Gly13 while being in proximity to Gly11, Tyr14,

Ser229, Gly230, and Arg307. The stereochemically defined methyl group in the P3 position made hydrophobic interactions with Gln12, Gly14, Leu30, and Ile10. The P2 aromatic ring was positioned between Thr231 and Gln73. The P1 phenyl ring displayed pi stacking interactions with Tyr71, Phe108, and Trp115 while having further contact with Gln73, Gly74, Lys107, and Ile110.¹¹⁷ The P1' carbonyl hydrogen bonds to the Thr72 backbone amide NH. The P2' position is involved in two hydrogen bonds, one of the amide NH of P2' to the carbonyl of Gly34 and the other of the carbonyl of P2' with the side chain hydroxyl of Tyr198. The valine side chain at the P2' position picks up hydrophobic interactions with Ser35, Val69, Ile126 and Arg128 in that region. The P3' isophthalic acid moiety interacts with the solvent exposed S3' pocket via hydrogen bonds from the carboxylates to the side chains of Thr72 and Arg128.¹¹⁷

(b) Inhibitors with *tert*-hydroxyl groups to mimic transition-state

Inhibitors with a *tert*-hydroxyl motif were investigated based on inhibitors of HIV-1 protease with a *tert*-hydroxyl transition state isostere. In these HIV-1 protease inhibitors, compounds maintained potency while obtaining better membrane permeability.¹¹⁸ Research efforts to emulate these results in BACE1 inhibitors resulted in compound **18** (Figure 16). In this example, stereochemistry at the tertiary center was shown to be not important, as both stereoisomers showed very similar activity, $IC_{50} = 0.23 \mu\text{M}$ and $0.32 \mu\text{M}$.¹¹⁹ However, this compound exhibited a very low membrane permeability of $1.2 \times 10^{-6} \text{ cm/s}$. Further investigations led to compounds such as **19**¹²⁰ and **20**.¹²¹ Compound **19** showed a slight decrease in potency, however compound **20** provided some insight into a unique binding mode of these compounds.

An X-ray crystal structure of the compound **20** and BACE1 complex showed that the N-terminal amine hydrogen bonded to Asp228 rather than the tertiary hydroxyl of the transition state isostere (Figure 17). Interestingly, the tertiary hydroxyl group hydrogen bonds to Arg128 while the benzyl group extends towards the protein surface and does not pick up any significant interactions in the binding pocket. This placed the carbonyl of the tetrazole near Arg235 and one of the nitrogens within hydrogen bonding distance of Tyr198. Further, the N-terminal carbonyl interacted with Thr72 of the flap region. The next valine amide NH hydrogen bonds to Gly34 and the carbonyl interacts with Tyr198. The subsequent leucine interacts with Pro70 of the flap through a hydrogen bond to the amide NH as well as positioning its carbonyl near to Tyr198. The carboxylic acid functionality at the C-terminus picks up polar interactions with Tyr68 and Lys75.

(c) Hydroxyethylene Isostere-based Inhibitors

Hydroxyethylene isosteric inhibitors were among the earliest examples of BACE1 inhibitors. The proof-of-concept inhibitors discussed previously, OM99-2 and OM00-3 both utilize a hydroxyethylene isostere core¹²²⁻¹²⁴ (Figure 5). These inhibitors were based on a leucine-alanine structure at the scissile site which mimicked the Swedish mutation of APP. However, while potent, these structures needed optimization to reduce molecular size and improve pharmacokinetic properties.^{70, 125}

Based upon the X-ray structure of **1**-bound BACE1, peptidomimetic inhibitor **21** was designed by truncating P3', P4' and P4-ligands from inhibitor **1**. Compound **21** displayed a K_i of 2.5 nM (Figure 18).¹²⁶ At the P2 position, both methylsulfone and methylcysteine ligands were investigated, however methionine, as shown in compound **21**, showed the most potent activity. This is possibly due to an interaction with Arg235.¹²⁷ Unfortunately, this class of inhibitors did not prove to be selective for BACE1.

Efforts towards the development of selective inhibitors, led to the design of compound **22** with a pyrazolylmethyl urethane at the P3 position (Figure 18).¹²⁸ This inhibitor showed a K_i of 0.3 nM and was selective for BACE1, showing 1186-fold selectivity over BACE2 and 436-fold selectivity over cathepsin D.¹²⁹

A crystal structure of **22** in the BACE1 active site (Figure 19) showed that one of the pyrazole nitrogens hydrogen bonds to Thr232 while one of the methyl substituents of the pyrazole ring sits in the hydrophobic S3 pocket. The P2 sulfone moiety forms hydrogen bonds with Arg235 and a tightly bound water molecule. These interactions may be responsible for the observed selectivity. Based upon the structural insights of the pyrazole derivative, compound **23** with a oxazolylmethyl P3 ligand was designed. Compound **23** displayed a K_i of 0.12 nM and a very high selectivity of greater than 3800-fold over BACE2 and greater than 2500-fold selectivity over cathepsin D.¹²⁹ Further modifications were investigated.¹³⁰

In an attempt to improve cell potency, inhibitors with a Leu-Ala isostere and P2 isophthalamides were investigated.^{131, 132} Incorporation of propyl isophthalamide across the P2 and P3 positions provided inhibitor **24** (Figure 20) which was less potent than previous inhibitors in Figure 18. However, optimization via the addition of a N-methylsulfonamide on the isophthalamide moiety to interact with residues in the S2 pocket, as well as the incorporation the oxazolylmethylamide moiety of previous inhibitors gave **25** with improved potency. Incorporation of hydrophobic groups in the P3 position resulted in inhibitor **26**. The (*R*)-methylbenzylamide was shown to be much more potent than either the benzylamide or the (*S*)-methylbenzylamide. While this compound only showed modest selectivity against BACE2 and cathepsin D, 28-fold and 37-fold respectively, it exhibited good cellular inhibition (IC_{50} 39 nM). An intraperitoneal injection of **26** to Tg2576 transgenic mice (8 mg/kg dose) showed a 30% reduction of plasma $A\beta_{40}$ levels after four hours.¹³¹

The X-ray crystal structure of compound **26** and BACE1 complex was determined to obtain binding site interactions (Figure 21). As can be seen, inhibitor forms a network of hydrogen bonding interactions with the catalytic aspartates. The P2 isophthalamide makes a number of key interactions in the S2 subsite. One of the sulfone oxygens forms a hydrogen bond with Arg235 and the P3 – phenylethyl moiety fills in the S3 subsite.

A series of derivatives with a Phe-Ala isostere were investigated (Figure 22). Compound **27** displayed an IC_{50} of 0.13 μ M.¹³³ It showed BACE2 selectivity of 2.8-fold. In this series of compounds, alanine at P2 was preferred, with other bulky or branched substituents at this position resulting in a dramatic loss of potency. Compound **28** with a Phe-Glu isostere was examined.¹³⁴ Compound **28** gave a K_i value of 1.7 μ M. While this compound showed 47-

fold selectivity over cathepsin D and 44-fold selectivity over renin, it did not show any selectivity over BACE2. Other examples, such as **29** and **30**, were designed and evaluated.¹³⁵⁻¹³⁷

Inhibitors utilizing a hydroxyethylene core with non-native P1 side chains have been investigated (Figure 23). A series of inhibitors displaying a difluorophenylalanine side chain at P1 were examined for the optimization at the prime side.¹³⁸ The P2' isobutylamide in compound **31**, was shown to be the best moiety at this position. At the P1' position, methyl was the preferred side chain, as seen previously. Compound **31** showed a BACE1 IC₅₀ of 30 nM and a cellular IC₅₀ of 3000 nM in HEK293 cells. Other difluorophenylalanine derivative, such as **32**, did not show much activity.¹³⁹ Inhibitors such as **33** with a benzyloxymethyl P1 ligand have been shown to have IC₅₀ values of less than 50 nM.¹⁴⁰

BACE1 inhibitors with hydroxyethylene isosteres containing unnatural amino acid-derived P1 and P1' side chains have been investigated (Figure 24).¹⁴¹ These inhibitors were designed to have optimal interactions in the P2' region. Compound **34** showed extensive interactions in the S2' subsite including a pi stacking interaction with Tyr71 and close contact of the methoxy substituent with Ser36, Asn37, and Ile126. In an effort to increase cell permeability by reducing polarity, compound **35** was designed.¹⁴² Despite the rather large lipophilic P1 ligand, this compound showed a BACE1 IC₅₀ of 69 nM. Unfortunately, this compound did not display cellular potency. Other examples such as compound **36** have shown moderate inhibitory activity.¹⁴³

(d) Hydroxyethylamine-based Inhibitors

BACE1 inhibitors with hydroxyethylamine transition-state isosteres have been investigated extensively. Earliest examples utilized were inhibitors **37** and **38** with a leucine side chain as the P1 ligand (Figure 25).¹⁴⁴ However, inhibitors with phenylalanine side chain are more widely utilized. In an attempt to optimize pharmacokinetic and pharmacodynamic properties, unnatural amino acid side chains have also been investigated.

Utilizing knowledge gained from hydroxyethylene-based inhibitors, peptidomimetic inhibitors containing hydroxyethylamine isosteres have been developed (Figure 26).¹⁴⁵ Inhibitor **39** showed an enzyme IC₅₀ of 15 nM and a cellular IC₅₀ of 29 nM while having 15-fold selectivity over BACE2, 500-fold selectivity over cathepsin D, and greater than 3000-fold selectivity over renin. An X-ray crystal structure of **39** and BACE1 complex showed that the α -methylbenzylamide fit in the S3 site, with *R*-hydroxyl stereochemistry preferred over *S* isomer. The P2 sulfonamide oxygen atoms were involved in hydrogen bonding with the backbone NH of Thr232 and Asn233. The hydroxyethylamine moiety interacts with the catalytic aspartic acids. The hydroxyl group hydrogen bonds to Asp32 while the α -amino group interacts with Asp228. Further investigation into these inhibitors resulted in compound **40**.¹⁴⁶ This inhibitor was designed to conformationally constrain the non-prime side of the inhibitor in an attempt to better access the S3 pocket. Compound **40** showed an IC₅₀ of 35 nM. It was speculated that the alkene linkage could be responsible for the moderate P_{app} efflux, however permeability calculations showed that the P_{app} value increased slightly.

Further investigation led to the development of inhibitors **41-44** (Figure 27).¹⁴⁷ The focus of this research was to reduce molecular weight and the number of amide bonds in an attempt to address cellular uptake and metabolic stability issues of previous inhibitors. A benzamide moiety was introduced on the non-prime side of the inhibitor. Compound **41** features a hydrogen bond acceptor at the meta position, however it was found that increasing the lipophilicity of this substituent, as in **42**, resulted in a moderate increase in potency. A crystal structure of the **42** and BACE1 complex showed that the sulfone moiety hydrogen bonded to Asn294, which left the S3 pocket unoccupied. Further optimization efforts led to compound **43**. It displayed an IC₅₀ of 605nM as well as selectivity over BACE2 and cathepsin D of 13-fold and 78-fold selectivity respectively. In this inhibitor, the carbonyl of the lactam moiety hydrogen bonds to Asn294 while the propoxy moiety fills in the S3 pocket. A linear, three atom chain was preferred at this position over shorter, longer, or branched derivatives. Compound **44** which utilized a nitrogen linked alkyl chain at P3 rather than the propoxy in compound **43** has shown to be the most potent and selective. It displayed IC₅₀ value of 13 nM and selectivity over BACE2 and cathepsin D of 139-fold and 207-fold respectively.¹⁴⁷

Further investigations of these compounds turned to the prime side, with focus on further reducing the molecular weight, number of heteroatoms, and polar surface area. Compounds **45** and **46** (Figure 28) were designed and evaluated in an attempt to address these issues.¹⁴⁸ Branched alkyl chain in compound **45**, allowed flexibility to optimally fill the pocket. However, it was seen that the prime side instead interacts with the enzyme in the extended conformation. Use of a meta-trifluoromethylbenzylamide at the prime side gave compound **46** which maintained potency and exhibited slightly better selectivity. A crystal structure of **46** complexed with BACE1 showed that the trifluoromethyl substituent filled the same pocket as the terminal methyl of the branched alkyl chain derivative **45**. Sultams were also investigated as a replacement to the lactam moiety on the non-prime side.¹⁴⁹ This resulted in compounds **47** and **48**. Introduction of a fluorine at the 2-position on the benzamide, **48**, increased cellular potency. When orally administered to TASTPM mice, a 250 mg/kg twice daily dose reduced brain A β ₄₀ and A β ₄₂ levels by 18% and 23% respectively. When administered with a Pgp inhibitor, this effect was enhanced to a 68% reduction for A β ₄₀ and a 55% reduction for A β ₄₂. Many other similar derivatives have been evaluated as BACE1 inhibitors.¹⁵⁰⁻¹⁵²

Tricyclic sultams have also been developed as P2 ligands in an effort to improve pharmacokinetic properties while eliminating a site of metabolism. Modeling studies suggested that the tricyclic derivatives could mimic the interactions desired while reducing the metabolic sites seen in prior compounds. Compound **49** (Figure 29) achieved this by maintaining nanomolar potency in both enzyme and cell assays while displaying increased oral bioavailability in both rats and dogs.¹⁵³ Compound **50**, showed that a 7,6,5- ring system was most active compared to 6,6,5- and 8,6,5- ring systems.¹⁵⁴ Compound **51** was developed to bind to the catalytic site as a hydrate.¹⁵⁵ However, it is found to exist in solution as a ketone. Other scaffolds, such as the pyrrolidinone indole derivative **52**, were also investigated, however there was no significant improvement in pharmacokinetics,

showing rapid clearance in a rat model.¹⁵⁶ A number of other related derivatives were synthesized and evaluated as BACE1 inhibitors.¹⁵⁷⁻¹⁵⁹

An X-ray crystal structure of inhibitor **50** and BACE1 complex was determined to obtain molecular insight (Figure 30). The structure shows that the tricyclic P2 ligand is involved in extensive interactions in the S2 and S3 subsites. Both sulfone oxygens form hydrogen bonds with backbone NHs of Thr232 and Asn233 as well as the side chain of Ser325 and Asn233. The tricyclic core appeared to fill in the hydrophobic sites of S2 and S3.

A combination of hydroxyethylamine isostere with a P2 isophthalamide and a P2' 3-methoxybenzylamine resulted in a very potent inhibitor. Compound **53** (Figure 31) showed an enzyme inhibitory K_i of 1.8 nM and a cellular IC_{50} of 0.001 μ M.¹⁶⁰ This inhibitor showed 39-fold selectivity over BACE2 and 23-fold selectivity over cathepsin D. A crystal structure of the **53** and BACE1 complex showed the hydroxyethylamine isostere forming hydrogen bonds with Asp32 and Asp228, as seen with other inhibitors in the class (Figure 32). The P3 phenyl group imposes a conformational shift of the 10s loop of the protein in order to span both the S3 and S4 pockets. The sulfonamide in the P2 position hydrogen bonds with Asn233 and Ser325 while having ionic interactions with the side chain of Arg235. The P2' methoxybenzene moiety makes adequate hydrophobic interaction in the S2' site, interacting with Gly34, Ile126, and Tyr198, as well as Pro70, Tyr71, and Thr72 of the flap region.¹⁶⁰

Compound **53** was intraperitoneally injected into Tg2576 mice, a 65% reduction of plasma $A\beta_{40}$ levels could be seen 3 hours after an 8 mg/kg dose. After a 4 mg/kg dose, 10% of the inhibitor was found in the brain after 1 hour, which decreased slowly over time. Long-term delivery of 33.4 mg/kg via an osmotic pump in Tg2576 transgenic mice showed rescue of cognitive decline with no toxicity after several months on the inhibitor in mice older than 16 months.¹⁶¹ Furthermore, no build-up of unprocessed APP was detected. Such build up has been hypothesized to be a possible concern of BACE1 inhibition. Other similar compounds have been investigated.¹⁶²⁻¹⁶⁶

Non-native P1 ligands, such as a difluorobenzyl moiety, have been investigated. (Figure 31) Compounds such as **54** showed good enzyme inhibitory and cellular activity and selectivity over cathepsin D.¹⁶⁷ The polar functionality at the P2 position helped enhance selectivity as the S2 site in cathepsin D is much more lipophilic than the S2 site in BACE1. A crystal structure of **54** in the BACE1 active site showed that the pyridine nitrogen interacts with Arg235, but does not form a hydrogen bond due to geometric constraints. Further investigations resulted in inhibitors **55** and **56**.¹⁶⁸ A crystal structure of the **55** and BACE1 complex revealed important interactions in the active site. The carbonyl oxygen of the N-terminal amide hydrogen bonded to the backbone nitrogen and side chain hydroxyl group of Thr232. The amide functionality form hydrogen bonds with the Gln73 backbone NH and the backbone carbonyl of Gly230, respectively. The hydroxyethylamine transition state isostere hydrogen bonds to the catalytic aspartic acid residues, the hydroxyl group to Asp32 and the amine nitrogen to Asp228. The nitrogen of the hydroxyethylamine isostere makes an additional hydrogen bond to the Gly34 carbonyl. Hydrophobic interactions also aid in the inhibitor affinity. One of the N-terminal propyl groups sits in the S3 subsite while the

isophthalate interacts with Thr230, Gln73, and Arg235. The hydrophobic side chains in the S1 site, Leu30, Gln73, Tyr71, Phe108, Trp115, and Leu118, nicely accommodate the difluorobenzyl moiety. Incorporating amide functionality at the C5 position of the isophthalamide increased both potency and cathepsin D selectivity (218-fold).¹⁶⁹ Many other inhibitors incorporating hydroxyethylamine isostere and isophthalamide derivatives as the P2 ligands have been synthesized and evaluated.¹⁷⁰⁻¹⁷⁵

Further research utilizing difluorophenylmethyl as the P1 ligand examined the replacement of isophthalamide functionality with indole. The presence of indole in other pharmaceuticals was known to facilitate brain penetration.¹⁷⁶ Substituted indole derivatives, such as **57** (Figure 33), retained enzyme inhibitory activity, but did not show promising cellular potency. Heterocyclic replacements of isophthalamide such as pyrrole, pyrrolidine, and reverse indole, were not promising. However 7-azaindole, as in compound **58**, showed an improvement in cellular activity. A 30 mg/kg intraperitoneal injection of **58** displayed a 51% reduction in plasma A β 1.5 hours post dose and a 37% reduction of plasma A β 5 hours post dose. Unfortunately, there was no reduction in brain A β seen up to 5 hours post dose. Other similar compounds have also been investigated.^{177, 178}

Other structural optimization efforts addressing the issues of cell permeability and Pgp efflux looked into reduction of size at non-prime side of the inhibitor. Compound **59** (Figure 34) displayed an IC₅₀ of 230 nM and a Pgp efflux ratio of 1.1.¹⁷⁹ A 30 mg/kg oral dose of **59** twice daily showed a reduction of cortical A β of 28% after 2.5 days. Further investigation resulted in inhibitors such as **60**, **61**, and **62**.¹⁸⁰ Unfortunately, inhibitors **60** and **61** showed more potent inhibitory activity against cathepsin D than BACE1. Compound **62** showed modest selectivity, however it did not show promising cell membrane permeability. Derivatization of these compounds has been investigated extensively.¹⁸¹⁻¹⁹⁵

A variety of substituted benzyl and alkyl derivatives as the P1 ligand have been synthesized and evaluated. Compound **63** (Figure 35) with a benzodioxolane P1 ligand exhibited potent activity.¹⁹⁶ A crystal structure of the **63** and BACE1 complex showed that the benzodioxolane ring occupied the S1 site and the hydroxyethylamine isostere hydrogen bonds to the catalytic aspartates as expected. The cyclobutane and neopentyl substituents on the prime side occupy the S1' and S2' sites respectively. Hydrogen bonds are formed between the amide NH with Gly230, and the carbonyl and methoxy functionality make a bidentate interaction with Thr72. When **63** was administered in rats at a 2 mg/kg iv dose or 5 mg/kg oral dose, a half life of about 3-5 hours was observed. Also, the clearance rate was moderate and the compound showed good oral bioavailability. A β ₄₀ reduction varied from 59-75% 4 hours post dose when dosage varied from 10 mg/kg to 100 mg/kg. Compound **64** was designed utilizing a 3-(2-thioazolyl)phenyl ligand at the P1 position.¹⁹⁷ Compound **64** exhibited a 59% reduction in brain A β levels after a 30 mg/kg oral dose in rats. Compound **65** with a terminal propene moiety as the P1 side chain showed an enzymatic IC₅₀ of 2 nM and a cellular IC₅₀ of 28 nM.¹⁹⁸

Inhibitors with constrained hydroxyethylamine isosteres have been developed. In these inhibitors, conformationally constrained cyclic amines were incorporated to interact with catalytic aspartates and fill in the S1' pocket. A representative example is compound **66**

(Figure 36) which showed an IC_{50} of 71 nM.¹⁹⁹ A crystal structure of **66** in the BACE1 active site showed that the imidazolidinone carbonyl makes contacts in the flap region, while the protonated nitrogen forms a hydrogen bond with Asp228 and Gly34. Piperazine sulfonamides such as **67** were also examined.²⁰⁰ While potent, these inhibitors were found to be Pgp substrates, showing no reduction in brain A β in CRND8 mice after 30 mg/kg, 100 mg/kg, and 300 mg/kg subcutaneous doses. Compounds such as **68**, containing a constrained carboxylic isostere, showed good enzyme inhibitory activity.²⁰¹ However, the peptidic nature of inhibitor **68** limited the cell membrane permeability. Compounds such as **69**, were found to be very potent in cellular assays.²⁰² In Pgp knockout mice, A β levels in both the brain and periphery were lowered when dosed with **69**. However, wild type mice showed no lowering of brain A β pointing to Pgp efflux as the limiting factor in the efficacy of compound **69**.

Compound **70** (Figure 37) was designed with a triazole moiety as the constraining hydroxyethylamine moiety.²⁰³ A crystal structure of the compound **70** and BACE1 complex was determined. It showed that the P3 phenyl ring spans both the S3 and S4 sites, which changes the conformation of the 10s loop. One of the oxygens of the P2 sulfonamide hydrogen bonds to Ser325 via a water bridge while also having ionic interactions with the Arg235 side chain. The other oxygen hydrogen bonds to the backbone nitrogen of Thr232 and Asn233. The hydroxyl group of the hydroxyethylamine isostere hydrogen bonds to the catalytic aspartic acid residues. In an attempt to enhance the cellular potency, pyrazole derivatives such as **71** and **72** were tried (Figure 36).²⁰³ Both showed better membrane permeability than previous triazole inhibitors. Many other examples of similarly constrained hydroxyethylamine inhibitors have been reported in patent literatures.²⁰⁴⁻²¹⁰

Conformationally constrained hydroxyethylamine template was designed to mimic the transition-state. Compounds were designed based upon cyclic sulfone and sulfoxide templates. Compound **73** (Figure 38) showed submicromolar activity in the enzyme inhibitory assay.²¹¹ X-ray crystallographic studies showed that the catalytic aspartates formed hydrogen bonds to the hydroxyethylamine isostere. The phenolic hydroxyl group hydrogen bonds to the backbone nitrogen of Phe108 and the sulfone moiety hydrogen bonds with Thr72 and Gln73, putting the enzyme in the closed flap conformation. The hydrophobic bromine resulted in improvement in potency and selectivity, however the phenol moiety has generally low metabolic stability. At the prime side it was found that hydrophobic 3-substituted aryl rings were necessary for potency in this class of compounds. Compound **74** showed to have an IC_{50} of 0.055 μ M and a relatively low Pgp efflux ratio of 2.1. While it gave moderate brain exposure in a mouse model, clearance tests showed it only had a half life of 6 minutes when exposed to rat liver microsomes. To improve stability, permeability, and Pgp efflux properties, compounds with fluorines (example compound **75**) were developed.²¹² However, these compounds showed higher efflux ratios and poor oral bioavailability. Compounds with a sulfoxide moiety instead of a sulfone were developed to improve cellular activity.²¹³ It was found that the axial sulfoxide, **76**, was more potent than the equatorial sulfoxide due to the hydrogen bonding capabilities to Thr72. Compound **76** exhibited high blood clearance and when dosed orally in mice at 20 μ Mol/kg with ritonavir,

a Pgp inhibitor. Compound **76** reduced brain A β ₄₀ 39% 4 hours post dose. Similar other derivatives have been investigated as BACE1 inhibitors.²¹⁴

(e) Carbinamine-derived Inhibitors

Carbinamines have been investigated as an attempt to increase blood-brain barrier penetration while maintaining the potency accomplished in previous inhibitors. The potential of carbinamines to mimic the transition-state has been examined. Compound **77** (Figure 39) evolved from the hydroxyethylamine isostere.²¹⁵ This compound resulted from truncation of classic hydroxyethylamine to a primary alcohol followed by optimization to the amine. Incorporation of the fluorine improved the Pgp efflux ratio. Unfortunately, this class of compounds displayed poor oral bioavailability.^{216,217}

Compounds such as **78** with a 1,3,4-oxadiazole ester mimic were shown to be very potent, with an IC₅₀ of 12 nM.²¹⁸ A proposed binding mode of this inhibitor in BACE1 active site is shown in Figure 40. Compound **79** was found to be a very potent and selective BACE1 inhibitor. It exhibited 42-fold selectivity over BACE2 and more than 250,000-fold selectivity over renin or cathepsin D.²¹⁹ After a 100 mg/kg intraperitoneal injection of **79** in mice, a 26% reduction in A β ₄₀ was seen four hours post dose, with a brain concentration of 1.8 μ M. When tested in rhesus monkeys at a low dose of 1.2 mg/kg IV bolus followed by a four hour infusion at 16 μ g/kg/min and a high dose of 3.5 mg/kg IV bolus followed by a four hour infusion at 48 μ g/kg/min, compound **79** showed a time and dose dependent reduction in A β , with an average plasma concentration of 3.8 μ M. Plasma A β levels were reduced by up to 65% four hours post dose and showed a return as early as eight hours, with a full recovery in 24 hours. Unfortunately, this compound showed less than 1% oral bioavailability when dosed alone. This increases to 83% when given with ritonavir to inhibit metabolism.²²⁰ Other examples of carbinamine as BACE1 inhibitors have been reported in patent literature.²²¹⁻²²⁴

(f) Reduced Amide-based Inhibitors

In this class of inhibitors, the nitrogen of the reduced amide appears to bind to the catalytic aspartic acids while other interactions aid in the further binding of the inhibitor in the active site. Compound **80** (Figure 41) was found through structure activity relationship studies of the P1' ligands.²²⁵ When the P1' position is methyl, as shown in **80**, or another small alkyl substituent (such as ethyl in compound **81**), the corresponding derivatives showed good cellular potency. Based upon the binding model of inhibitor **81**, inhibitor **82** was designed to interact with residues in the active site. Inhibitor **82** was found to be a very potent and selective compound.²²⁶ It displayed a K_i of 17 pM and showed 7000-fold selectivity over BACE2 and 250,000-fold selectivity over cathepsin D. An X-ray crystal structure of **82** and BACE1 complex showed (Figure 42) that the nitrogen of the reduced amide isostere hydrogen bonded to Asp228 while the other catalytic aspartic acid, Asp32, forms a hydrogen bond network within the active site with Gly34, Ser35, and Gly230. The P3 phenyl group extends across both the S3 and S4 sites, imposing a conformational shift of the 10s loop of the protein, as seen previously. The stereochemistry of the hydroxyl group was found to be very important at the P1' position, as the diastereomer of this position was much less potent. This is due to the orientation of the hydroxyl group towards Tyr198 in the active site in the

X-ray structure. Further, the allothreonine moiety is critical for selectivity, as derivative **81**, without the hydroxyl group showed only 55-fold and 300-fold selectivity for BACE2 and cathepsin D respectively. A high-throughput in situ synthesis and screening study afforded the testing of 120 reduced amide derivatives as BACE1 inhibitors.²²⁷ In enzyme inhibitory assay, these compounds (representative example, compound **83**) were found to have micromolar activity. Other related reduced amide based inhibitors have been evaluated.²²⁸⁻²³¹

(g) Macrocyclic Inhibitors

Macrocyclic inhibitors have been developed placing the macrocyclic moiety mainly on the non-prime side of the inhibitor. Different transition state isosteres, such as hydroxyethylene, hydroxyethylamine, carbinamine, and reduced amide isosteres have been utilized in macrocyclic inhibitors. The macrocycle is used to stabilize the biologically active conformation of the inhibitor to optimize the interactions in the active site while allowing for some flexibility to form the shape of the active site. Macrocyclic inhibitors with a Leu-Ala isostere, **84** and **85** (Figure 43) were designed based upon the X-ray structure of OM99-2 bound BACE1. The structure showed an intramolecular hydrogen bond between P2 Asn and P4-Glu side chains. It was observed that increasing ring size from a 14 member ring, to a 15 member ring, to a 16 member ring increased potency across each addition of a carbon.²³² Inhibitor **85** displayed a K_i of 14.2 nM. Reduction of the alkene in the macrocycle gave saturated inhibitor **84** which showed a slight decrease in potency to 25.1 nM. A crystal structure of **84** and BACE1 complex (Figure 44) showed the interaction of the hydroxyethylene isostere with Asp32 and Asp228. The S1 and S1' sites are adequately filled by the P1 leucine and P1' alanine. The P2 macrocyclic urethane fills the hydrophobic pocket while having hydrogen bonding interaction such as the carbonyl of the asparagine moiety with Arg235 of the active site.

Macrocyclic inhibitors were designed by formation of ring cycles between the P1 ligand and the P2 backbone amide nitrogen. A representative example is inhibitor **86**.²³³ It showed an IC_{50} of 65 nM. This compound showed enhanced cellular and enzyme inhibitory potency. Cocrystallization of **86** with BACE1 allowed for the elucidation of a crystal structure of the complex. This showed that interactions from P3 to P3' were very similar to those of OM99-2, however compound **86** showed less than perfect occupancy of the S1 site. Molecular modeling studies suggested modifications that can fill this subsite.²³⁴ It was found that the 16 member macrocycle of **87** was more potent than the corresponding 15 member macrocycle. A crystal structure of inhibitor **87** and BACE1 complex supported the predictions of the computational modeling.

Macrocyclic inhibitors utilizing a hydroxyethylamine transition state isostere have been developed to reduce the number of amide bonds and hydrogen bond donors and acceptors to enhance pharmacokinetic properties. Compounds **88** and **89** (Figure 45) exhibited IC_{50} values of 22 nM and 2 nM respectively.²³⁵ An X-ray crystal structure of inhibitor **88** and BACE1 complex was determined. The structure showed better hydrophobic contacts of Ile118, Leu30, and Trp115 with the alkyl portion of the macrocycle (Figure 46). Also, the N-methyl of the macrocycle forced the flap region into a slightly open conformation due to

an interaction with Gly230. The hydroxyethylamine isostere hydrogen bonded to the catalytic aspartic acid residues, as seen in previous hydroxyethylamine inhibitors. Inhibitor **88** showed 53-fold selectivity over cathepsin D, however its clinical efficacy was shown to be limited due to Pgp efflux, as the efflux ratio was calculated to be 15 for this compound. While potency was gained in macrocyclic inhibitor **89**, Pgp efflux was quite high with a ratio of 9.4. Furthermore, selectivity over cathepsin D disappeared. In an attempt to increase blood-brain barrier penetration, lipophilicity issues were addressed. A decrease in lipophilicity resulted in inhibitors **90** and **91**.²³⁶ Inhibitor **90**, showed nanomolar potency, however the efflux ratio was very high, 23, which results in low brain exposure. Addition of a spirocyclic cyclopropane in inhibitor **91**, increased potency with greater membrane permeability and lower Pgp efflux ratios.

Further design of macrocyclic inhibitors with hydroxyethylamine isostere included the addition of phenyl substitution on the macrocycle. As represented in compound **92** (Figure 47) the (*R*)- stereochemistry at the phenyl substitution was important for access to a hydrophobic subpocket in the S3 site. While this compound showed good enzyme inhibitory potency of 3.2 nM, the cell membrane permeability was poor. Macrocyclic inhibitor **93** showed a BACE1 enzymatic IC₅₀ of 17 nM and was 22-fold selective over cathepsin D.²³⁷ Other macrocyclic inhibitors such as **94**, also displayed potent enzyme inhibitor activity.²³⁸⁻²⁴¹

A series of carbinamine-based macrocyclic inhibitors has been designed in order to stabilize the biologically active conformation of acyclic carbinamine inhibitors. During the development of these inhibitors, it was observed that macrolactones were more active than the corresponding macroethers. This is possibly due to additional interactions in the flap region of the protein.²⁴² While inhibitor **95** (Figure 48) was potent with an IC₅₀ of 2 nM, it displayed low membrane permeability, a high efflux ratio of 16, and high metabolism. In an attempt to increase brain penetration, an increase in steric bulk near the amide bond of the macrocycle was sought. Inhibitor **96** achieved greater brain penetration showing an efflux ratio of 1. However, this gain was countered with a loss of potency in inhibitory activity (IC₅₀ of 380 nM). Replacement of the amide functionality of isophthalamide with a secondary amine provided inhibitor **97** with an IC₅₀ of 400 nM.²⁴³

Macrocyclic inhibitors with reduced amide isosteres have been investigated as well. The reduced peptidic character of the reduced amide isostere was thought to improve brain penetration. Macrocycles such as **98** were designed and synthesized.²⁴⁴ It was observed that a 14 member macrocycle had better membrane permeability and a lower Pgp efflux ratio than macrocycles with smaller rings. When inhibitor **98** was dosed at 100 mg/kg via IV bolus in AAP-YAC mice, Aβ₄₀ was reduced 25% and brain concentration of **98** was 1100 nM. Other examples of reduced amide macrocyclic BACE1 inhibitors are reported in the patent literature.^{245, 246}

7. Nonpeptide Inhibitors

The development of small molecule nonpeptide inhibitors have evolved from high-throughput screening or fragment based screening of scaffolds, followed by chemical

optimization. The major objectives for the search of small molecule nonpeptide inhibitors are to develop inhibitors smaller in size, with less peptide character, and better metabolic stability. Also, small molecule inhibitors may have better blood-brain-barrier penetration ability and a lower Pgp efflux ratio. Inhibitors can also be developed based on computational screening and modeling methods, which can narrow a large compound library down to a few hundred compounds. Some isolated natural products have also been shown to have BACE1 inhibitory properties. While many scaffolds have been utilized, the scaffolds shown in Figure 49 will be discussed in this section.

(a) Acyl Guanidine-based Inhibitors

A high throughput screening of a library of compounds provided an initial hit compound **99**, which featured an acyl guanidine moiety (Figure 50). This hit has a BACE1 IC_{50} of 3.7 μ M and a crystal structure of the **99** and BACE1 complex showed that the acyl guanidine moiety was responsible for forming four hydrogen bonds to the catalytic aspartic acid residues.²⁴⁷ Further development of this hit gave inhibitor **100**. This compound displayed an IC_{50} value of 110 nM, however it was only modestly selective showing only 3-fold selectivity over BACE2 and 54-fold selectivity over cathepsin D. A crystal structure of **100** and BACE1 complex revealed that the acyl guanidine moiety hydrogen bonded to the catalytic aspartic acid residues while the substitution at the amine of the acyl guanidine moiety extended into the S1' pocket to pick up hydrogen bonds with Arg235 and Thr329 via water mediated hydrogen bonds. The para-npropyloxyphenyl substitution on the pyrrole ring extends across the S1-S3 subsites. Compound **101**, with an adamantyl substitution on the pyrrole ring, showed similar potency to previous compounds.²⁴⁸ A crystal structure of **101** with BACE1 showed that the compound binds similarly to compound **100**, however it suffers from poor membrane permeability. Compound **102** with a bromobenzoate substitution exhibited reduction of potency.²⁴⁹ A crystal structure revealed that the 3-bromobenzoyl moiety packs the S3 pocket, however it must twist the amide bond unfavorably out of the plane to do so, which could be the cause for the decrease in potency. Compound **103** showed enhanced inhibitory potency compared to compound **102**.^{250, 251}

Another high throughput screening hit, **104**, showed a K_i of 3900 nM (Figure 51).²⁵² Optimization efforts resulted in compound **105**, with a K_i of 5 nM. However, when dosed subcutaneously in rats, only plasma $A\beta_{40}$ was lowered, with little to no reduction in brain or cerebrospinal fluid $A\beta$ levels, suggesting that inhibitor **105** is subject to high levels of Pgp efflux. Other examples of this type of scaffold include compound **106** which displayed an IC_{50} of less than 100 nM.²⁵³

A virtual screening suggested an indole guanidine fragment, **107** (Figure 52), for optimization.²⁵⁴ Compounds **108** and **109** were optimized from this fragment hit, showing IC_{50} values of 1.01 μ M and 0.044 μ M respectively. A crystal structure of compound **108** and BACE1 complex showed that the acyl guanidine moiety bonded to the catalytic aspartic acid residues as seen previously. The carbonyl of the acyl guanidine formed a direct hydrogen bond with the Gln73 backbone as well as two water-mediated hydrogen bonds to the Gln73 and Thr72 side chains. The indole moiety forms a cation- π interaction with the Arg235 side chain in the S1' site. Overall, this inhibitor binds to the enzyme in a semi-closed flap

conformation. Compound **109** binds very similarly to **108**, however the incorporation of the nitrile functionality on the indole formed a new hydrogen bond to Ser328, which is responsible for the increase in potency. Other inhibitors utilizing this scaffold, such as **110** and **111**, have been shown to have IC₅₀ values of less than 100 nM.^{255, 256} Scaffolds with a terminal guanidine moiety have also been shown to have micromolar potency.^{257, 258}

(b) 2-Aminopyridine-based Inhibitors

2-Aminopyridine-based small molecule BACE1 inhibitors have also been explored. Compound **112** (Figure 53) was identified as BACE1 inhibitor with an IC₅₀ of 25 μM.²⁵⁹ The 3-methoxy-biaryl moiety changes the conformation of the flap region to an open conformation due to the rotation of the Tyr71 to above the aminopyridine. A twist in the biaryl region fills the nonprime hydrophobic pocket while the methoxy substitution displaces water in the S3 pocket and hydrogen bonds to the backbone amide nitrogen of Gly13. Moving the biaryl substitution from the 6-position to the 3-position, as in compound **113**, was speculated to fill the S1-S3 sites. Unfortunately, compound **113** was less potent and showed an IC₅₀ of 24 μM. Optimization efforts resulted in compound **114** with an IC₅₀ of 0.69 μM. In compound **114**, the indole nitrogen is able to hydrogen bond to Gly230 and the 2,3-diaminopyridine moiety is positioned under the flap. Other inhibitors, such as **115**, utilize the pyrrole moiety as seen in previous acyl guanidine inhibitors.^{260, 261} The binding mode of compound **115** is shown in Figure 54. The aminopyridine functionality hydrogen bonds to Asp32 and Asp228 while having a π edge interaction with Tyr71. Other aminopyridine derivatives have also been synthesized and evaluated for BACE1 inhibitory activity.^{262, 263}

(c) Aminoimidazole-based Inhibitors

Based on the high throughput screening hit aminoimidazole derivative **116** (Figure 55), a series of potent small molecule BACE1 inhibitors have been developed. Compound **117**, displayed good enzyme inhibitory potency and showed low Pgp efflux ratio of 3.6.²⁶⁴ Compound **118** showed a BACE1 IC₅₀ of 7.4 μM.²⁶⁵ A modeling study of this compound in the BACE1 active site suggested that the amino group hydrogen bonds to the catalytic aspartic acid residues while the unsubstituted N3 nitrogen of the imidazole ring makes electrostatic and hydrogen bonding interactions with the side chains of Asp228 and Asp32 (Figure 56). Furthermore, the fluorine atom interacts with the Trp76 side chain while the benzyl moiety forms π stacking interactions with Tyr71 and hydrophobic interactions with Arg235. It was also suggested that the poly methoxy groups may hydrogen bond to Asn233 and Lys321. Compound **119** displayed an IC₅₀ value of 24 nM, however it was susceptible to high Pgp efflux and was shown to be much more potent against BACE2 (IC₅₀ 0.84 μM) than BACE1.²⁶⁶

A series of fused pyrimidine imidazole inhibitors has also been investigated. High throughput hit compound **120** (Figure 57) was found to bind to BACE1 with the flap in a more open position.²⁶⁷ With the objectives of improving metabolic stability and to reduce polar total surface area of inhibitors, compound **121** was developed with an IC₅₀ of 20 nM. Further optimization provided compound **122** showing a low nanomolar inhibitor with a pIC₅₀ value of 7.5.²⁶⁸ When dosed orally in wild type mice, compound **122**, a decrease of

brain A β ₄₀ levels of 17% 1.5 hours post dose. Compound **123**, with a spirocyclic cyclobutane moiety, showed an IC₅₀ of 10 nM.²⁶⁹ Further optimization resulted in a series of BACE1 inhibitors with moderate to good potency.²⁷⁰⁻²⁷⁵

(e) Amino/iminohydantoin-based Inhibitors

Aminohydantoin-based inhibitors have been developed based on the high throughput hit **124** (Figure 58), which showed an IC₅₀ of 3.4 μ M. Further optimization of this hit provided compound **125** which showed an inhibitor with an IC₅₀ of 10 μ M.²⁷⁶ A possible binding mode of compound **125** in BACE1 active site is shown in Figure 59. When a 100 mg/kg oral dose was given to Tg2576 mice, plasma A β ₄₀ levels showed a 69% decrease 8 hours post dose. Unfortunately, brain A β levels were not significantly lowered, presumably due to poor brain exposure. Based upon high throughput hit, compound **126** was developed.²⁷⁷ This inhibitor had a BACE1 IC₅₀ of 40 nM and was 427-fold more potent for BACE1 than cathepsin D. Unfortunately, compound **126** was slightly more potent for BACE2 than BACE1, with a BACE2 IC₅₀ of 30 nM. The aminohydantoin scaffold has been further explored with a variety of functionalities extending from phenyl rings to biaryl rings.²⁷⁸⁻²⁸⁹

From acyl guanidine-type high throughput hit **127** (Figure 60), iminohydantoin-based inhibitors have been developed in an attempt to interact with the hydrophobic area from S1 to S3 in the BACE1 active site. Compound **128** had an IC₅₀ of 605 nM and was found to penetrate the brain, with a Pgp efflux ratio 0.9.²⁹⁰ Unfortunately, this compound was not shown to be selective over cathepsin D. Compound **129** showed reduced potency compared to **128**, but showed significantly better selectivity over cathepsin D compared to **128**. Spiropiperidine iminohydantoin compound **130** showed an IC₅₀ of 2.8 μ M.²⁹¹ The X-ray crystallographic studies of **130** in the BACE1 active site showed that this inhibitor sits higher in the active site than previously seen which does not allow for the flap to fully close over the inhibitor with the Tyr71 residue shifting into the S1 region. Further, the S2 and S3 sites are left unoccupied. Unfortunately, compound **130** did not show any selectivity over BACE2, with a BACE2 IC₅₀ of 1.5 μ M. Further, it was found to be an excellent substrate for Pgp, with an efflux ratio of 19.

(g) Aminothiazoline and Aminooxazoline-based inhibitors

Starting from aminothiazole hit **131**, a weak inhibitor with an IC₅₀ of 38 μ M, compound **132** was designed.²⁹² The replacement of the spirocycle resulted in inhibitor **132** with IC₅₀ value of 1.1 μ M. This inhibitor binds to the enzyme in a flap open conformation with both the internal and external nitrogens of the aminothiazole moiety hydrogen bonding to the catalytic aspartic acid residues. The methoxyphenyl moiety acts like Tyr71, which mimics the closed state stabilization by hydrogen bonding to Trp76. Further investigation provided aminothiazoline inhibitor **133** which exhibited an IC₅₀ of 1.1 nM.²⁹³ Bicyclic aminooxazolines were designed to extend into the P3 and P2' pocket.²⁹⁴ Compound **134** exhibited micromolar inhibitory activity. Aminooxazoline derivative **135** showed an IC₅₀ of 0.05 μ M.²⁹⁵

Aminooxazoline inhibitors have been developed from lead compound **136** (Figure 62).²⁹⁶ Compound **136** was more potent against BACE2 (IC₅₀= 52 nM) than BACE1. Compound

137 was also more potent against BACE2. Compound **138** showed an enzyme IC₅₀ of 12 nM and an efflux ratio of 1.9. Four hours post 10 mg/kg oral dose, A β production was down 95%. Furthermore, the oral bioavailability of **138** was found to be 68%. Compounds such as **139** were found to have good *in vitro* properties, with an enzymatic IC₅₀ of 120 nM and a cellular IC₅₀ of 67 nM.²⁹⁷ However, it showed no *in vivo* activity. A variety of other aminooxazoline inhibitors have also been developed.²⁹⁸⁻³⁰⁶

The corresponding sulfur containing heterocycles, such as aminothiadiazines have also been investigated.³⁰⁷ Compound **140** (Figure 63) showed an IC₅₀ of 9.9 μ M. A modeling study showed that the naphthylbenzylamide extends into the S3 site while the amino group hydrogen bonds to Asp32 and Gly34. The second catalytic aspartic acid residue, Asp228, is hydrogen bonded to one of the internal nitrogens, while the oxygen of the benzyloxy moiety hydrogen bonds to Thr231. Compound **140** displayed an efflux ratio of 0.98, suggesting it would not be a Pgp substrate. Compounds **141** and **142** showed potent BACE1 inhibitory activity.^{308, 309} Iminopyrimidinone **143** showed very potent activity.³¹⁰ It was found that smaller substitution at C6, such as methyl in **143** was optimum for potency. A crystal structure showed that the propynyl moiety protrudes into the S3 site and forms hydrophobic interactions with Ala335. A closed flap conformation brings Tyr71 close to the methylene of the iminopyrimidinone as well as forming a pocket that can accommodate the chlorine. This compound showed low clearance in rat and human hepatocytes and a 69% oral bioavailability in rats. Expansion from 6-membered heterocycles to 7-membered heterocycles has been investigated. Representative derivatives **144-147** (Figure 64) showed low nanomolar enzyme inhibitory activity.³¹¹⁻³¹⁴

(h) Dihydroquinazoline-based Inhibitors

Dihydroquinazoline-based BACE1 inhibitors evolved from the aminoquinazoline fragment hit, **148** (Figure 65).³¹⁵ Optimization of this hit provided compound **149**, with a K_i of 11 nM. The stereochemistry (*S*-configuration) at the cyclohexyl moiety is preferred to better fill the S1' pocket while the N-cyclohexyl moiety fills the S1 site. While this inhibitor had modest selectivity over renin and cathepsin D, it was found to be a Pgp substrate. Compound **150** incorporated a specific heterocyclic substitution to better interact in the active site.³¹⁶ Initially, when N-methyl was replaced with methylthiazole, potency was reduced significantly. However, incorporation of a methoxymethyl substituent on the thiazole ring, resulted in improvement of enzyme inhibitory and cell activity. A molecular model of inhibitor **150** is shown in Figure 66. As can be seen the methyl ether oxygen is within proximity to form a hydrogen bond with Thr 232. Other substituted dihydroquinazoline-derived inhibitors including inhibitor **151** have been reported.³¹⁷⁻³¹⁹

(i) Aminoquinoline-based Inhibitors

Fragment screening resulted in aminoquinoline, derivative **152** (Figure 67) with a K_d of 900 μ M. Optimization of this hit resulted in compounds **153** and **154**.³²⁰ Aromatic substitution at the 6-position of the aminoquinoline fragment showed better potency than substitution at any other position. Further, ortho- or meta- substitution on the ring gave an increase in potency, while para- substitution was not accommodated in the active site. Incorporation of an amide at the 3-position of the aminoquinoline resulted in access to the S2' pocket.

Monosubstituted amides were more active than disubstituted derivatives. In the case of **153**, the N-cyclohexyl substitution was directed towards the S2' site while the methyl of the o-tolyl moiety was situated in the P1 site. Further optimization to improve pharmacokinetic properties led to compound **154** with a 3-chloro-2-pyridinyl 6-substituent. When a 60 mg/kg dose of compound **154** was administered subcutaneously to rats, a 42% reduction of cerebrospinal fluid A β levels was observed two hours post-dose. However, metabolic stability of this compound was less satisfactory as it exhibited high clearance in human and rat liver microsomes. Inhibitor **155**, with an adamantylamide moiety showed a K_i of 66 nM.³²¹

(j) Pyrrolidine-based Inhibitors

A high throughput screening of a library of compounds resulted in pyrrolidine hit **156** (Figure 68), with an IC₅₀ value of 240 μ M.³²² Optimization efforts led to derivative **157**, showing an IC₅₀ value of 29 nM. Model studies showed that the pyrrolidine nitrogen formed a bidentate hydrogen bonding network with the catalytic aspartic acid residues and the disubstituted piperidine substituent was situated in a pocket under the flap region of the enzyme. However, this compound was not selective over BACE2, showing an identical activity to that of BACE1. An X-ray fragment screening resulted in spiropyrrolidine fragment **158**.³²³ Optimization of this lead compound by substitution on the pyrrolidine provided compound **158**. The para nitrile substitution of the benzyloxy moiety was carried out to interact with Arg128 while the meta-substitution aimed to fill the S2' site.

(k) Macrocyclic Nonpeptide Inhibitors

Utilizing strategies similar to that of peptidomimetic macrocycles, a variety of nonpeptide macrocyclic inhibitors have been developed. Macrocycles allow for the bioactive conformation of an inhibitor to be stabilized, while still allowing for enough flexibility to fit to the active site of the enzyme. A high throughput screening resulted in compound **160** (Figure 69) with a K_i of 0.9 μ M.³²⁴ It was found that this hit binds in the active site in a hairpin shape. To constrain the inhibitor to the hairpin shape, macrocycle **161** was developed, which displayed an IC₅₀ of 5 nM. When tested in vivo, via I.V., intraperitoneal, or oral delivery, only trace amounts of compound **161** was found in the brain, suggesting it is subject to high levels of Pgp efflux. Other types of scaffolds, such as acyl guanidine and iminohydantoin have also been subjected to macrocyclization.³²⁵⁻³²⁹ Macrocyclic inhibitors **162** and **163** displayed potent BACE1 inhibitory activity.

(l) Miscellaneous Nonpeptide Scaffolds

A high throughput screening resulted in hit compound **164** (Figure 70) with an IC₅₀ value of 25 μ M.³³⁰ From this result, compound **165** was developed, showing an IC₅₀ value of 1.4 μ M. This compound showed more than 350-fold selectivity over cathepsin D and renin, and 97-fold selectivity over BACE2. X-ray crystallographic studies showed that **165** binds in the S1 to S4 sites and does not have any direct contact to the catalytic aspartic acid residues. Rather, a hydrogen bond is formed from the oxyacetamide nitrogen to the water molecule bound between the two aspartic acids. Piperazine derivative **166** displayed IC₅₀ values of 79 nM.³³¹ Modeling studies suggested that the amide nitrogen hydrogen bonds to Asp32 and

Asp228 while the rest of the molecule picks up hydrophobic interactions in the active site. Compound **166** had a cellular potency of 2.37 μM . Compound **167** which incorporates a coumarin moiety in the piperazine scaffold displayed an IC_{50} of 93 nM.³³²

Acetylcholinesterase inhibitor **168** (Figure 71) was identified as a lead compound.³³³ Lead optimization resulted in compound **169** with an IC_{50} of 99 nM. Molecular docking studies suggested the protonated nitrogen interacts with the catalytic aspartic acids while the N-benzyl moiety fits into either the S1 or S1' site. A tyramine hit was optimized to compound **170**, which picks up interactions in the S3 pocket via the para-tolyl substitution on the tyramine hit.³³⁴ Spirocyclic sulfonamide **171** showed a BACE1 IC_{50} of 20.9 μM .³³⁵ Substituted aryl derivative **172** showed improvement in potency to 100 nM. The ortho-alkoxy substitution on the phenolic moiety is thought to have intramolecular hydrogen bonds that interfere with Pgp efflux recognition. Subcutaneous 100 mg/kg and 300 mg/kg doses of **172** in wild type mice showed dose dependent reductions in brain and cerebrospinal fluid $\text{A}\beta_{40}$ levels three hours post dose.

8. Natural Products with BACE1 Inhibitory Activity

There are a variety of natural products isolated that have been shown to have BACE1 inhibitory activity. While most are unlikely to become drug candidates, elucidation of the structures of the compounds may provide insight into binding specificities and provide new scaffolds to explore more potent and selective BACE1 inhibitors. Epigallocatechin gallate, **173** (Figure 72) was isolated from green tea. It was shown to be a non-competitive inhibitor with an IC_{50} of 1.6 μM .³³⁶ The stereochemistry has no effect on activity. However, the pyrogallol group at the C2 position was essential for activity. Compound **174**, isolated from Smilax Rhizoma, was found to inhibit BACE1 with an IC_{50} of 4.2 μM . It is the first example of a stilbenoid with BACE1 activity. Kuwanon C, **175**, a flavonoid isolated from the stem bark of Morus lhou, is a noncompetitive inhibitor with an IC_{50} of 3.4 μM .³³⁷ Molecular modeling of **175** suggested the resorcinol moiety hydrogen bonds to Thr231, Thr329, and Asp228 while the prenyl groups form hydrophobic interactions in the active site. Compound **176**, extracted from the fruit of ficus benjamina var. nuda was found to be a moderate inhibitor of BACE1 with an IC_{50} of 45 μM .³³⁸ Biflavanoid **177** was extracted from cephalotaxus harringtonia var fastigiata. It showed an IC_{50} of 56 μM against BACE1.³³⁹

Synthetic derivatives of bergenin, derived from natural bergenin isolated from the Bergenia species, provided some modestly potent BACE1 inhibitors, such as **180** (Figure 36).³⁴⁰ Geraniin, **179**, was isolated from geranium thunbergii. It was found to have a BACE1 IC_{50} of 4.0 μM .³⁴¹ Loganin, **180** extracted from corni fructus was found to be a noncompetitive inhibitor of BACE1 with an IC_{50} of 55 μM .³⁴²

9. Nonpeptide Inhibitors from Computational Methods

Computational discovery of BACE1 inhibitors arises from high throughput screening of compound libraries. In silico screening is advantageous for its ability to narrow down large compound libraries to a smaller number of reliable hits, thus making the testing of these compounds much less resource dependent. In some studies, only a particular scaffold or

functionality is investigated, while in others, full libraries are scanned. Computational screening allows for lead compounds to be elucidated from large libraries of compounds with very little time and resource constraints. A screening of 300,000 molecules with at least one hydroxyl group afforded ten compounds, all with a phenylurea moiety.³⁴³ 32,000 phenylurea compounds were then screened, which led to commercially available compounds being purchased and assayed, resulting in compounds such as **181** (Figure 73), with an IC₅₀ of 57.8 μM. Two separate in silico screenings, one with 10,067 compounds and one with 306,022 compounds were performed. A total of 88 hits were found, many with a 1,3,5-triazine moiety.³⁴⁴ From these 88 hits, 10 were found to be active. Compounds such as **182** were discovered, with an IC₅₀ of 7.1 μM. Other screenings are performed with the intention of discovering new pharmacophores. A receptor based virtual screening of 280,000 compounds resulted in 42 hits.³⁴⁵ Of these, 15 were potential inhibitors including compound **183**. Using eHiTS software, a high throughput screening of 250,000 commercially available compounds resulted in the purchase of six compounds for assay.³⁴⁶ Compound **184** displayed an IC₅₀ of 2.4 μM. A docking study showed that inhibitor **184** binds in the active site in a planar conformation that is stabilized by an intramolecular hydrogen bond to the phenolic hydroxyl. Further, the para-tolyl amide hydrogen bonds to Asp228.

A receptor based screening of 280,000 compounds resulted in the purchase of 20 compounds for assay.³⁴⁷ Inhibitor **185** (Figure 74) was discovered in this study as a submicromolar inhibitor. Triazine **186** was identified as a 120 nM inhibitor of BACE1 via an in silico approach.³⁴⁸ Computational screening has also been utilized to identify new scaffolds that may be optimized to inhibitors. A virtual screening of two commercially available databases resulted in compounds such as **187**, all with a common structural motif responsible for the binding to the catalytic aspartic acid residues.³⁴⁹

9. Clinical Development of BACE1 Inhibitors

While no BACE1 inhibitors have been FDA approved to date, some have made it through various stages of clinical trials. CTS21166 was the first BACE1 inhibitor to pass Phase 1 clinical trials. Preclinically, it showed single nanomolar potency against BACE1 and decent oral bioavailability, brain penetration, and metabolic clearance. Toxicology studies found a tolerance that lent itself toward clinical development. In two Phase 1 trials, healthy volunteers received up to 225 mg intravenously or 200 mg orally. CTS21166 showed reduction of Aβ₄₀ levels up to 80% 4-8 hours post dose with sustained reduction up to 72 hours and displayed a human oral bioavailability of 40.5%.³⁵⁰

BACE1 inhibitor AZD3839 was designed and developed at AstraZeneca and selected for clinical development. The lead structure **188** (Figure 76) was identified by NMR-based fragment screening. Subsequent lead optimization and design of new structural classes through scaffold hopping approaches led to a series of potent BACE1 inhibitors **189-191** with isoindole structural template. One of the notable features of these inhibitors is that fluorine can be introduced on the aromatic rings to manipulate the pharmacological properties. Introduction of difluoromethyl group on the pyridine in inhibitor **191** led to fluoroderivative **192** (AZD3839).

The binding mode of AZD3839 was determined by X-ray structural studies of inhibitor and BACE1 complex (Figure 77). It showed that the inhibitor binds in a flap-open conformation of the enzyme. The catalytic aspartates form a network of hydrogen bonds with the amidine group. The phenyl ring nestles in the S1 subpocket while the pyrimidine ring projects toward the S3 pocket. The substituted pyridine ring fills in the S2' subpocket and the pyridine nitrogen forms a hydrogen bond with Trp76.

AstraZeneca recently announced that AZD3839 completed phase I clinical trials with healthy volunteers. A single oral dose of up to 300 mg showed rapid absorption of AZD3839 followed by rapid initial decline. $A\beta_{40}$ and $A\beta_{42}$ levels were decreased in a dose-dependent manner at the 300 mg dose, 57.8% for $A\beta_{40}$ compared to a 25.0% reduction in the placebo group, and 39.3% for $A\beta_{42}$ compared to a 7.56% reduction in the placebo group. No deaths or serious adverse effects were reported, however 31% of volunteers who received AZD3839 and 39% of volunteers who received the placebo reported mild side effects such as dizziness, headache, and orthostatic hypertension.³⁵¹

Another recent clinical BACE1 inhibitor is LY2811376. A fragment-based screening provided initial lead structure amino-benzothiazine **193** (Figure 78).³⁵² Subsequent deplanarizing of the aminothiazine provided inhibitor **194** with significant improvement in potency. Determination of X-ray structure of inhibitor **194** and BACE1 complex and subsequent structure-based optimization provided inhibitor **195** with inhibitor activity in a new single digit micromolar range. Introduction of fluorine to improve metabolic stability and improve log P resulted in inhibitor **196** (LY2811376) which was selected for clinical development. This inhibitor was shown to be safe and well tolerated in healthy human volunteers. After oral dosing of 30 or 90 mg of LY2811376P have been shown to have prominent and long-lasting $A\beta$ reductions in lumbar CSF.³⁵² The X-ray structure of inhibitor **196** and BACE1 complex (Figure 79) shows that the amino-thiazine forms a network of hydrogen bonds with the catalytic aspartates in a flap-open conformation of BACE1. The pyrimidine ring fills in the S3 and the difluorobenzene scaffold occupies the S1-S2 pocket.

BACE1 inhibitor MK-8931 was tested for safety and tolerability as well as pharmacokinetic and pharmacodynamics properties in moderate to mild symptomatic AD patients. Once daily oral doses of 12 mg, 40 mg, and 60 mg resulted in dose dependent reduction of $A\beta_{40}$ in the cerebrospinal fluid up to 57%, 79% and 84% respectively. No serious adverse events were reported, however mild to moderate side effects, including headache, dizziness, nausea, and vomiting were experienced in some cases.³⁵³

10. Conclusion

β -secretase (BACE1) continues to be an attractive drug design target for the treatment of Alzheimer's disease. This review outlines the evolution of a variety of structural chemotypes of β -secretase inhibitors that have been reported since 2000. These include, pseudo-peptide inhibitors, a range of peptidomimetic inhibitors and a variety of nonpeptide heterocyclic inhibitors. The determination of the X-ray structure of a mechanism-based inhibitor and BACE1 complex, coupled with previous medicinal chemistry experience with the design of renin and HIV-1 protease inhibitors led to structure-based design of potent peptidomimetic

BACE1 inhibitors. Many of these inhibitors exhibited impressive intrinsic potency. However, the emergence of an effective BACE1 inhibitor drug has not yet materialized due to a number of challenging issues. First of all, due to the location of β -secretase target in the brain, BACE1 inhibitors need to have access to the target CNS compartment. As a result, inhibitors are required to have low molecular weight, and reduced susceptibility to P-glycoprotein or other transporters to achieve effective blood-brain-barrier penetration. In addition, inhibitors need to have high selectivity over other aspartic acid proteases such as BACE2 and cathepsin D which show high active site homology with BACE1. Peptidomimetic BACE1 inhibitors have had high molecular weight and other drawbacks with BBB penetration.

To alleviate the issues related to high molecular weight and peptidomimetic native, massive high-throughput and fragment-based screening efforts led to the evolution of a number of structural classes of small molecule nonpeptide BACE1 inhibitor leads. Subsequent lead optimization provided a broad range of preclinical BACE1 inhibitors with promising pharmacological properties. In recent years, a few of these new classes of BACE1 inhibitors advanced to clinical development including inhibitor AZD3839 from AstraZeneca and LY2811376 from Eli Lilly. Also, Merck Research Laboratories has announced that MK8931 has advanced to phase IIa/b clinical development. Structure-based design led to the development of a variety of BACE1 inhibitors. Clinical development of CTS21166 was conducted by CoMentis and this inhibitor was shown to reduce human plasma A β . Continued efforts through structure-based design strive to meet the many and varied challenges presented by therapeutic inhibition of BACE1 target.

Acknowledgements

This research was supported by the National Institutes of Health. We would like to thank Dr. Jordan Tang (Oklahoma Medical Research Foundation) for our productive collaboration on BACE1 inhibitors. We also thank Dr. Kalapala Venkateswara Rao (Purdue University) for helpful discussions.

References

1. Selkoe DJ. *Physiol Rev.* 2001; 81:741–766. [PubMed: 11274343]
2. Sinha, S. *Aspartic Acid Proteases as Therapeutic Targets.* Ghosh, AK., editor. Vol. 45. Wiley-VCH; 2010. p. 393-412.
3. Selkoe DJ. *Nature.* 1999; 399:A23–A31. [PubMed: 10392577]
4. Selkoe DJ. *JAMA.* 2000; 283:1615–1617. [PubMed: 10735401]
5. Selkoe DJ. *Nature.* 1991; 354:432–433. [PubMed: 1684220]
6. Kang J, Lemaire HG, Unterbeck A, Salbaum JM, Masters CL, Grzeschik KH, Multhaup G, Beyreuther K, Muller-Hill B. *Nature.* 1987; 325:733–736. [PubMed: 2881207]
7. Selkoe DJ. *Annu Rev Cell Biol.* 1994; 10:373–403. [PubMed: 7888181]
8. Naslund J, Haroutunian V, Mohs R, Davis KL, Davies P, Greengard P, Buxbaum JD. *J Am Med Assoc.* 2000; 283:1571–1577.
9. Christie RH, Bacskai BJ, Zipfel WR, Williams RM, Kajdasz ST, Webb WW, Hyman BT. *The Journal of Neuroscience : the official journal of the Society for Neuroscience.* 2001; 21:858–864. [PubMed: 11157072]
10. Bussiere T, Friend PD, Sadeghi N, Wicinski B, Lin GI, Bouras C, Giannakopoulos P, Robakis NK, Morrison JH, Perl DP, Hof PR. *Neuroscience.* 2002; 112:75–91. [PubMed: 12044473]

11. Ohno M, Cole SL, Yasvoina M, Zhao J, Citron M, Berry R, Disterhoft JF, Vassar R. *Neurobiol Dis.* 2007; 26:134–145. [PubMed: 17258906]
12. Sinha S, Lieberburg I. *Proc Natl Acad Sci U S A.* 1999; 96:11049–11053. [PubMed: 10500121]
13. Daugherty BL, Green SA. *Traffic.* 2001; 2:908–916. [PubMed: 11737828]
14. Ishiura S, Tsukahara T, Tabira T, Sugita H. *FEBS Letters.* 1989; 257:388–392. [PubMed: 2573543]
15. Weidemann A, Konig G, Bunke D, Fischer P, Salbaum JM, Masters CL, Beyreuther K. *Cell.* 1989; 57:115–126. [PubMed: 2649245]
16. Yamazaki T, Koo EH, Selkoe DJ. *The Journal of neuroscience : the official journal of the Society for Neuroscience.* 1997; 17:1004–1010. [PubMed: 8994055]
17. Kandalepas PC, Sadleir KR, Eimer WA, Zhao J, Nicholson DA, Vassar R. *Acta Neuropathologica.* 2013; 126:329–352. [PubMed: 23820808]
18. Seubert P, Oltersdorf T, Lee MG, Barbour R, Blomquist C, Davis DL, Bryant K, Fritz LC, Galasko D, Thal LJ, et al. *Nature.* 1993; 361:260–263. [PubMed: 7678698]
19. Gralle M, Botelho MG, Wouters FS. *J Biol Chem.* 2009; 284:15016–15025. [PubMed: 19336403]
20. Haass C, Lemere C, Capell A, Citron M, Seubert P, Schenk D, Lannfelt L, Selkoe DJ. *Nature Medicine.* 1995; 1:1291–1296.
21. Mullan M, Crawford F, Axelman K, Houlden H, Lilius L, Winblad B, Lannfelt L. *Nature Genetics.* 1992; 1:345–347. [PubMed: 1302033]
22. Citron M, Vigo-Pelfrey C, Teplow DB, Miller C, Schenk D, Johnston J, Winblad B, Venizelos N, Lannfelt L, Selkoe DJ. *Proc Natl Acad Sci USA.* 1994; 91:11993–11997. [PubMed: 7991571]
23. Kumar-Singh S. *Human Molecular Genetics.* 2000; 9:2589–2598. [PubMed: 11063718]
24. Ancolio K, Dumanchin C, Barelli H, Warter JM, Brice A, Campion D, Frebourg T, Checler F. *Proceedings of the National Academy of Sciences.* 1999; 96:4119–4124.
25. Eckman CB, Mehta ND, Crook R, Perez-tur J, Prihar G, Pfeiffer E, Graff-Radford N, Hinder P, Yager D, Zenk B, Refolo LM, Mihail Prada C, Younkin SG, Hutton M, Hardy J. *Human Molecular Genetics.* 1997; 6:2087–2089. [PubMed: 9328472]
26. Murrell J, Farlow M, Ghetti B, Benson M. *Science.* 1991; 254:97–99. [PubMed: 1925564]
27. Chartier-Harlin MC, Crawford F, Houlden H, Warren A, Hughes D, Fidani L, Goate A, Rossor M, Roques P, Hardy J, et al. *Nature.* 1991; 353:844–846. [PubMed: 1944558]
28. Goate A, Chartier-Harlin MC, Mullan M, Brown J, Crawford F, Fidani L, Giuffra L, Haynes A, Irving N, James L, et al. *Nature.* 1991; 349:704–706. [PubMed: 1671712]
29. Murrell JR. *Archives of Neurology.* 2000; 57:885. [PubMed: 10867787]
30. Kwok JBJ, Li Q-X, Hallupp M, Whyte S, Ames D, Beyreuther K, Masters CL, Schofield PR. *Annals of Neurology.* 2000; 47:249–253. [PubMed: 10665499]
31. Van Broeckhoven C, Haan J, Bakker E, Hardy J, Van Hul W, Wehnert A, Vegter-Van der Vlis M, Roos R. *Science.* 1990; 248:1120–1122. [PubMed: 1971458]
32. Hendriks L, van Duijn CM, Cras P, Cruts M, Van Hul W, van Harskamp F, Warren A, McInnis MG, Antonarakis SE, Martin JJ, et al. *Nat Genet.* 1992; 1:218–221. [PubMed: 1303239]
33. Hardy J, Selkoe DJ. *Science.* 2002; 297:353–356. [PubMed: 12130773]
34. Selkoe DJ. *Science.* 2002; 298:789–791. [PubMed: 12399581]
35. Buxbaum J, Liu K, Luo Y, Slack JL, Stocking KL, Peschon JJ, Johnson RS, Castner BJ, Cerretti DP, Black RA. *The Journal of Biological Chemistry.* 1998; 273:27765–27767. [PubMed: 9774383]
36. Lammich S, Kojro E, Postina R, Gilbert S, Pfeiffer R, Jasionowski M, Haass C, Fahrenholz F. *Proc Natl Acad Sci U S A.* 1999; 96:3922–3927. [PubMed: 10097139]
37. Wolfe MS, Xia W, Ostaszewski BL, Diehl TS, Kimberly WT, Selkoe DJ. *Nature.* 1999; 398:513–517. [PubMed: 10206644]
38. Haass C, De Strooper B. *Science.* 1999; 286:916–919. [PubMed: 10542139]
39. Haass C. *EMBO J.* 2004; 23:483–488. [PubMed: 14749724]
40. Esler WP, Kimberly WT, Ostaszewski BL, Diehl TS, Moore CL, Tsai JY, Rahmati T, Xia W, Selkoe DJ, Wolfe MS. *Nat Cell Biol.* 2000; 2:428–434. [PubMed: 10878808]

41. Diment S, Leech MS, Stahl PD. *Journal of Biological Chemistry*. 1988; 263:6901–6907. [PubMed: 3360812]
42. Saftig P, Peters C, von Figura K, Craessaerts K, Van Leuven F, De Strooper B. *The Journal of Biological Chemistry*. 1996; 271:27241–27244. [PubMed: 8910296]
43. Thompson A, Grueninger-Leitch F, Huber G, Malherbe P. *Molecular Brain Research*. 1997; 48:206–014. [PubMed: 9332717]
44. Yan R, Bienkowski MJ, Shuck ME, Miao H, Tory MC, Pauley AM, Brashier JR, Stratman NC, Mathews WR, Buhl AE, Carter DB, Tomasselli AG, Parodi LA, Henrikson RL, Gurney ME. *Nature*. 1999; 402:533–537. [PubMed: 10591213]
45. Nelson RB, Siman R, Iqbal MA, Potter H. *J Neurochem*. 1993; 61:567–577. [PubMed: 8336143]
46. Sahasrabudhe SR, Brown AM, Hulmes JD, Jacobsen JS, Vitek MP, Blume AJ, Sonnenberg JL. *J Biol Chem*. 1993; 268:16699–16705. [PubMed: 8344949]
47. Bennett BD, Babu-Khan S, Loeloff R, Louis JC, Curran E, Citron M, Vassar R. *J Biol Chem*. 2000; 275:20647–20651. [PubMed: 10749877]
48. Huber AB, Brosamle C, Mechler H, Huber G. *Brain Res*. 1999; 837:193–202. [PubMed: 10434003]
49. Hussain I, Powell D, Howlett DR, Tew DG, Meek TD, Chapman C, Gloger IS, Murphy KE, Southan CD, Ryan DM, Smith TS, Simmons DL, Walsh FS, Dingwall C, Christie G. *Molecular and Cellular Neuroscience*. 1999; 14:419–427. [PubMed: 10656250]
50. Vassar R, Bennett BD, Babu-Khan S, Kahn S, Mendiaz EA, Denis P, Teplow DB, Ross S, Amarante P, Loeloff R, Luo Y, Fisher S, Fuller J, Edenson S, Lile J, Jarosinski MA, Biere AL, Curran E, Burgess T, Louis JC, Collins F, Treanor J, Rogers G, Citron M. *Science*. 1999; 286:735–741. [PubMed: 10531052]
51. Sinha S, Anderson JP, Barbour R, Basi GS, Caccavello R, Davis D, Doan M, Dovey HF, Frigon N, Hong J, Jacobson-Croak K, Jewett N, Keim P, Knops J, Lieberburg I, Power M, Tan H, Tatsuno G, Tung J, Schenk D, Seubert P, Suomensaaari SM, Wang S, Walker D, Zhao J, McConlogue L, John V. *Nature*. 1999; 402:537–540. [PubMed: 10591214]
52. Lin X, Koelsch G, Wu S, Downs D, Dashti A, Tang J. *Proc Natl Acad Sci U S A*. 2000; 97:1456–1460. [PubMed: 10677483]
53. Benjannet S, Elagoz A, Wickham L, Mamarbachi M, Munzer JS, Basak A, Lazure C, Cromlish JA, Sisodia S, Checler F, Chretien M, Seidah NG. *J Biol Chem*. 2001; 276:10879–10887. [PubMed: 11152688]
54. Haniu M, Denis P, Young Y, Mendiaz EA, Fuller J, Hui JO, Bennett BD, Kahn S, Ross S, Burgess T, Katta V, Rogers G, Vassar R, Citron M. *J Biol Chem*. 2000; 275:21099–21106. [PubMed: 10887202]
55. Shi XP, Chen E, Yin KC, Na S, Garsky VM, Lai MT, Li YM, Platchek M, Register RB, Sardana MK, Tang MJ, Thiebeau J, Wood T, Shafer JA, Gardell SJ. *J Biol Chem*. 2001; 276:10366–10373. [PubMed: 11266439]
56. Ermolieff J, Loy JA, Koelsch G, Tang J. *Biochemistry*. 2000; 39:12450–12456. [PubMed: 11015226]
57. Huse JT, Pijak DS, Leslie GJ, Lee VM, Doms RW. *J Biol Chem*. 2000; 275:33729–33737. [PubMed: 10924510]
58. Fischer F, Molinari M, Bodendorf U, Paganetti P. *J Neurochem*. 2002; 80:1079–1088. [PubMed: 11953458]
59. Koo EH, Squazzo SL. *J Biol Chem*. 1994; 269:17386–17389. [PubMed: 8021238]
60. Hong L, Tang J. *Biochemistry*. 2004; 43:4689–4695. [PubMed: 15096037]
61. Vassar R, Kovacs DM, Yan R, Wong PC. *The Journal of neuroscience : the official journal of the Society for Neuroscience*. 2009; 29:12787–12794. [PubMed: 19828790]
62. Vassar R. *Journal of Molecular Neuroscience*. 2001; 17:157–170. [PubMed: 11816789]
63. Seiffert D, Bradley JD, Rominger CM, Rominger DH, Yang F, Meredith JE Jr, Wang Q, Roach AH, Thompson LA, Spitz SM, Higaki JN, Prakash SR, Combs AP, Copeland RA, Arneric SP, Hartig PR, Robertson DW, Cordell B, Stern AM, Olson RE, Zaczek R. *J Biol Chem*. 2000; 275:34086–34091. [PubMed: 10915801]

64. Kamnetz F, Tomita T, Hsieh H, Seabrook G, Borchelt D, Iwatsubo T, Sisodia S, Malinow R. *Neuron*. 2003; 37:925–937. [PubMed: 12670422]
65. Willem M, Garratt AN, Novak B, Citron M, Kaufmann S, Rittger A, DeStrooper B, Saftig P, Birchmeier C, Haass C. *Science*. 2006; 314:664–666. [PubMed: 16990514]
66. Luo Y, Bolon B, Kahn S, Bennett BD, Babu-Khan S, Denis P, Fan W, Kha H, Zhang J, Gong Y, Martin L, Louis JC, Yan Q, Richards WG, Citron M, Vassar R. *Nature Neuroscience*. 2001; 4:231–232. [PubMed: 11224535]
67. Roberds SL, Anderson JP, Basi G, Bienkowski MJ, Branstetter DG, Chen KS, Freedman SB, Frigon NL, Games D, Hu K, Johnson-Wood K, Keapenman KE, Kawabe TT, Kola I, Kuehn R, Lee M, Liu W, Motter R, Nichols NF, Power M, Robertson DW, Schenk D, Schoor M, Shopp GM, Shuck ME, Sinha S, Svensson KA, Tatsuno G, Tintrup H, Wijsman J, Wright S, McConlogue L. *Human Molecular Genetics*. 2001; 10:1317–1324. [PubMed: 11406613]
68. Nishitomi K, Sakaguchi G, Horikoshi Y, Gray AJ, Maeda M, Hirata-Fukae C, Becker AG, Hosono M, Sakaguchi I, Minami SS, Nakajima Y, Li HF, Takeyama C, Kihara T, Ota A, Wong PC, Aisen PS, Kato A, Kinoshita N, Matsuoka Y. *J Neurochem*. 2006; 99:1555–1563. [PubMed: 17083447]
69. Ohno M, Sametsky EA, Younkin LH, Oakley H, Younkin SG, Citron M, Vassar R, Disterhoft JF. *Neuron*. 2004; 41:27–33. [PubMed: 14715132]
70. Ghosh AK, Shin DW, Downs D, Koelsch G, Lin XL, Ermolieff J, Tang J. *Journal of the American Chemical Society*. 2000; 122:3522–3523.
71. Hong L, Koelsch G, Lin X, Wu S, Terzyan S, Ghosh AK, Zhang XC, Tang J. *Science*. 2000; 290:150–153. [PubMed: 11021803]
72. Hong L, Turner RT 3rd, Koelsch G, Shin D, Ghosh AK, Tang J. *Biochemistry*. 2002; 41:10963–10967. [PubMed: 12206667]
73. Turner RT 3rd, Koelsch G, Hong L, Castanheira P, Ermolieff J, Ghosh AK, Tang J. *Biochemistry*. 2001; 40:10001–10006. [PubMed: 11513577]
74. Gruninger-Leitch F, Schlatter D, Kung E, Nelbock P, Dobeli H. *J Biol Chem*. 2002; 277:4687–4693. [PubMed: 11741910]
75. Farzan M, Schnitzler CE, Vasilieva N, Leung D, Choe H. *PNAS*. 2000; 97:9712–9717. [PubMed: 10931940]
76. Cai H, Wang Y, McCarthy D, Wen H, Borchelt DR, Price DL, Wong PC. *Nature Neuroscience*. 2001; 4:233–234. [PubMed: 11224536]
77. Turner RT, Loy JA, Nguyen C, Devasamudram T, Ghosh AK, Koelsch G, Tang J. *Biochemistry*. 2002; 41:8742–8746. [PubMed: 12093293]
78. Turner RT 3rd, Hong L, Koelsch G, Ghosh AK, Tang J. *Biochemistry*. 2005; 44:105–112. [PubMed: 15628850]
79. Benes P, Vetvicka V, Fusek M. *Crit Rev Oncol Hematol*. 2008; 68:12–28. [PubMed: 18396408]
80. Koike M, Nakanishi H, Saftig P, Ezaki J, Isahara K, Ohsawa Y, Schulz-Schaeffer W, Watanabe T, Waguri S, Kametaka S, Shibata M, Yamamoto K, Kominami E, Peters C, von Figura K, Uchiyama Y. *The Journal of neuroscience : the official journal of the Society for Neuroscience*. 2000; 20:6898–6906. [PubMed: 10995834]
81. Baechle D, Flad T, Cansier A, Steffen H, Schittek B, Tolson J, Herrmann T, Dihazi H, Beck A, Mueller GA, Mueller M, Stevanovic S, Garbe C, Mueller CA, Kalbacher H. *Journal of Biological Chemistry*. 2006; 281:5406–5415. [PubMed: 16354654]
82. Hong L, Tang J. *Biochemistry*. 2004; 43:4689–4695. [PubMed: 15096037]
83. Chang WP, Koelsch G, Wong S, Downs D, Da H, Weerasena V, Gordon B, Devasamudram T, Bilcer G, Ghosh AK, Tang J. *J Neurochem*. 2004; 89:1409–1416. [PubMed: 15189343]
84. Rajendran L, Schneider A, Schlechtingen G, Weidlich S, Ries J, Braxmeier T, Schwille P, Schulz JB, Schroeder C, Simons M, Jennings G, Knolker HJ, Simons K. *Science*. 2008; 320:520–523. [PubMed: 18436784]
85. Meredith JE Jr, Thompson LA, Toyn JH, Marcin L, Barten DM, Marcinkeviciene J, Kopcho L, Kim Y, Lin A, Guss V, Burton C, Iben L, Polson C, Cantone J, Ford M, Drexler D, Fiedler T, Lentz KA, Grace JE Jr, Kolb J, Corsa J, Pierdomenico M, Jones K, Olson RE, Macor JE, Albright CF. *J Pharmacol Exp Ther*. 2008; 326:502–513. [PubMed: 18499745]

86. Laird FM, Cai H, Savonenko AV, Farah MH, He K, Melnikova T, Wen H, Chiang HC, Xu G, Koliatsos VE, Borchelt DR, Price DL, Lee HK, Wong PC. *The Journal of neuroscience : the official journal of the Society for Neuroscience*. 2005; 25:11693–11709. [PubMed: 16354928]
87. Zhou L, Barao S, Laga M, Bockstael K, Borgers M, Gijzen H, Annaert W, Moechars D, Mercken M, Gevaert K, De Strooper B. *J Biol Chem*. 2012; 287:25927–25940. [PubMed: 22692213]
88. Kuhn PH, Koroniak K, Hogl S, Colombo A, Zeitschel U, Willem M, Volbracht C, Schepers U, Imhof A, Hoffmeister A, Haass C, Rossner S, Brase S, Lichtenthaler SF. *EMBO J*. 2012; 31:3157–3168. [PubMed: 22728825]
89. Hu X, Hicks CW, He W, Wong P, Macklin WB, Trapp BD, Yan R. *Nat Neurosci*. 2006; 9:1520–1525. [PubMed: 17099708]
90. Hu X, Zhou X, He W, Yang J, Xiong W, Wong P, Wilson CG, Yan R. *The Journal of neuroscience : the official journal of the Society for Neuroscience*. 2010; 30:8819–8829. [PubMed: 20592204]
91. Kobayashi D, Zeller M, Cole T, Buttini M, McConlogue L, Sinha S, Freedman S, Morris RG, Chen KS. *Neurobiol Aging*. 2008; 29:861–873. [PubMed: 17331621]
92. Hitt BD, Jaramillo TC, Chetkovich DM, Vassar R. *Molecular Neurodegeneration*. 2012; 5:31. [PubMed: 20731874]
93. Savonenko AV, Melnikova T, Laird FM, Stewart KA, Price DL, Wong PC. *Proc Natl Acad Sci U S A*. 2008; 105:5585–5590. [PubMed: 18385378]
94. Hitt B, Riordan SM, Kukreja L, Eimer WA, Rajapaksha TW, Vassar R. *J Biol Chem*. 2012; 287:38408–38425. [PubMed: 22988240]
95. Rajapaksha TW, Eimer WA, Bozza TC, Vassar R. *Molecular Neurodegeneration*. 2011; 6:88. [PubMed: 22204380]
96. Cao L, Rickenbacher GT, Rodriguez S, Moulia TW, Albers MW. *Sci Rep*. 2012; 2:231. [PubMed: 22355745]
97. Cai J, Qi X, Kociok N, Skosyrski S, Emilio A, Ruan Q, Han S, Liu L, Chen Z, Bowes Rickman C, Golde T, Grant MB, Saftig P, Serneels L, de Strooper B, Joussem AM, Boulton ME. *EMBO Mol Med*. 2012; 4:980–991. [PubMed: 22903875]
98. Luna S, Cameron DJ, Ethell DW. *PLoS One*. 2013; 8:e75052. [PubMed: 24040383]
99. John, V.; Tung, J.; Fang, L.; Mamo, SS. *Int. Pat.* 2000. WO2000077030
100. Peters, S.; Fuchs, K.; Eickmeier, C.; Stransky, W.; Dorner-Ciossek, C.; Handschuh, S.; Nar, H.; Klinder, K.; Kostka, M. *US Pat.* 2007. US7238774
101. Hu J, Cwi CL, Smiley DL, Timm D, Erickson JA, McGee JE, Yang HC, Mendel D, May PC, Shapiro M, McCarthy JR. *Bioorg Med Chem Lett*. 2003; 13:4335–4339. [PubMed: 14643321]
102. Dorner-Ciossek, C.; Fuchs, K.; Handschuh, S.; Kostka, M.; Peters, S.; Haass, C. *Int. Pat.* 2004. WO2004101603
103. Peters, S.; Fuchs, K.; Eickmeier, C.; Stransky, W.; Dorner-Ciossek, C.; Handschuh, S.; Nar, H.; Klinder, K.; Kostka, M. *US Pat.* 2006. US20060100158
104. Peters, S.; Fuchs, K.; Eickmeier, C.; Stransky, W.; Dorner-Ciossek, C.; Handschuh, S.; Nar, H.; Klinder, K.; Kostka, M. *Int. Pat.* 2006. WO2006050861
105. Hu B, Fan KY, Bridges K, Chopra R, Lovering F, Cole D, Zhou P, Ellingboe J, Jin G, Cowling R, Bard J. *Bioorg Med Chem Lett*. 2004; 14:3457–3460. [PubMed: 15177452]
106. Schostarez, HJ.; Chrusciel, RA. *Int. Pat.* 2003. WO2003006021
107. Kiso, Y. *US Pat.* 2007. US7312188
108. Shuto D, Kasai S, Kimura T, Liu P, Hidaka K, Hamada T, Shibakawa S, Hayashi Y, Hattori C, Szabo B, Ishiura S, Kiso Y. *Bioorg Med Chem Lett*. 2003; 13:4273–4276. [PubMed: 14643307]
109. Kimura T, Shuto D, Kasai S, Liu P, Hidaka K, Hamada T, Hayashi Y, Hattori C, Asai M, Kitazume S, Saido TC, Ishiura S, Kiso Y. *Bioorg Med Chem Lett*. 2004; 14:1527–1531. [PubMed: 15006396]
110. Kimura T, Shuto D, Hamada Y, Igawa N, Kasai S, Liu P, Hidaka K, Hamada T, Hayashi Y, Kiso Y. *Bioorg Med Chem Lett*. 2005; 15:211–215. [PubMed: 15582441]
111. Asai M, Hattori C, Iwata N, Saido TC, Sasagawa N, Szabo B, Hashimoto Y, Maruyama K, Tanuma S, Kiso Y, Ishiura S. *J Neurochem*. 2006; 96:533–540. [PubMed: 16336629]

112. Kimura T, Hamada Y, Stochaj M, Ikari H, Nagamine A, Abdel-Rahman H, Igawa N, Hidaka K, Nguyen JT, Saito K, Hayashi Y, Kiso Y. *Bioorg Med Chem Lett*. 2006; 16:2380–2386. [PubMed: 16481167]
113. Hamada Y, Igawa N, Ikari H, Ziora Z, Nguyen JT, Yamani A, Hidaka K, Kimura T, Saito K, Hayashi Y, Ebina M, Ishiura S, Kiso Y. *Bioorg Med Chem Lett*. 2006; 16:4354–4359. [PubMed: 16757166]
114. Ziora Z, Kasai S, Hidaka K, Nagamine A, Kimura T, Hayashi Y, Kiso Y. *Bioorg Med Chem Lett*. 2007; 17:1629–1633. [PubMed: 17251016]
115. Hamada Y, Abdel-Rahman H, Yamani A, Nguyen JT, Stochaj M, Hidaka K, Kimura T, Hayashi Y, Saito K, Ishiura S, Kiso Y. *Bioorg Med Chem Lett*. 2008; 18:1649–1653. [PubMed: 18249539]
116. Hom RK, Fang LY, Mamo S, Tung JS, Guinn AC, Walker DE, Davis DL, Gailunas AF, Thorsett ED, Sinha S, Knops JE, Jewett NE, Anderson JP, John V. *J Med Chem*. 2003; 46:1799–1802. [PubMed: 12723942]
117. Back M, Nyhlen J, Kvarnstrom I, Appelgren S, Borkakoti N, Jansson K, Lindberg J, Nystrom S, Hallberg A, Rosenquist A, Samuelsson B. *Bioorg Med Chem*. 2008; 16:9471–9486. [PubMed: 18842420]
118. Ekegren JK, Unge T, Safa MZ, Wallberg H, Samuelsson B, Hallberg A. *J Med Chem*. 2005; 48:8098–8102. [PubMed: 16335934]
119. Wangsell F, Russo F, Savmarker J, Rosenquist A, Samuelsson B, Larhed M. *Bioorg Med Chem Lett*. 2009; 19:4711–4714. [PubMed: 19576765]
120. Russo F, Wångsell F, Sävmarker J, Jacobsson M, Larhed M. *Tetrahedron*. 2009; 65:10047–10059.
121. Wangsell F, Nordeman P, Savmarker J, Emanuelsson R, Jansson K, Lindberg J, Rosenquist A, Samuelsson B, Larhed M. *Bioorg Med Chem*. 2011; 19:145–155. [PubMed: 21183353]
122. Tang, J.; Hong, L.; Ghosh, AK. *Int. Pat.* 2001. WO2001000665
123. Ghosh, AK.; Tang, J.; Bilcer, G.; Chang, W.; Hong, L.; Koelsch, GE.; Loy, JA.; Turner, RT., 3rd; Devasamudram, T. *US Pat.* 2004. US20040121947
124. Tang, J.; Ghosh, AK. *US Pat.* 2007. US7244708
125. Tang, J.; Hong, L.; Ghosh, AK. *Aspartic Acid Proteases as Therapeutic Targets*. Ghosh, AK., editor. Vol. 45. Wiley-VCH; 2010. p. 413-440.
126. Ghosh AK, Bilcer G, Harwood C, Kawahama R, Shin D, Hussain KA, Hong L, Loy JA, Nguyen C, Koelsch G, Ermolieff J, Tang J. *J Med Chem*. 2001; 44:2865–2868. [PubMed: 11520194]
127. Ghosh, AK.; Tang, J.; Bilcer, G.; Chang, W.; Hong, L.; Koelsch, G.; Loy, J.; Turner, I.; R. T.. *Int. Pat.* 2003. WO2003039454
128. Ghosh, AK.; Lei, H.; Devasamudram, T.; Liu, C.; Tang, J.; Bilcer, G. *US Pat.* 2008. US7335632
129. Ghosh AK, Kumaragurubaran N, Hong L, Lei H, Hussain KA, Liu CF, Devasamudram T, Weerasena V, Turner R, Koelsch G, Bilcer G, Tang J. *J Am Chem Soc*. 2006; 128:5310–5311. [PubMed: 16620080]
130. Ghosh, A.; Lei, H.; Devasamudram, T.; Lui, C.; Tang, J.; Bilcer, G. *Int. Pat.* 2006. WO2006034296
131. Ghosh AK, Kumaragurubaran N, Hong L, Kulkarni SS, Xu XM, Chang WP, Weerasena V, Turner R, Koelsch G, Bilcer G, Tang J. *Journal of Medicinal Chemistry*. 2007; 50:2399–2407. [PubMed: 17432843]
132. Ghosh, AK.; Lei, H.; Devasamudram, T.; Liu, C.; Tang, J.; Bilcer, G. *Int. Pat.* 2006. WO2006034277
133. Chen SH, Lamar J, Guo D, Kohn T, Yang HC, McGee J, Timm D, Erickson J, Yip Y, May P, McCarthy J. *Bioorg Med Chem Lett*. 2004; 14:245–250. [PubMed: 14684336]
134. Brady SF, Singh S, Crouthamel MC, Holloway MK, Coburn CA, Garsky VM, Bogusky M, Pennington MW, Vacca JP, Hazuda D, Lai MT. *Bioorg Med Chem Lett*. 2004; 14:601–604. [PubMed: 14741251]
135. Faller, A.; Milner, PH.; Ward, JG. *Int. Pat.* 2003. WO2003045903

136. Faller, A.; Macpherson, DT.; Milner, PH.; Stanway, SJ.; Trouw, LS. *Int. Pat.* 2003. WO2003045913
137. Demont, EH.; Redshaw, S.; Walter, DS. *Int. Pat.* 2004. WO2004111022
138. Hom RK, Gailunas AF, Mamo S, Fang LY, Tung JS, Walker DE, Davis D, Thorsett ED, Jewett NE, Moon JB, John V. *J Med Chem.* 2004; 47:158–164. [PubMed: 14695829]
139. Hom, R.; Mamo, S.; Tung, J.; Gailunas, A.; John, V.; Fang, L. *US Pat.* 2003. US20030013881
140. Kvarnstrom, I.; Wangsell, F.; Rosenquist, A.; Samuelsson, B.; Sahlberg, C.; Sund, C.; Belda, O.; Ivanov, V.; Oden, L.; Noren, R. *Int. Pat.* 2008. WO2008119772
141. Meredith JA, Bjorklund C, Adolfsson H, Jansson K, Hallberg A, Rosenquist A, Samuelsson B. *European Journal of Medicinal Chemistry.* 2010; 45:542–554. [PubMed: 19995674]
142. Sandgren V, Back M, Kvarnstrom I, Dahlgren A. *The Open Medicinal Chemistry Journal.* 2013; 7:1–15. [PubMed: 23585822]
143. Kvarnstrom, I.; Back, M.; Sandgren, V.; Oscarson, S.; Bjorklund, C.; Rosenquist, A.; Samuelsson, B.; Johansson, PO.; Dorange, I. *Int. Pat.* 2008. WO2008119773
144. Tamamura H, Kato T, Otaka A, Fujii N. *Organic & Biomolecular Chemistry.* 2003; 1:2468. [PubMed: 12956063]
145. Stachel SJ, Coburn CA, Steele TG, Jones KG, Loutzenhiser EF, Gregro AR, Rajapakse HA, Lai MT, Crouthamel MC, Xu M, Tugusheva K, Lineberger JE, Pietrak BL, Espeseth AS, Shi XP, Chen-Dodson E, Holloway MK, Munshi S, Simon AJ, Kuo L, Vacca JP. *J Med Chem.* 2004; 47:6447–6450. [PubMed: 15588077]
146. Stachel SJ, Coburn CA, Steele TG, Crouthamel MC, Pietrak BL, Lai MT, Holloway MK, Munshi SK, Graham SL, Vacca JP. *Bioorg Med Chem Lett.* 2006; 16:641–644. [PubMed: 16263281]
147. Clarke B, Demont E, Dingwall C, Dunsdon R, Faller A, Hawkins J, Hussain I, MacPherson D, Maile G, Matico R, Milner P, Mosley J, Naylor A, O'Brien A, Redshaw S, Riddell D, Rowland P, Soleil V, Smith KJ, Stanway S, Stemp G, Sweitzer S, Theobald P, Vesey D, Walter DS, Ward J, Wayne G. *Bioorg Med Chem Lett.* 2008; 18:1011–1016. [PubMed: 18171614]
148. Clarke B, Demont E, Dingwall C, Dunsdon R, Faller A, Hawkins J, Hussain I, MacPherson D, Maile G, Matico R, Milner P, Mosley J, Naylor A, O'Brien A, Redshaw S, Riddell D, Rowland P, Soleil V, Smith KJ, Stanway S, Stemp G, Sweitzer S, Theobald P, Vesey D, Walter DS, Ward J, Wayne G. *Bioorg Med Chem Lett.* 2008; 18:1017–1021. [PubMed: 18166458]
149. Beswick P, Charrier N, Clarke B, Demont E, Dingwall C, Dunsdon R, Faller A, Gleave R, Hawkins J, Hussain I, Johnson CN, MacPherson D, Maile G, Matico R, Milner P, Mosley J, Naylor A, O'Brien A, Redshaw S, Riddell D, Rowland P, Skidmore J, Soleil V, Smith KJ, Stanway S, Stemp G, Stuart A, Sweitzer S, Theobald P, Vesey D, Walter DS, Ward J, Wayne G. *Bioorg Med Chem Lett.* 2008; 18:1022–1026. [PubMed: 18171615]
150. Demont, EH.; Redshaw, S.; Walter, DS. *Int. Pat.* 2004. WO2004080376
151. Demont, EH.; Faller, A.; Macpherson, DT.; Milner, PH.; Naylor, A.; Redshaw, S.; Stanway, SJ.; Vesey, DR.; Walter, DS. *Int. Pat.* 2004. WO2004050619
152. Demont, EH.; Redshaw, S.; Walter, DS. *Int. Pat.* 2005. WO2005113525
153. Charrier N, Clarke B, Cutler L, Demont E, Dingwall C, Dunsdon R, East P, Hawkins J, Howes C, Hussain I, Jeffrey P, Maile G, Matico R, Mosley J, Naylor A, O'Brien A, Redshaw S, Rowland P, Soleil V, Smith KJ, Sweitzer S, Theobald P, Vesey D, Walter DS, Wayne G. *J Med Chem.* 2008; 51:3313–3317. [PubMed: 18457381]
154. Charrier N, Clarke B, Demont E, Dingwall C, Dunsdon R, Hawkins J, Hubbard J, Hussain I, Maile G, Matico R, Mosley J, Naylor A, O'Brien A, Redshaw S, Rowland P, Soleil V, Smith KJ, Sweitzer S, Theobald P, Vesey D, Walter DS, Wayne G. *Bioorg Med Chem Lett.* 2009; 19:3669–3673. [PubMed: 19477642]
155. Charrier N, Clarke B, Cutler L, Demont E, Dingwall C, Dunsdon R, Hawkins J, Howes C, Hubbard J, Hussain I, Maile G, Matico R, Mosley J, Naylor A, O'Brien A, Redshaw S, Rowland P, Soleil V, Smith KJ, Sweitzer S, Theobald P, Vesey D, Walter DS, Wayne G. *Bioorg Med Chem Lett.* 2009; 19:3674–3678. [PubMed: 19406640]
156. Charrier N, Clarke B, Cutler L, Demont E, Dingwall C, Dunsdon R, Hawkins J, Howes C, Hubbard J, Hussain I, Maile G, Matico R, Mosley J, Naylor A, O'Brien A, Redshaw S, Rowland

- P, Soleil V, Smith KJ, Sweitzer S, Theobald P, Vesey D, Walter DS, Wayne G. *Bioorg Med Chem Lett.* 2009; 19:3664–3668. [PubMed: 19428244]
157. Demont, EH.; Redshaw, S.; Walter, DS. *Int. Pat.* 2004. WO2004094430
158. Redshaw, S.; Demont, EH.; Walter, DS. *Int. Pat.* 2005. WO2005058915
159. Demont, EH.; Redshaw, S.; Walter, DS. *Int. Pat.* 2006. WO2006103088
160. Ghosh AK, Kumaragurubaran N, Hong L, Kulkarni S, Xu X, Miller HB, Reddy DS, Weerasena V, Turner R, Chang W, Koelsch G, Tang J. *Bioorg Med Chem Lett.* 2008; 18:1031–1036. [PubMed: 18180160]
161. Chang WP, Huang X, Downs D, Cirrito JR, Koelsch G, Holtzman DM, Ghosh AK, Tang J. *FASEB J.* 2011; 25:775–784. [PubMed: 21059748]
162. Bueno Melendo, AB.; Chen, SH.; Erickson, JA.; Gonzalez-Garcia, MR.; Guo, D.; Marcos Llorente, A.; McCarthy, JR.; Shepherd, TA.; Sheehan, SM.; Yip, YYM. *Int. Pat.* 2005. WO2005108391
163. Cumming, JN.; Iserloh, U.; Stamford, A.; Strickland, C.; Voigt, JH.; Wu, Y.; Huang, Y.; Xia, Y.; Chackalamannil, S.; Guo, T.; Hobbs, DW.; Le, TXH.; L. J. F.; Saionz, KW.; Babu, SD. *Int. Pat.* 2005. WO2005016876
164. Xue, Q.; Albrecht, BK.; Andersen, DL.; Bartberger, M.; Brown, J.; Brown, R.; Chaffee, SC.; Cheng, Y.; Croghan, M.; Graceffa, R.; Harried, S.; Hitchcock, S.; Hungate, R.; Judd, T.; Kaller, M.; Kreiman, C.; La, D.; Lopez, P.; Masse, CE.; Monenschein, H.; Nguyen, T.; Nixey, T.; Patel, VF.; Pennington, L.; Weiss, M.; Yang, B.; Zhong, W. *Int. Pat.* 2007. WO2007061930
165. Zhong, W.; Hitchcock, S.; Patel, VF.; Croghan, M.; Dineen, T.; Harried, S.; Horne, D.; Judd, T.; Kaller, M.; Kreiman, C.; Lopez, P.; Monenschein, H.; Nguyen, T.; Weiss, M.; Xue, Q.; Yang, B. *Int. Pat.* 2008. WO2008147547
166. Ghosh, AK.; Liu, CF.; Devasamudram, T.; Lei, H.; Swanson, LM.; Ankala, SV.; Lilly, JC.; Bilcer, GM. *Int. Pat.* 2009. WO2009015369
167. Freskos JN, Fobian YM, Benson TE, Moon JB, Bienkowski MJ, Brown DL, Emmons TL, Heintz R, Laborde A, McDonald JJ, Mischke BV, Molyneaux JM, Mullins PB, Bryan Prince D, Paddock DJ, Tomasselli AG, Winterrowd G. *Bioorg Med Chem Lett.* 2007; 17:78–81. [PubMed: 17049233]
168. Maillard MC, Hom RK, Benson TE, Moon JB, Mamo S, Bienkowski M, Tomasselli AG, Woods DD, Prince DB, Paddock DJ, Emmons TL, Tucker JA, Dappen MS, Brogley L, Thorsett ED, Jewett N, Sinha S, John V. *J Med Chem.* 2007; 50:776–781. [PubMed: 17300163]
169. Kortum SW, Benson TE, Bienkowski MJ, Emmons TL, Prince DB, Paddock DJ, Tomasselli AG, Moon JB, LaBorde A, TenBrink RE. *Bioorg Med Chem Lett.* 2007; 17:3378–3383. [PubMed: 17434734]
170. Schostarez, HJ.; Chrusciel, RA.; Centko, RS. *Int. Pat.* 2002. WO2002084768
171. Fang, LY.; John, V. *Int. Pat.* 2002. WO200202506
172. Beck, JP.; Gailunas, A.; Hom, R.; Jagodzinska, B.; John, V.; Maillard, M. *Int. Pat.* 2002. WO200202520
173. John, V.; Maillard, M.; Jagodzinska, B.; Beck, JP.; Gailunas, A.; Fang, L.; Sealy, J.; Tenbrink, R.; Freskos, J.; Mickelson, J.; Samala, L.; Hom, R. *Int. Pat.* 2003. WO2003040096
174. Pulley, SR.; Toker, JA. *Int. Pat.* 2004. WO2004050609
175. Kleinman, EF.; Murray, JC. *Int. Pat.* 2006. WO2006032999
176. Marcin LR, Higgins MA, Zusi FC, Zhang Y, Dee MF, Parker MF, Muckelbauer JK, Camac DM, Morin PE, Ramamurthy V, Tebben AJ, Lentz KA, Grace JE, Marcinkeviciene JA, Kopcho LM, Burton CR, Barten DM, Toyn JH, Meredith JE, Albright CF, Bronson JJ, Macor JE, Thompson LA. *Bioorg Med Chem Lett.* 2011; 21:537–541. [PubMed: 21078556]
177. Gailunas, A.; Hom, R.; John, V.; Maillard, M.; Chrusciel, RA.; Fisher, J.; Jacobs, J.; Freskos, JN.; Brown, DL.; Fobian, YM. *Int. Pat.* 2003. WO2003006423
178. Decicco, CP.; Tebben, AJ.; Thompson, LA.; Combs, AP. *Int. Pat.* 2004. WO2004013098
179. Truong AP, Toth G, Probst GD, Sealy JM, Bowers S, Wone DW, Dressen D, Hom RK, Konradi AW, Sham HL, Wu J, Peterson BT, Ruslim L, Bova MP, Kholodenko D, Motter RN, Bard F, Santiago P, Ni H, Chian D, Soriano F, Cole T, Brigham EF, Wong K, Zmolek W, Goldbach E,

- Samant B, Chen L, Zhang H, Nakamura DF, Quinn KP, Yednock TA, Sauer JM. *Bioorg Med Chem Lett.* 2010; 20:6231–6236. [PubMed: 20833041]
180. Ng RA, Sun M, Bowers S, Hom RK, Probst GD, John V, Fang LY, Maillard M, Gailunas A, Brogley L, Neitz RJ, Tung JS, Pleiss MA, Konradi AW, Sham HL, Dappen MS, Adler M, Yao N, Zmolek W, Nakamura D, Quinn KP, Sauer JM, Bova MP, Ruslim L, Artis DR, Yednock TA. *Bioorg Med Chem Lett.* 2013; 23:4674–4679. [PubMed: 23856050]
181. Tenbrink, R.; Maillard, M.; Warpehoski, M. *Int. Pat.* 2003. WO2003050073
182. Aquino, J.; John, V.; Tucker, JA.; Hom, R.; Pulley, S.; Tenbrink, R. *Int. Pat.* 2004. WO2004094384
183. John, V.; Maillard, M.; Tucker, J.; Jagodzinska, B.; Brogley, L.; Tung, J.; Shah, N.; Neitz, RJ. *Int. Pat.* 2005. WO2005087752
184. John, V.; Maillard, M.; Fang, L.; Tucker, J.; Brogley, L.; Aquino, J.; Bowers, S.; Probst, G.; Tung, J. *Int. Pat.* 2005. WO2005087714
185. John, V.; Hom, R.; Sealy, J.; Aquino, J.; Probst, G. *Int. Pat.* 2005. WO2005070402
186. John, V.; Maillard, M.; Tucker, J.; Aquino, J.; Hom, R.; Tung, J.; Dressen, D.; Shah, N.; Neitz, RJ. *Int. Pat.* 2005. WO2005087215
187. John, V.; Maillard, M.; Jagodzinska, B.; Aquino, J.; Probst, G.; Tung, JS. *Int. Pat.* 2006. WO2006010095
188. Butler, TW. *Int. Pat.* 2006. WO2006064324
189. Sealy, J.; Hom, R.; John, V.; Probst, G.; Tung, JS. *Int. Pat.* 2006. WO2006010094
190. Bronk, BS.; Butler, TW. *Int. Pat.* 2006. WO2006085216
191. Albrecht, BK.; Andersen, DL.; Bartberger, M.; Brown, J.; Brown, R.; Chaffee, SC.; Cheng, Y.; Croghan, M.; Graceffa, R.; Harried, S.; Hitchcock, S.; Hungate, R.; Judd, T.; Kaller, M.; Kreiman, C.; La, D.; Lopez, P.; Masse, CE.; Monenschein, H.; Nguyen, T.; Nixey, T.; Patel, VF.; Pennington, L.; Weiss, M.; Xue, Q.; Yang, B.; Zhong, W. *Int. Pat.* 2007. WO2007062007
192. Hom, R.; Toth, G.; Probst, G.; Bowers, S.; Truong, A.; Tung, JS. *Int. Pat.* 2007. WO2007047306
193. Kleinman, EF. *Int. Pat.* 2007. WO2007110727
194. Boyd, JG.; Butler, TW.; O'Neill, BT. *Int. Pat.* 2007. WO2007060526
195. Neitz, RJ.; Tisdale, E.; Jagodzinska, B.; Truong, A.; Tung, JS. *Int. Pat.* 2007. WO2007047305
196. Weiss MM, Williamson T, Babu-Khan S, Bartberger MD, Brown J, Chen K, Cheng Y, Citron M, Croghan MD, Dineen TA, Esmay J, Graceffa RF, Harried SS, Hickman D, Hitchcock SA, Horne DB, Huang H, Imbeah-Ampiah R, Judd T, Kaller MR, Kreiman CR, La DS, Li V, Lopez P, Louie S, Monenschein H, Nguyen TT, Pennington LD, Rattan C, San Miguel T, Sickmier EA, Wahl RC, Wen PH, Wood S, Xue Q, Yang BH, Patel VF, Zhong W. *J Med Chem.* 2012; 55:9009–9024. [PubMed: 22468639]
197. Dineen TA, Weiss MM, Williamson T, Acton P, Babu-Khan S, Bartberger MD, Brown J, Chen K, Cheng Y, Citron M, Croghan MD, Dunn RT 2nd, Esmay J, Graceffa RF, Harried SS, Hickman D, Hitchcock SA, Horne DB, Huang H, Imbeah-Ampiah R, Judd T, Kaller MR, Kreiman CR, La DS, Li V, Lopez P, Louie S, Monenschein H, Nguyen TT, Pennington LD, San Miguel T, Sickmier EA, Vargas HM, Wahl RC, Wen PH, Whittington DA, Wood S, Xue Q, Yang BH, Patel VF, Zhong W. *J Med Chem.* 2012; 55:9025–9044. [PubMed: 22468684]
198. Zhong, W.; Hitchcock, S.; Patel, VF.; Croghan, M.; Dineen, T.; Horne, D.; Kaller, M.; Kreiman, C.; Lopez, P.; Monenschein, H.; Nguyen, T.; Pennington, L.; Xue, Q.; Yang, B. *Int. Pat.* 2008. WO2008147544
199. Barrow JC, Rittle KE, Ngo PL, Selnick HG, Graham SL, Pitzemberger SM, McGaughey GB, Colussi D, Lai MT, Huang Q, Tugusheva K, Espeseth AS, Simon AJ, Munshi SK, Vacca JP. *ChemMedChem.* 2007; 2:995–999. [PubMed: 17458843]
200. Cumming J, Babu S, Huang Y, Carrol C, Chen X, Favreau L, Greenlee W, Guo T, Kennedy M, Kuvelkar R, Le T, Li G, McHugh N, Orth P, Ozgur L, Parker E, Saionz K, Stamford A, Strickland C, Tadesse D, Voigt J, Zhang L, Zhang Q. *Bioorg Med Chem Lett.* 2010; 20:2837–2842. [PubMed: 20347593]

201. Hanessian S, Yun H, Hou Y, Yang G, Bayraktarian M, Therrien E, Moitessier N, Roggo S, Veenstra S, Tintelnot-Blomley M, Rondeau JM, Ostermeier C, Strauss A, Ramage P, Paganetti P, Neumann U, Betschart C. *J Med Chem.* 2005; 48:5175–5190. [PubMed: 16078837]
202. Thompson LA, Shi J, Decicco CP, Tebben AJ, Olson RE, Boy KM, Guernon JM, Good AC, Liauw A, Zheng C, Copeland RA, Combs AP, Trainor GL, Camac DM, Muckelbauer JK, Lentz KA, Grace JE, Burton CR, Toyn JH, Barten DM, Marcinkeviciene J, Meredith JE, Albright CF, Macor JE. *Bioorg Med Chem Lett.* 2011; 21:6909–6915. [PubMed: 21974952]
203. Zou Y, Xu L, Chen W, Zhu Y, Chen T, Fu Y, Li L, Ma L, Xiong B, Wang X, Li J, He J, Zhang H, Xu Y, Li J, Shen J. *Eur J Med Chem.* 2013; 68C:270–283. [PubMed: 23988410]
204. Cumming, JN.; Iserloh, U.; Stamford, A.; Strickland, C.; Voigt, JH.; Wu, G.; Huang, Y.; Chackalamannil, S.; Guo, T.; Hobbs, DW.; Le, TXH.; Lowrie, JF.; Saionz, KW.; Babu, SD. *Int. Pat.* 2005. WO2005016876
205. Cumming, JN.; Huang, Y.; Li, G.; Iserloh, U.; Stamford, A.; Strickland, C.; Voigt, JH.; Wu, Y.; Pan, J.; Guo, T.; Hobbs, DW.; Le, TXH.; Lowrie, JF. *Int. Pat.* 2005. WO2005014540
206. Thompson, LA., III; Boy, KM.; Shi, J.; Macor, JE. *Int. Pat.* 2006. WO20060229309
207. Durham, TB.; Hahn, PJ.; Kohn, TJ.; McCarthy, JR.; Broughton, HB.; Dally, RD.; Gonzalez-Garcia, MR.; Henry, KJ., Jr.; Shepherd, TA.; Erickson, JA.; Bueno-Melendo, AB. *Int. Pat.* 2006. WO2006034093
208. Huang, Y.; Li, G.; Stamford, AW. *Int. Pat.* 2006. WO2006014762
209. Thompson III, LA.; Boy, KM.; Shi, J.; Macor, JE. *Int. Pat.* 2006. WO2006099532
210. Barrow, JC.; Rittle, KE.; Bondiskey, PL. *Int. Pat.* 2007. WO2007058862
211. Rueeger H, Rondeau JM, McCarthy C, Mobitz H, Tintelnot-Blomley M, Neumann U, Desrayaud S. *Bioorg Med Chem Lett.* 2011; 21:1942–1947. [PubMed: 21388807]
212. Rueeger H, Lueoend R, Rogel O, Rondeau JM, Mobitz H, Machauer R, Jacobson L, Staufenbiel M, Desrayaud S, Neumann U. *J Med Chem.* 2012; 55:3364–3386. [PubMed: 22380629]
213. Rueeger H, Lueoend R, Machauer R, Veenstra SJ, Jacobson LH, Staufenbiel M, Desrayaud S, Rondeau JM, Mobitz H, Neumann U. *Bioorg Med Chem Lett.* 2013; 23:5300–5306. [PubMed: 23981898]
214. Briard, E.; Lueoend, RM.; Machauer, R.; Moebitz, H.; Rogel, O.; Rondeau, JM.; Rueeger, H.; Tintelnot-Blomley, M.; Veenstra, SJ. *Int. Pat.* 2009. WO2009024615
215. Stanton MG, Stauffer SR, Gregro AR, Steinbeiser M, Nantermet P, Sankaranarayanan S, Price EA, Wu G, Crouthamel MC, Ellis J, Lai MT, Espeseth AS, Shi XP, Jin L, Colussi D, Pietrak B, Huang Q, Xu M, Simon AJ, Graham SL, Vacca JP, Selnick H. *J Med Chem.* 2007; 50:3431–3433. [PubMed: 17583334]
216. Maillard, M.; Baldwin, ET.; Beck, JT.; Hughes, R.; John, V.; Pulley, SR.; Tenbrink, R. *Int. Pat.* 2004. WO2004024081
217. Coburn, CA.; Stachel, SJ.; Vacca, JP. *Int. Pat.* 2004. WO2004043916
218. Rajapakse HA, Nantermet PG, Selnick HG, Munshi S, McGaughey GB, Lindsley SR, Young MB, Lai MT, Espeseth AS, Shi XP, Colussi D, Pietrak B, Crouthamel MC, Tugusheva K, Huang Q, Xu M, Simon AJ, Kuo L, Hazuda DJ, Graham S, Vacca JP. *J Med Chem.* 2006; 49:7270–7273. [PubMed: 17149856]
219. Sankaranarayanan S, Holahan MA, Colussi D, Crouthamel MC, Devanarayan V, Ellis J, Espeseth A, Gates AT, Graham SL, Gregro AR, Hazuda D, Hochman JH, Holloway K, Jin L, Kahana J, Lai MT, Lineberger J, McGaughey G, Moore KP, Nantermet P, Pietrak B, Price EA, Rajapakse H, Stauffer S, Steinbeiser MA, Seabrook G, Selnick HG, Shi XP, Stanton MG, Swestock J, Tugusheva K, Tyler KX, Vacca JP, Wong J, Wu G, Xu M, Cook JJ, Simon AJ. *J Pharmacol Exp Ther.* 2009; 328:131–140. [PubMed: 18854490]
220. Nantermet PG, Rajapakse HA, Stanton MG, Stauffer SR, Barrow JC, Gregro AR, Moore KP, Steinbeiser MA, Swestock J, Selnick HG, Graham SL, McGaughey GB, Colussi D, Lai MT, Sankaranarayanan S, Simon AJ, Munshi S, Cook JJ, Holahan MA, Michener MS, Vacca JP. *ChemMedChem.* 2009; 4:37–40. [PubMed: 19085994]
221. Barrow, JC.; McGaughey, GB.; Nantermet, PG.; Rajapakse, HA.; Selnick, HG.; Stauffer, SR.; Vacca, JP.; Stachel, SJ.; Coburn, CA.; Stanton, MG. *Int. Pat.* 2005. WO2005103043

222. Nantermet, PG.; Stanton, MG.; Rajapakse, HA.; Selnick, HG.; Barrow, JC.; Stauffer, SR.; Vacca, JP.; Moore, KP.; Stachel, SJ. *Int. Pat.* 2006. WO2006057945
223. Nantermet, PG.; Rajapakse, HA. *Int. Pat.* 2007. WO2007019080
224. Nantermet, PG. *Int. Pat.* 2007. WO2007019078
225. Coburn CA, Stachel SJ, Jones KG, Steele TG, Rush DM, DiMuzio J, Pietrak BL, Lai MT, Huang Q, Lineberger J, Jin L, Munshi S, Katharine Holloway M, Espeseth A, Simon A, Hazuda D, Graham SL, Vacca JP. *Bioorg Med Chem Lett.* 2006; 16:3635–3638. [PubMed: 16690314]
226. Ghosh AK, Venkateswara Rao K, Yadav ND, Anderson DD, Gavande N, Huang X, Terzyan S, Tang J. *J Med Chem.* 2012; 55:9195–9207. [PubMed: 22954357]
227. Monceaux CJ, Hirata-Fukae C, Lam PC, Totrov MM, Matsuoka Y, Carlier PR. *Bioorg Med Chem Lett.* 2011; 21:3992–3996. [PubMed: 21621412]
228. Jagodzinska, B.; Warpehoski, MA.; Shaltout, RM. *Int. Pat.* 2003. WO2003057721
229. Peters, S.; Eickmeier, C.; Fuchs, K.; Stransky, W.; Dorner-Ciossek, C.; Kostka, M.; Handschuh, S.; Bauer, M.; Nar, H.; Bornemann, K.; Klinder, K.; Rademann, J.; Weik, S. *Int. Pat.* 2005. WO2005113582
230. Eickmeier, C.; Fuchs, K.; Peters, S.; Dorner-Ciossek, C.; Heine, N.; Handschuh, S.; Klinder, K.; Kostka, M. *Int. Pat.* 2006. WO2006103038
231. Peters, S.; Meier, C.; Fuchs, K.; Stransky, W.; Dorner-Ciossek, C.; Kostka, M.; Handschuh, S.; Nar, H.; Bornemann, K.; Klinder, K.; Bauer, M. *Int. Pat.* 2007. WO2007014946
232. Ghosh AK, Devasamudram T, Hong L, DeZutter C, Xu X, Weerasena V, Koelsch G, Bilcer G, Tang J. *Bioorg Med Chem Lett.* 2005; 15:15–20. [PubMed: 15582402]
233. Rojo I, Martin JA, Broughton H, Timm D, Erickson J, Yang HC, McCarthy JR. *Bioorg Med Chem Lett.* 2006; 16:191–195. [PubMed: 16249081]
234. Machauer R, Veenstra S, Rondeau JM, Tintelnot-Blomley M, Betschart C, Neumann U, Paganetti P. *Bioorg Med Chem Lett.* 2009; 19:1361–1365. [PubMed: 19195886]
235. Machauer R, Laumen K, Veenstra S, Rondeau JM, Tintelnot-Blomley M, Betschart C, Jatou AL, Desrayaud S, Staufienbiel M, Rabe S, Paganetti P, Neumann U. *Bioorg Med Chem Lett.* 2009; 19:1366–1370. [PubMed: 19195887]
236. Lerchner A, Machauer R, Betschart C, Veenstra S, Rueeger H, McCarthy C, Tintelnot-Blomley M, Jatou AL, Rabe S, Desrayaud S, Enz A, Staufienbiel M, Paganetti P, Rondeau JM, Neumann U. *Bioorg Med Chem Lett.* 2010; 20:603–607. [PubMed: 19963375]
237. Pennington LD, Whittington DA, Bartberger MD, Jordan SR, Monenschein H, Nguyen TT, Yang BH, Xue QM, Vounatsos F, Wahl RC, Chen K, Wood S, Citron M, Patel VF, Hitchcock SA, Zhong W. *Bioorg Med Chem Lett.* 2013; 23:4459–4464. [PubMed: 23769639]
238. Pulley, SR.; Beck, JP.; Tenbrink, RE.; Jacobs, JS. *Int. Pat.* 2002. WO2002100399
239. Pulley, SR.; Beck, JP.; Tenbrink, RE. *Int. Pat.* 2002. WO2002100856
240. Auberson, Y.; Betschart, C.; Glatthar, R.; Laumen, K.; Machauer, R.; Tintelnot-Blomley, M.; Troxler, TJ.; Veenstra, SJ. *Int. Pat.* 2005. WO2005049585
241. Stamford, AW.; Huang, Y.; Li, G.; Strickland, CO.; Voigt, JH. *Int. Pat.* 2006. WO2006014944
242. Lindsley SR, Moore KP, Rajapakse HA, Selnick HG, Young MB, Zhu H, Munshi S, Kuo L, McGaughey GB, Colussi D, Crouthamel MC, Lai MT, Pietrak B, Price EA, Sankaranarayanan S, Simon AJ, Seabrook GR, Hazuda DJ, Pudvah NT, Hochman JH, Graham SL, Vacca JP, Nantermet PG. *Bioorg Med Chem Lett.* 2007; 17:4057–4061. [PubMed: 17482814]
243. Moore KP, Zhu H, Rajapakse HA, McGaughey GB, Colussi D, Price EA, Sankaranarayanan S, Simon AJ, Pudvah NT, Hochman JH, Allison T, Munshi SK, Graham SL, Vacca JP, Nantermet PG. *Bioorg Med Chem Lett.* 2007; 17:5831–5835. [PubMed: 17827011]
244. Stachel SJ, Coburn CA, Sankaranarayanan S, Price EA, Wu G, Crouthamel M, Pietrak BL, Huang Q, Lineberger J, Espeseth AS, Jin L, Ellis J, Holloway MK, Munshi S, Allison T, Hazuda D, Simon AJ, Graham SL, Vacca JP. *J Med Chem.* 2006; 49:6147–6150. [PubMed: 17034118]
245. Coburn, CA.; Stachel, SJ.; Vacca, JP. *Int. Pat.* 2004. WO2004062625
246. Coburn, C.; Stachel, SJ.; Vacca, JP. *Int. Pat.* 2005. WO2005018545
247. Cole DC, Manas ES, Stock JR, Condon JS, Jennings LD, Aulabaugh A, Chopra R, Cowling R, Ellingboe JW, Fan KY, Harrison BL, Hu Y, Jacobsen S, Jin G, Lin L, Lovering FE, Malamas

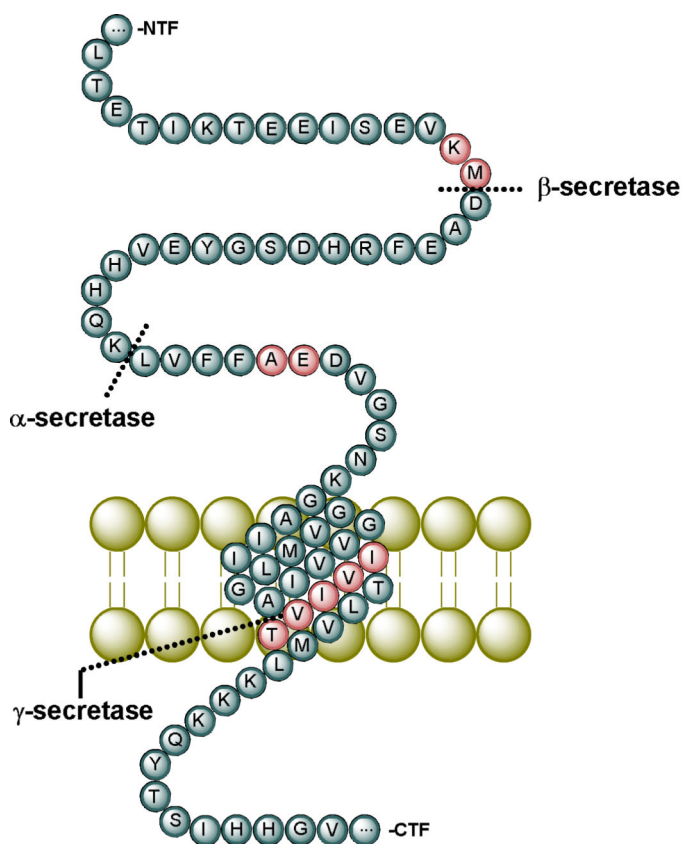
- MS, Stahl ML, Strand J, Sukhdeo MN, Svenson K, Turner MJ, Wagner E, Wu J, Zhou P, Bard J. *J Med Chem.* 2006; 49:6158–6161. [PubMed: 17034121]
248. Jennings LD, Cole DC, Stock JR, Sukhdeo MN, Ellingboe JW, Cowling R, Jin G, Manas ES, Fan KY, Malamas MS, Harrison BL, Jacobsen S, Chopra R, Lohse PA, Moore WJ, O'Donnell MM, Hu Y, Robichaud AJ, Turner MJ, Wagner E, Bard J. *Bioorg Med Chem Lett.* 2008; 18:767–771. [PubMed: 18068983]
249. Cole DC, Stock JR, Chopra R, Cowling R, Ellingboe JW, Fan KY, Harrison BL, Hu Y, Jacobsen S, Jennings LD, Jin G, Lohse PA, Malamas MS, Manas ES, Moore WJ, O'Donnell MM, Olland AM, Robichaud AJ, Svenson K, Wu J, Wagner E, Bard J. *Bioorg Med Chem Lett.* 2008; 18:1063–1066. [PubMed: 18162398]
250. Cole, DC.; Manas, ES.; Jennings, LD.; Lovering, FE.; Stock, JR.; Moore, WJ.; Ellingboe, JW.; Condon, JS.; Sukhdeo, MN.; Zhou, P.; Wu, J.; Morris, KM. U.S. Pat. 2006. US20060183790
251. Fobare, WF.; Solvibile, WR, Jr.. U.S. Pat. 2006. US20060183792
252. Gerritz SW, Zhai W, Shi S, Zhu S, Toyn JH, Meredith JE Jr, Iben LG, Burton CR, Albright CF, Good AC, Tebben AJ, Muckelbauer JK, Camac DM, Metzler W, Cook LS, Padmanabha R, Lentz KA, Sofia MJ, Poss MA, Macor JE, Thompson LA 3rd. *J Med Chem.* 2012; 55:9208–9223. [PubMed: 23030502]
253. Gerritz, S.; Shi, S.; Zhu, S. U.S. Pat. 2006. US20060287287
254. Zou Y, Li L, Chen W, Chen T, Ma L, Wang X, Xiong B, Xu Y, Shen J. *Molecules.* 2013; 18:5706–5722. [PubMed: 23681056]
255. Thompson, LA.; Shi, J.; Zusi, FC.; Dee, MF.; Macor, JE. U.S. Pat. 2007. US20070049589
256. Wu, YJ.; Gerritz, S.; Shi, S.; Zhu, S. U.S. Pat. 2007. WO20070232581
257. Hu, B. U.S. Pat. 2006. US20060183943
258. Berg, S.; Kolmodin, K. Int. Pat. 2007. WO2007120096
259. Congreve M, Aharony D, Albert J, Callaghan O, Campbell J, Carr RA, Chessari G, Cowan S, Edwards PD, Frederickson M, McMenamin R, Murray CW, Patel S, Wallis N. *J Med Chem.* 2007; 50:1124–1132. [PubMed: 17315857]
260. Malamas MS, Barnes K, Hui Y, Johnson M, Lovering F, Condon J, Fobare W, Solvibile W, Turner J, Hu Y, Manas ES, Fan K, Olland A, Chopra R, Bard J, Pangalos MN, Reinhart P, Robichaud AJ. *Bioorg Med Chem Lett.* 2010; 20:2068–2073. [PubMed: 20223661]
261. Malamas, MS.; Fobare, WF.; Solvibile, WR., Jr.; Lovering, FE.; Condon, JS.; Robichaud, AJ. U.S. Pat. 2006. US20060173049
262. Albert, JS.; Callaghan, J.; Carr, RAE.; Chessari, G.; Cowan, S.; Congreve, MS.; Edwards, P.; Frederickson, M.; Murray, CW.; Patel, S. U.S. Pat. 2008. US20080287399
263. Coburn, C.; Holloway, MK.; Stachel, SJ. U.S. Pat. 2008. US20080161363
264. Hills ID, Holloway MK, de Leon P, Nomland A, Zhu H, Rajapakse H, Allison TJ, Munshi SK, Colussi D, Pietrak BL, Toolan D, Haugabook SJ, Graham SL, Stachel SJ. *Bioorg Med Chem Lett.* 2009; 19:4993–4995. [PubMed: 19640712]
265. Chiriano G, De Simone A, Mancini F, Perez DI, Cavalli A, Bolognesi ML, Legname G, Martinez A, Andrisano V, Carloni P, Roberti M. *Eur J Med Chem.* 2012; 48:206–213. [PubMed: 22209418]
266. Gravenfors Y, Viklund J, Blid J, Ginman T, Karlstrom S, Kihlstrom J, Kolmodin K, Lindstrom J, von Berg S, von Kieseritzky F, Bogar K, Slivo C, Swahn BM, Olsson LL, Johansson P, Eketjall S, Falting J, Jeppsson F, Stromberg K, Janson J, Rahm F. *J Med Chem.* 2012; 55:9297–9311. [PubMed: 23017051]
267. Malamas MS, Erdei J, Gunawan I, Barnes K, Johnson M, Hui Y, Turner J, Hu Y, Wagner E, Fan K, Olland A, Bard J, Robichaud AJ. *J Med Chem.* 2009; 52:6314–6323. [PubMed: 19757823]
268. Swahn BM, Holenz J, Kihlstrom J, Kolmodin K, Lindstrom J, Plobeck N, Rotticci D, Sehgelmeble F, Sundstrom M, Berg S, Falting J, Georgievska B, Gustavsson S, Neelissen J, Ek M, Olsson LL, Berg S. *Bioorg Med Chem Lett.* 2012; 22:1854–1859. [PubMed: 22325942]
269. Malamas, MS.; Erdei, JJ.; Gunawan, IS.; Barnes, KD.; Johnson, MR.; Hui, Y. U.S. Pat. 2005. US20050282826

270. Malamas, MS.; Erdei, JJ.; Gunawan, IS.; Nowak, PW.; Harrison, BL. U.S. Pat. 2006. US20060160828
271. Berg, S.; Holenz, J.; Hogdin, K.; Kolmodin, K.; Plobeck, N.; Rotticci, D.; Sehgelmeble, F. U.S. Pat. 2007. US20070299087
272. Berg, S.; Hogdin, K.; Kihlstrom, J.; Plobeck, N.; Sehgelmeble, F.; Wirstam, M. U.S. Pat. 2008. US20080051420
273. Berg, S.; Holenz, J.; Hogdin, K.; Kihlstrom, J.; Kolmodin, K.; Lindstrom, J.; Plobeck, N.; Rotticci, D.; Sehgelmeble, F.; Wirstam, M. Int. Pat. 2008. US20080058349
274. Berg, S.; Holenz, J.; Hogdin, K.; Kolmodin, K.; Plobeck, N.; Rotticci, D.; Sehgelmeble, F.; Wirstam, M. U.S. Pat. 2008. US20080214577
275. Malamas, MS.; Barnes, KD.; Johnson, MR. U.S. Pat. 2008. US20080051390
276. Malamas MS, Erdei J, Gunawan I, Turner J, Hu Y, Wagner E, Fan K, Chopra R, Olland A, Bard J, Jacobsen S, Magolda RL, Pangalos M, Robichaud AJ. *J Med Chem.* 2010; 53:1146–1158. [PubMed: 19968289]
277. Nowak P, Cole DC, Aulabaugh A, Bard J, Chopra R, Cowling R, Fan KY, Hu B, Jacobsen S, Jani M, Jin G, Lo MC, Malamas MS, Manas ES, Narasimhan R, Reinhart P, Robichaud AJ, Stock JR, Subrath J, Svenson K, Turner J, Wagner E, Zhou P, Ellingboe JW. *Bioorg Med Chem Lett.* 2010; 20:632–635. [PubMed: 19959359]
278. Malamas, MS.; Erdei, JJ.; Gunawan, IS.; Zhou, P.; Yan, Y.; Quagliato, DA. U.S. Pat. 2005. US20050282825
279. Berg, S.; Burrows, J.; Chessari, G.; Congreve, MS.; Hedstrom, J.; Hellberg, S.; Hogdin, K.; Kihlstrom, J.; Kolmodin, K.; Lindstrom, J.; Murray, C.; Patel, S. Int. Pat. 2007. WO2007058602
280. Malamas, MS.; Erdei, JJ.; Fobare, WF.; Quagliato, DA.; Antane, SA.; Robichaud, AJ. U.S. Pat. 2007. US20070072925
281. Malamas, MS.; Gunawan, IS.; Erdei, JJ.; Nowak, PW.; Stock, JR.; Yan, Y. U.S. Pat. 2007. US20070027199
282. Malamas, MS.; Zhou, P.; Fobare, WF.; Solvibile, WR.; Gunawan, IS.; Erdei, JJ.; Yan, Y.; Andrae, PM.; Quagliato, DA. U.S. Pat. 2007. US20070004786
283. Zhou, P.; Malamas, MS.; Li, Y.; Robichaud, AJ.; Quagliato, DA. U.S. Pat. 2007. US20070004730
284. Berg, S.; Hallberg, J.; Hogdin, K.; Karlstrom, S.; Kers, A.; Plobeck, N.; Rakos, L. Int. Pat. 2008. WO2008076044
285. Berg, S.; Holenz, J.; Karlstrom, S.; Kihlstrom, J.; Lindstrom, J.; Rakos, L. U.S. Pat. 2008. US20080176862
286. Berg, S.; Karlstrom, S.; Kolmodin, K.; Lindstrom, J.; Nystrom, JE.; Sehgelmeble, F.; Soderman, P. U.S. Pat. 2008. US20080161269
287. Burrows, JN.; Hellberg, S.; Hogdin, K.; Karlstrom, S.; Kolmodin, K.; Lindstrom, J.; Slivo, C. Int. Pat. 2008. WO2008150217
288. Malamas, MS.; Robichaud, AJ.; Porte, AM.; Morris, KM.; Solvibile, WR.; Kim, JI. U.S. Pat. 2009. US20090048320
289. Malamas, MS.; Robichaud, AJ.; Porte, AM.; Solvibile, WR.; Morris, KM.; Antane, SA.; Kim, JI.; McDevitt, RE. U.S. Pat. 2009. US20090042964
290. Zhu Z, Sun ZY, Ye Y, Voigt J, Strickland C, Smith EM, Cumming J, Wang L, Wong J, Wang YS, Wyss DF, Chen X, Kuvelkar R, Kennedy ME, Favreau L, Parker E, McKittrick BA, Stamford A, Czarniecki M, Greenlee W, Hunter JC. *J Med Chem.* 2010; 53:951–965. [PubMed: 20043696]
291. Barrow JC, Stauffer SR, Rittle KE, Ngo PL, Yang Z, Selnick HG, Graham SL, Munshi S, McGaughey GB, Holloway MK, Simon AJ, Price EA, Sankaranarayanan S, Colussi D, Tugusheva K, Lai MT, Espeseth AS, Xu M, Huang Q, Wolfe A, Pietrak B, Zuck P, Levorse DA, Hazuda D, Vacca JP. *J Med Chem.* 2008; 51:6259–6262. [PubMed: 18811140]
292. Stachel SJ, Coburn CA, Rush D, Jones KL, Zhu H, Rajapakse H, Graham SL, Simon A, Katharine Holloway M, Allison TJ, Munshi SK, Espeseth AS, Zuck P, Colussi D, Wolfe A,

- Pietrak BL, Lai MT, Vacca JP. *Bioorg Med Chem Lett*. 2009; 19:2977–2980. [PubMed: 19409780]
293. Hicken, EJ.; Hunt, KW.; Rodriguez, ME.; Tang, TP.; Siu, M. *Int. Pat.* 2013. WO2013148851
294. Huestis MP, Liu W, Volgraf M, Purkey HE, Yu C, Wang W, Smith D, Vigers G, Dutcher D, Hunt KW, Siu M. *Tetrahedron Letters*. 2013; 54:5802–5807.
295. Andreini, M.; Gabellieri, E.; Guba, W.; Marconi, G.; Narquizian, R.; Power, E.; Travagli, M.; Woltering, T.; Wostl, W. *U.S. Pat.* 2009. US20090209529
296. Hilpert H, Guba W, Woltering TJ, Wostl W, Pinard E, Mauser H, Mayweg AV, Rogers-Evans M, Humm R, Krummenacher D, Muser T, Schnider C, Jacobsen H, Ozmen L, Bergadano A, Banner DW, Hochstrasser R, Kuglstatter A, David-Pierson P, Fischer H, Polara A, Narquizian R. *J Med Chem*. 2013; 56:3980–3995. [PubMed: 23590342]
297. Woltering TJ, Wostl W, Hilpert H, Rogers-Evans M, Pinard E, Mayweg A, Gobel M, Banner DW, Benz J, Travagli M, Pollastrini M, Marconi G, Gabellieri E, Guba W, Mauser H, Andreini M, Jacobsen H, Power E, Narquizian R. *Bioorg Med Chem Lett*. 2013; 23:4239–4243. [PubMed: 23735744]
298. Borroni, E.; Gobbi, L.; Hilpert, H.; Honer, M.; Muri, D.; Narquizian, R.; Polara, A. *Int. Pat.* 2012. WO2012168175
299. Hilpert, H.; Humm, R. *Int. Pat.* 2012. WO2012107371
300. Hilpert, H.; Narquizian, R.; Pinard, E.; Polara, A.; Rogers-Evans, M.; Woltering, T.; Wostl, W. *Int. Pat.* 2012. WO2012156284
301. Hilpert, H.; Wostl, W. *Int. Pat.* 2012. WO2012139993
302. Narquizian, R.; Pinard, E.; Wostl, W. *Int. Pat.* 2012. WO2012163790
303. Woltering, T. *Int. Pat.* 2012. WO2012168164
304. Hilpert, H.; Humm, R.; Woltering, T. *Int. Pat.* 2013. WO2013110622
305. Hilpert, H.; Pinard, E.; Woltering, T. *Int. Pat.* 2013. WO2013041499
306. Lueoend, RM.; Machauer, R.; Rueeeger, H.; Veenstra, SJ. *Int. Pat.* 2013. WO2013027188
307. Shangguan S, Wang F, Liao Y, Yu H, Li J, Huang W, Hu H, Yu L, Hu Y, Sheng R. *Molecules*. 2013; 18:3577–3594. [PubMed: 23519200]
308. Kobayashi, N.; Ueda, K.; Itoh, N.; Suzuki, S.; Sakaguchi, G.; Kato, A.; Yukimasa, A.; Hori, A.; Koriyama, Y.; Haraguchi, H.; Yasui, K.; Kanda, Y. *U.S. Pat.* 2009. US20090082560
309. Beck, JP.; Green, SJ.; Lopez, JE.; Mathes, BM.; Mergott, DJ.; Porter, WJ.; Rankovic, Z.; Shi, Y.; Watson, BM.; Winneroski, LL, Jr. *U.S. Pat.* 2013. US20130261111
310. Stamford AW, Scott JD, Li SW, Babu S, Tadesse D, Hunter R, Wu Y, Misiaszek J, Cumming JN, Gilbert EJ, Huang C, McKittrick BA, Hong L, Guo T, Zhu Z, Strickland C, Orth P, Voigt JH, Kennedy ME, Chen X, Kuvelkar R, Hodgson R, Hyde LA, Cox K, Favreau L, Parker EM, Greenlee WJ. *ACS Med Chem Lett*. 2012; 3:897–902. [PubMed: 23412139]
311. Gabellieri, E.; Guba, W.; Hilpert, H.; Mauser, H.; Mayweg, AV.; Rogers-Evans, M.; Rombach, D.; Thomas, A.; Woltering, T.; Wostl, W. *Int. Pat.* 2012. WO2012126791
312. Hilpert, H.; Narquizian, R. *Int. Pat.* 2012. WO2012110459
313. Hilpert, H.; Rogers-Evans, M.; Rombach, D. *Int. Pat.* 2012. WO2012119883
314. Narquizian, R.; Woltering, T.; Wostl, W. *Int. Pat.* 2012. WO2012136603
315. Baxter EW, Conway KA, Kennis L, Bischoff F, Mercken MH, Winter HL, Reynolds CH, Tounge BA, Luo C, Scott MK, Huang Y, Braeken M, Pieters SM, Berthelot DJ, Masure S, Bruinzeel WD, Jordan AD, Parker MH, Boyd RE, Qu J, Alexander RS, Brenneeman DE, Reitz AB. *J Med Chem*. 2007; 50:4261–4264. [PubMed: 17685503]
316. Ghosh AK, Pandey S, Gangarajula S, Kulkarni S, Xu X, Rao KV, Huang X, Tang J. *Bioorg Med Chem Lett*. 2012; 22:5460–5465. [PubMed: 22863204]
317. Baxter, E.; Boyd, R.; Coats, S.; Jordan, A.; Reitz, A.; Reynolds, CH.; Scott, M.; Schulz, M.; De Winter, HLJ. *Int. Pat.* 2006. WO2006017844
318. Bishoff, FP.; Bracken, M.; Pieters, SM.; Mercken, MH.; De Winter, HLJ.; Berthelot, DJC. *Int. Pat.* 2006. WO2006024932

319. Baxter, EB.; Creighton, CJ.; Huang, Y.; Luo, C.; Parker, MH.; Reitz, AB.; Reynolds, CH.; Ross, TM.; Strobel, E.; Tounge, BA. U.S. Pat. 2007. US20070259898
320. Cheng Y, Judd TC, Bartberger MD, Brown J, Chen K, Fremeau RT Jr, Hickman D, Hitchcock SA, Jordan B, Li V, Lopez P, Louie SW, Luo Y, Michelsen K, Nixey T, Powers TS, Rattan C, Sickmier EA, St Jean DJ Jr, Wahl RC, Wen PH, Wood S. *J Med Chem.* 2011; 54:5836–5857. [PubMed: 21707077]
321. Baxter, EW.; Reitz, AB.; Creighton, CJ. U.S. Pat. 2007. US20070232642
322. Stachel SJ, Steele TG, Petrocchi A, Haugabook SJ, McGaughey G, Katharine Holloway M, Allison T, Munshi S, Zuck P, Colussi D, Tugasheva K, Wolfe A, Graham SL, Vacca JP. *Bioorg Med Chem Lett.* 2012; 22:240–244. [PubMed: 22130130]
323. Efremov IV, Vajdos FF, Borzilleri KA, Capetta S, Chen H, Dorff PH, Dutra JK, Goldstein SW, Mansour M, McColl A, Noell S, Oborski CE, O'Connell TN, O'Sullivan TJ, Pandit J, Wang H, Wei B, Withka JM. *J Med Chem.* 2012; 55:9069–9088. [PubMed: 22468999]
324. Huang Y, Strobel ED, Ho CY, Reynolds CH, Conway KA, Piesvaux JA, Brenneman DE, Yohrling GJ, Moore Arnold H, Rosenthal D, Alexander RS, Tounge BA, Mercken M, Vandermeeren M, Parker MH, Reitz AB, Baxter EW. *Bioorg Med Chem Lett.* 2010; 20:3158–3160. [PubMed: 20399652]
325. Iserloh, U.; Zhu, Z.; Stamford, A.; Voigt, JH. U.S. Pat. 2006. US20060281729
326. Baxter, E.; Reitz, A.; Parker, MH.; Huang, Y.; Ho, CY.; Strobel, E.; Reynolds, CH. U.S. Pat. 2007. US20070232630
327. Nantermet, PG.; Holloway, MK.; Moore, KP.; Stauffer, SR. Int. Pat. 2008. WO2008045250
328. Shi, S.; Gerritz, S.; Zhu, S. U.S. Pat. 2008. US20080262055
329. Wu, YJ.; Gerritz, S.; Shi, S.; Zhu, S. U.S. Pat. 2008. US20080139523
330. Coburn CA, Stachel SJ, Li YM, Rush DM, Steele TG, Chen-Dodson E, Holloway MK, Xu M, Huang Q, Lai MT, DiMuzio J, Crouthamel MC, Shi XP, Sardana V, Chen Z, Munshi S, Kuo L, Makara GM, Annis DA, Tadikonda PK, Nash HM, Vacca JP, Wang T. *J Med Chem.* 2004; 47:6117–6119. [PubMed: 15566281]
331. Garino C, Tomita T, Pietrancosta N, Laras Y, Rosas R, Herbette G, Maignet B, Quelever G, Iwatsubo T, Kraus JL. *J Med Chem.* 2006; 49:4275–4285. [PubMed: 16821787]
332. Garino C, Pietrancosta N, Laras Y, Moret V, Rolland A, Quelever G, Kraus JL. *Bioorg Med Chem Lett.* 2006; 16:1995–1999. [PubMed: 16412632]
333. Piazza L, Cavalli A, Colizzi F, Belluti F, Bartolini M, Mancini F, Recanatini M, Andrisano V, Rampa A. *Bioorg Med Chem Lett.* 2008; 18:423–426. [PubMed: 17998161]
334. Kuglstatter A, Stahl M, Peters JU, Huber W, Stihle M, Schlatter D, Benz J, Ruf A, Roth D, Enderle T, Hennig M. *Bioorg Med Chem Lett.* 2008; 18:1304–1307. [PubMed: 18226904]
335. Brodney MA, Barreiro G, Ogilvie K, Hajos-Korcsok E, Murray J, Vajdos F, Ambroise C, Christoffersen C, Fisher K, Lanyon L, Liu J, Nolan CE, Withka JM, Borzilleri KA, Efremov I, Oborski CE, Varghese A, O'Neill BT. *J Med Chem.* 2012; 55:9224–9239. [PubMed: 22984865]
336. Jeon S-Y, Bae K, Seong Y-H, Song K-S. *Bioorganic & Medicinal Chemistry Letters.* 2003; 13:3905–3908. [PubMed: 14592472]
337. Cho JK, Ryu YB, Curtis-Long MJ, Kim JY, Kim D, Lee S, Lee WS, Park KH. *Bioorg Med Chem Lett.* 2011; 21:2945–2948. [PubMed: 21511472]
338. Dai J, Shen D, Yoshida WY, Parrish SM, Williams PG. *Planta Med.* 2012; 78:1357–1362. [PubMed: 22763739]
339. Takahashi K, Sasaki H, Kitoh Y, Miki K, Kinoshita K, Koyama K, Kaneda M. *Heterocycles.* 2012; 85:2749.
340. Kashima Y, Miyazawa M. *Journal of Oleo Science.* 2013; 62:391–401. [PubMed: 23728330]
341. Youn K, Jun M. *Planta Med.* 2013; 79:1038–1042. [PubMed: 23877922]
342. Youn K, Jeong WS, Jun M. *Nat Prod Res.* 2013; 27:1471–1474. [PubMed: 22931211]
343. Huang D, Luthi U, Kolb P, Edler K, Cecchini M, Audetat S, Barberis A, Caflisch A. *J Med Chem.* 2005; 48:5108–5111. [PubMed: 16078830]
344. Huang D, Luthi U, Kolb P, Cecchini M, Barberis A, Caflisch A. *J Am Chem Soc.* 2006; 128:5436–5443. [PubMed: 16620115]

345. Xu W, Chen G, Liew OW, Zuo Z, Jiang H, Zhu W. *Bioorg Med Chem Lett*. 2009; 19:3188–3192. [PubMed: 19447035]
346. Yi Mok N, Chadwick J, Kellett KA, Hooper NM, Johnson AP, Fishwick CW. *Bioorg Med Chem Lett*. 2009; 19:6770–6774. [PubMed: 19854048]
347. Xu W, Chen G, Zhu W, Zuo Z. *Bioorg Med Chem Lett*. 2010; 20:5763–5766. [PubMed: 20732815]
348. Xu W, Chen G, Zhu W, Zuo Z. *Bioorg Med Chem Lett*. 2010; 20:6203–6207. [PubMed: 20850315]
349. Chiriano G, Sartini A, Mancini F, Andrisano V, Bolognesi ML, Roberti M, Recanatini M, Carloni P, Cavalli A. *Chem Biol Drug Des*. 2011; 77:268–271. [PubMed: 21244641]
350. Hsu, HH. BACE Lead Target for Orchestrated Therapy of Alzheimer's Disease. John, V., editor. John Wiley & Sons, Inc.; Hoboken, NJ, USA: 2010. p. 197-216.
351. AstraZeneca. Clinical Study Report Synopsis. 2012
352. May PC, Dean RA, Lowe SL, Martenyi F, Sheehan SM, Boggs LN, Monk SA, Mathes BM, Mergott DJ, Watson BM, Stout SL, Timm DE, Smith Labell E, Gonzales CR, Nakano M, Jhee SS, Yen M, Ereshefsky L, Lindstrom TD, Calligaro DO, Cocke PJ, Greg Hall D, Friedrich S, Citron M, Audia JE. *The Journal of neuroscience : the official journal of the Society for Neuroscience*. 2011; 31:16507–16516. [PubMed: 22090477]
353. Merck. M. Newsroom. 2013



COMMON APP MUTATIONS		
Mutation	Type	Effect
K670N/M671L	Swedish	Increase in β -secretase processing

A692G	Flemish	Increased A β aggregation
E693Q	Dutch	Increased A β aggregation
T714I	Austrian	Increase in A β 42 levels
V715M	French	Increase in A β 42 levels
I716V	Florida	Increase in A β 42 levels
V717L/V717F	Indiana/London	Increase in A β 42 levels
L723P	Australian	Increase in A β 42 levels

Figure 1.
APP processing pathways and common mutations (red)

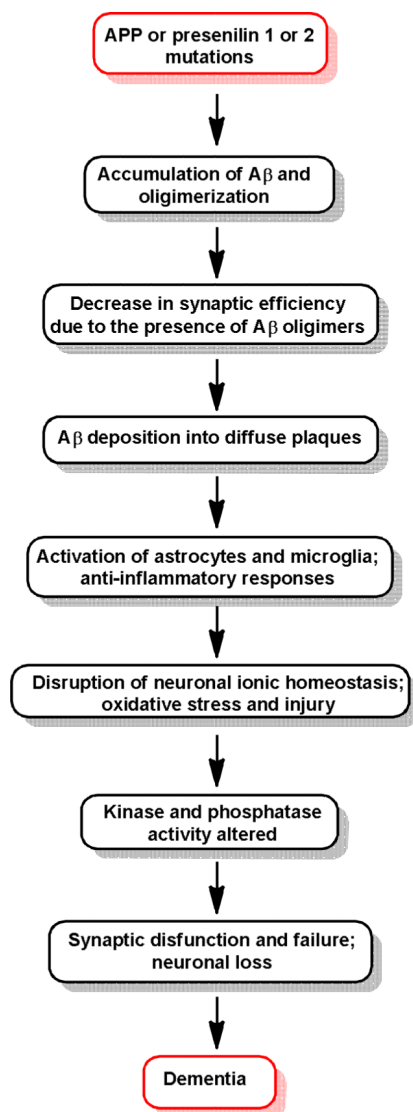


Figure 2. The amyloid hypothesis of the progression of Alzheimer's disease³⁴

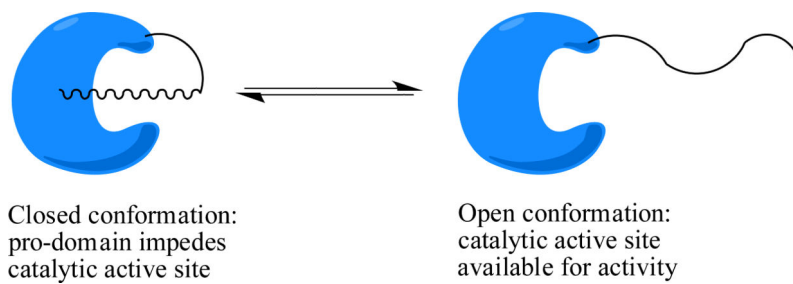


Figure 3.
Open and closed conformations of pro-BACE1

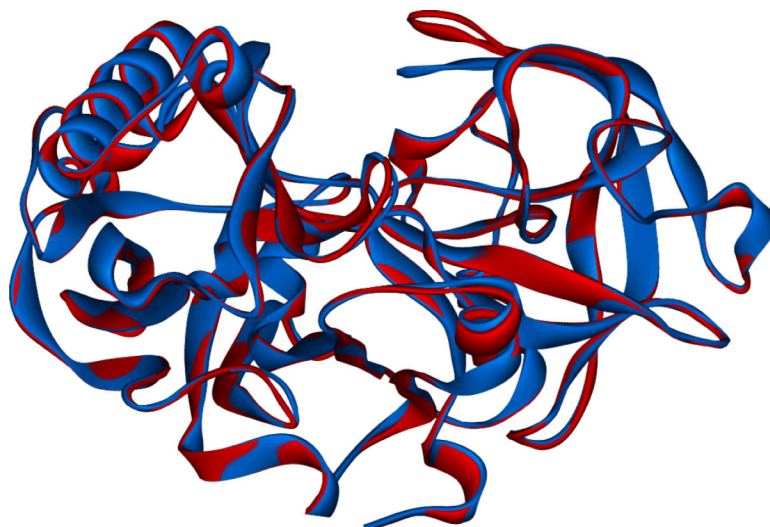


Figure 4. Open flap (red, PDB: 1SGZ) and closed flap (blue, PDB: 1M4H) conformations of mature BACE1

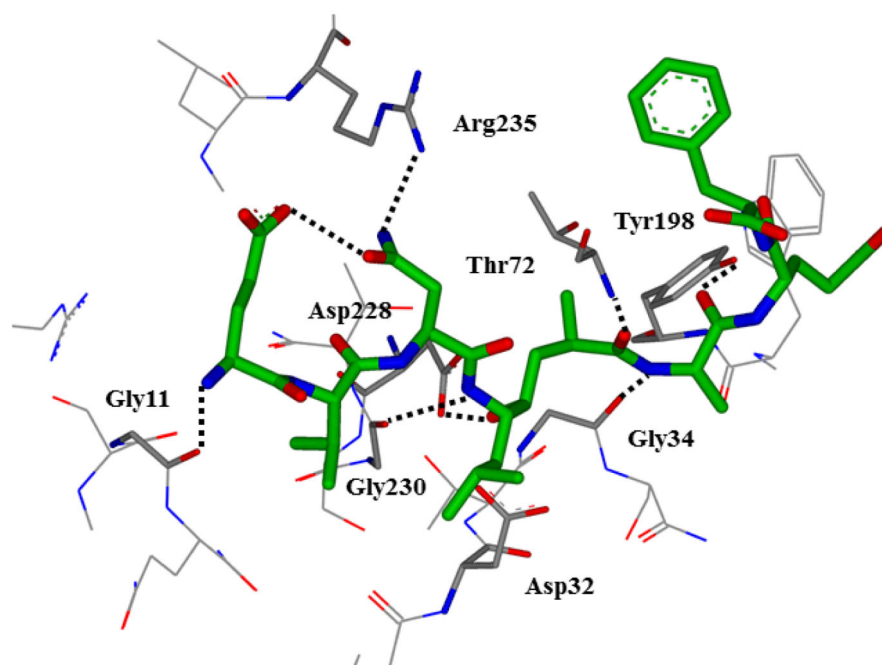
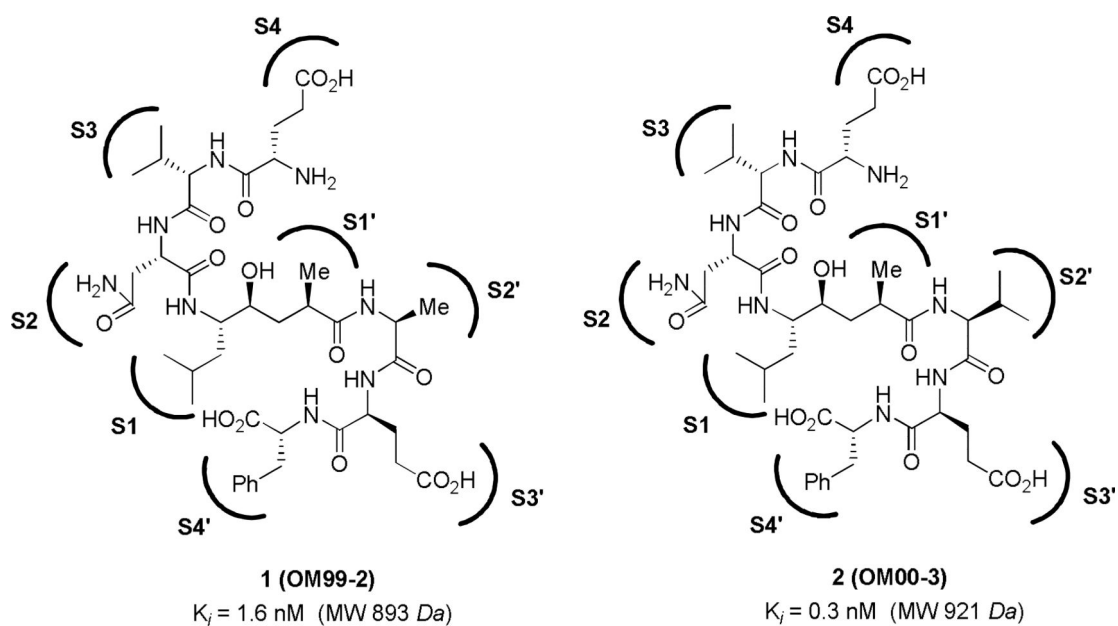


Figure 5. Structures and activity of substrate-based design inhibitors **1** and **2**. Crystal structure of inhibitor **1** (green) in the BACE1 active site (gray). PDB: 1FKN Hydrogen bonds are shown as black dashed lines. Nonbonding residues are shown as gray lines.

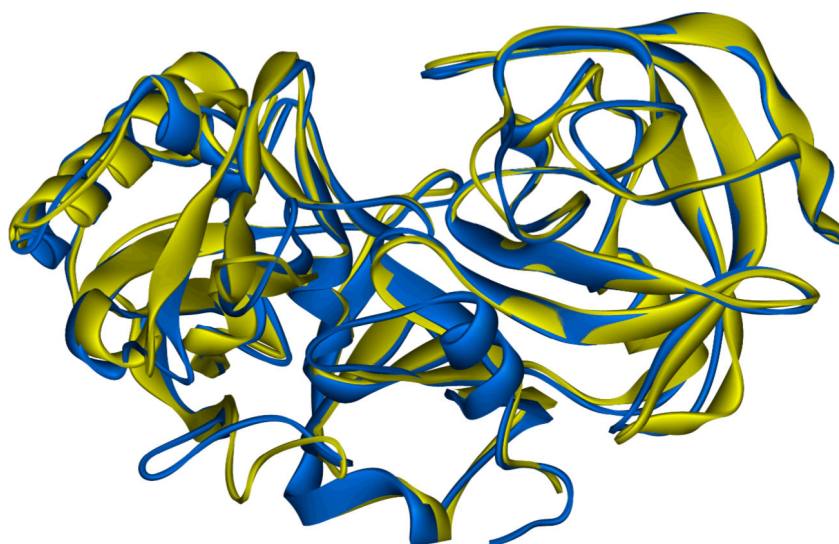


Figure 6. Overlay of inhibitor-bound BACE1 (blue, PDB:1FKN) and inhibitor bound BACE2 (yellow, PDB:2EWY) Inhibitors are hidden for clarity.

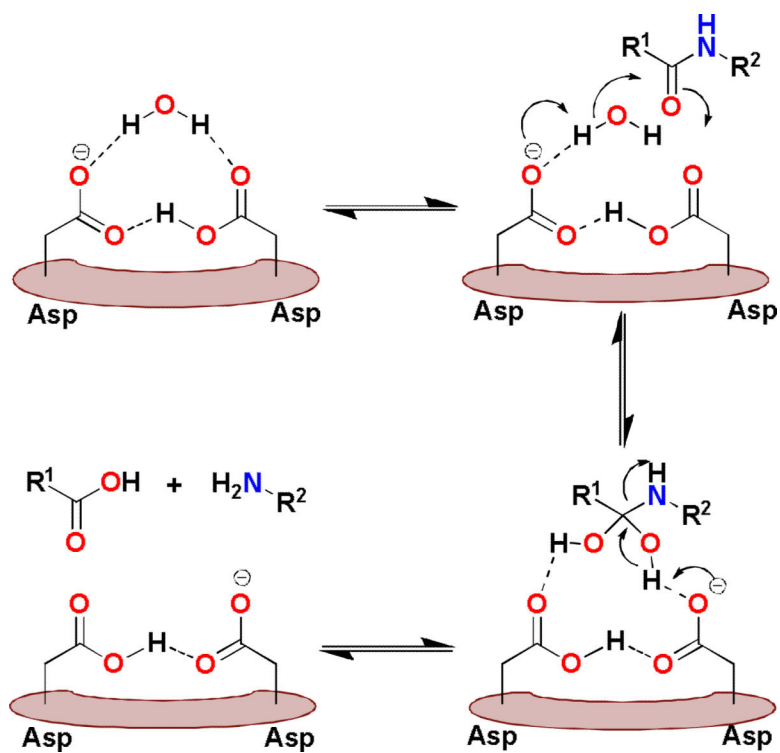


Figure 7.
Mechanism of aspartic acid protease catalytic action

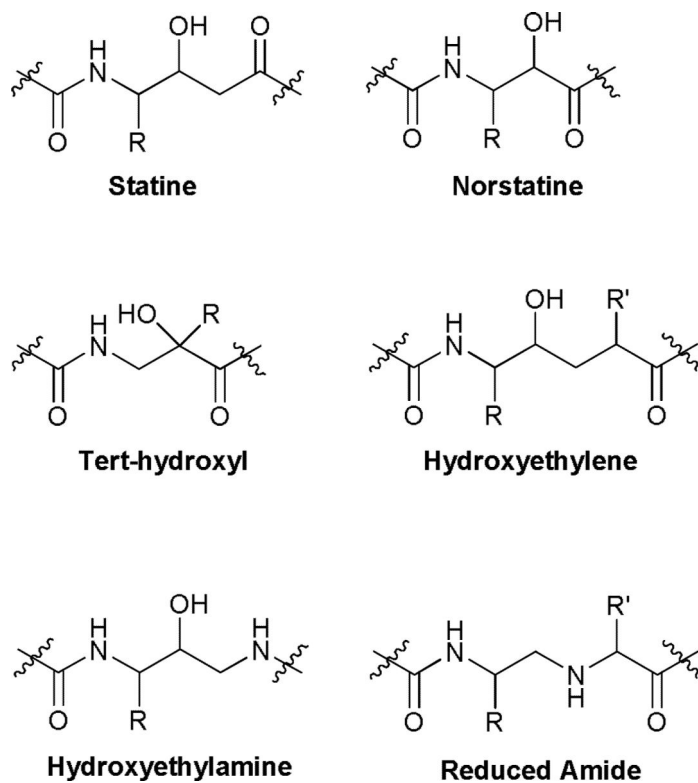


Figure 8.
Commonly used transition-state isosteres in peptidomimetic inhibitors

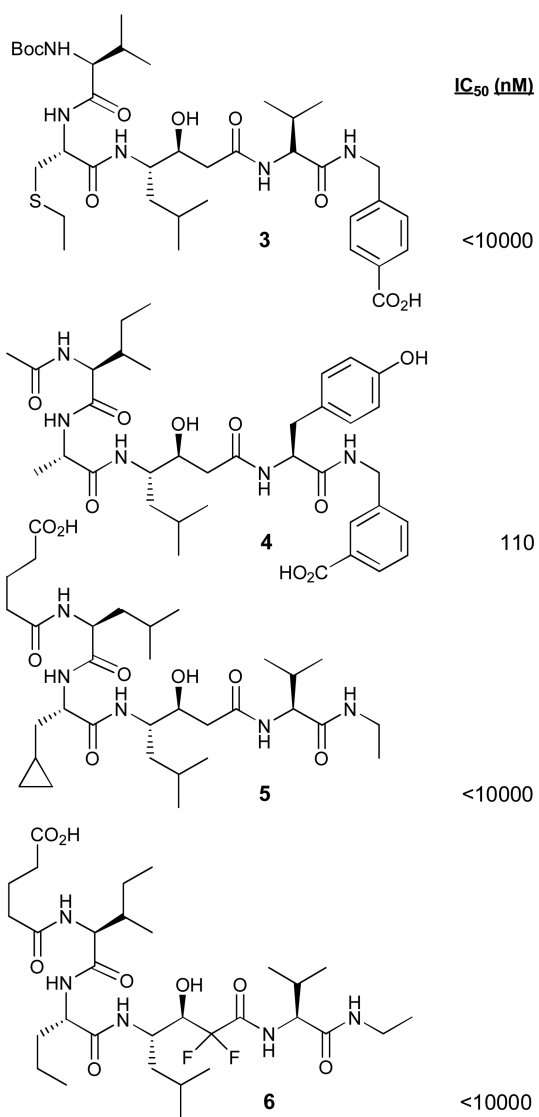


Figure 9.
Statine-based BACE1 inhibitors **3-6**

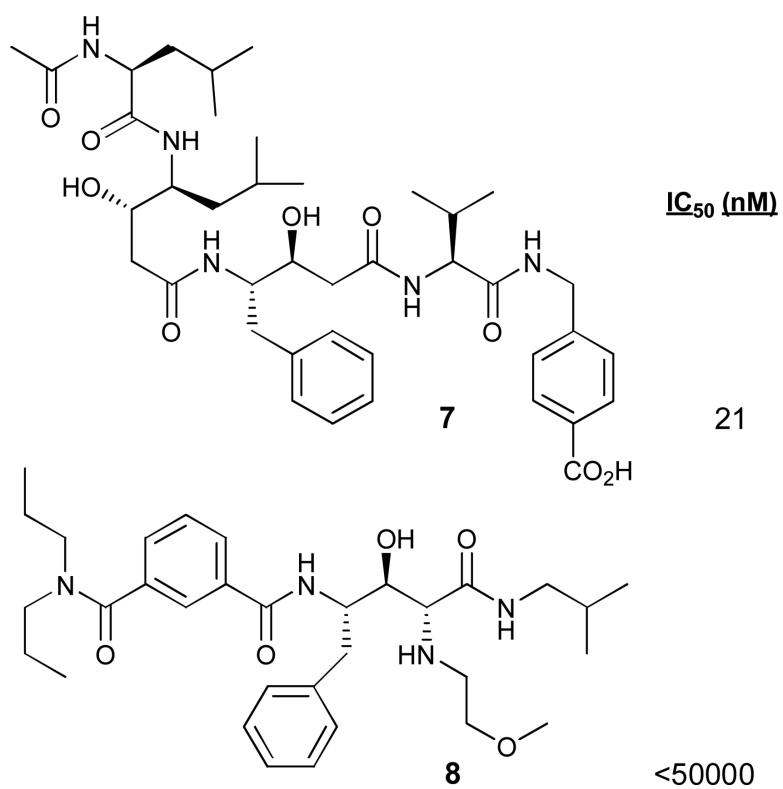


Figure 10.
Phenylstatine derived BACE1 inhibitors **7** and **8**

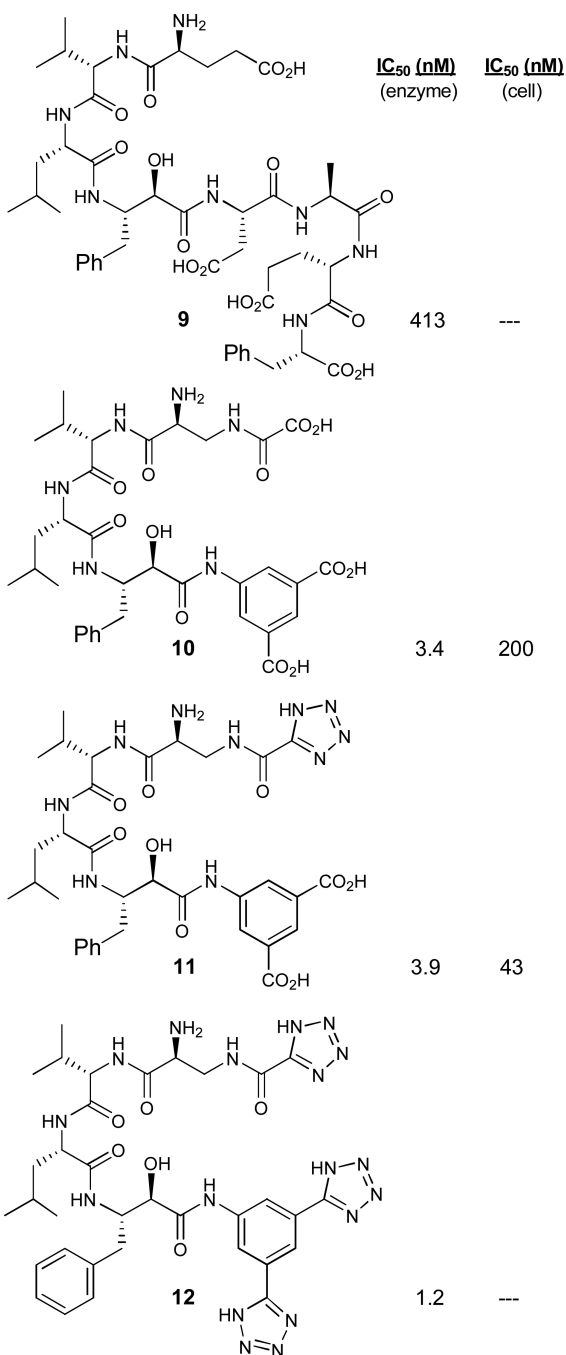


Figure 11.
Development of phenylnorstatine-based BACE1 inhibitors **9-12**

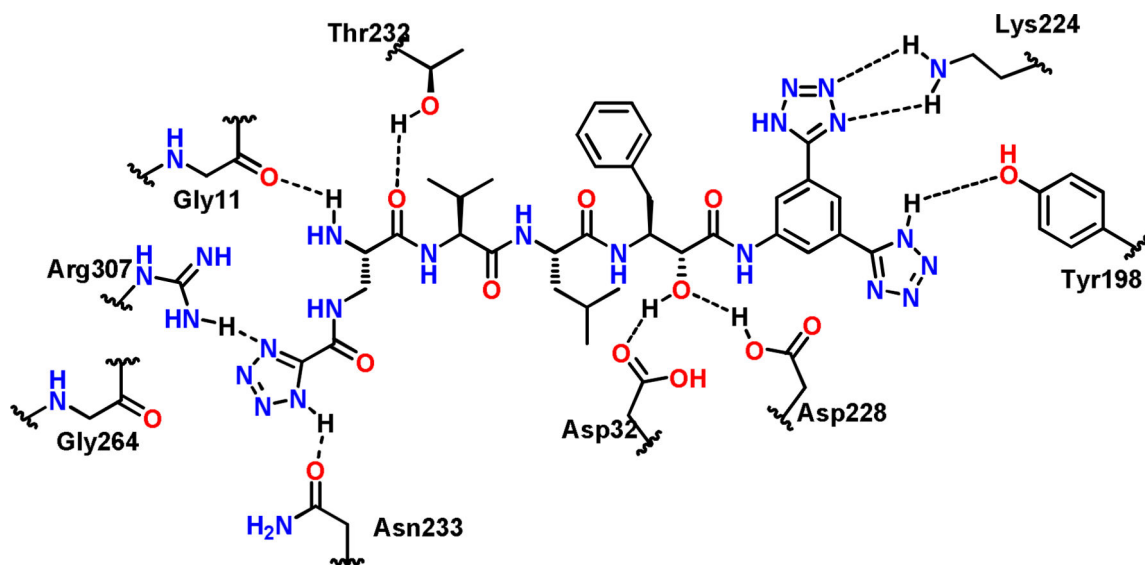


Figure 12.
Binding mode of BACE1 inhibitor 12

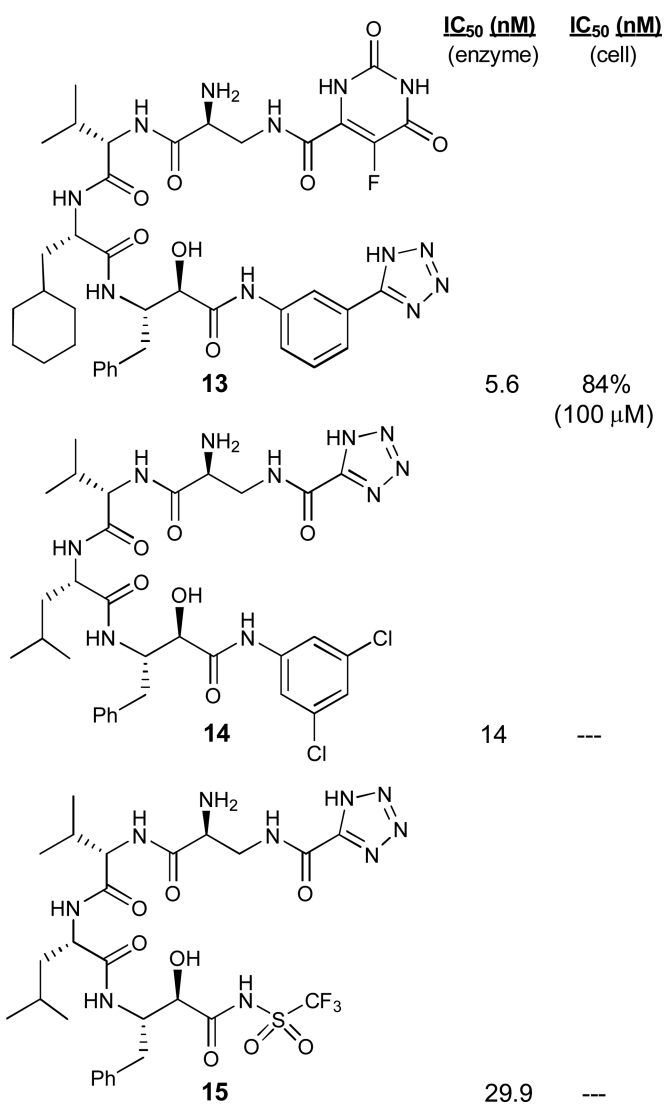


Figure 13.
Optimization of phenylnorstatine inhibitors **13-15**.

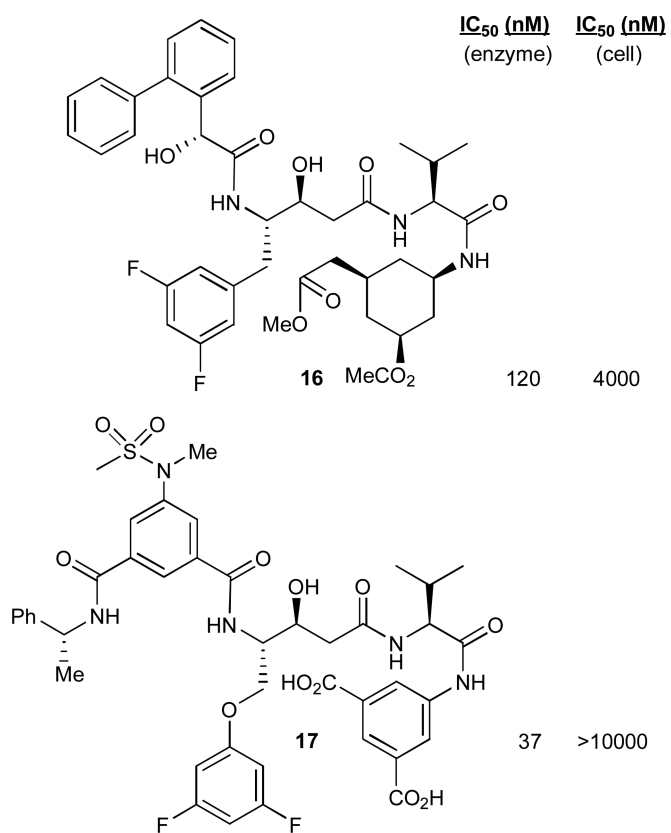


Figure 14.
BACE1 inhibitors **16** and **17** with fluoro-statine derivatives

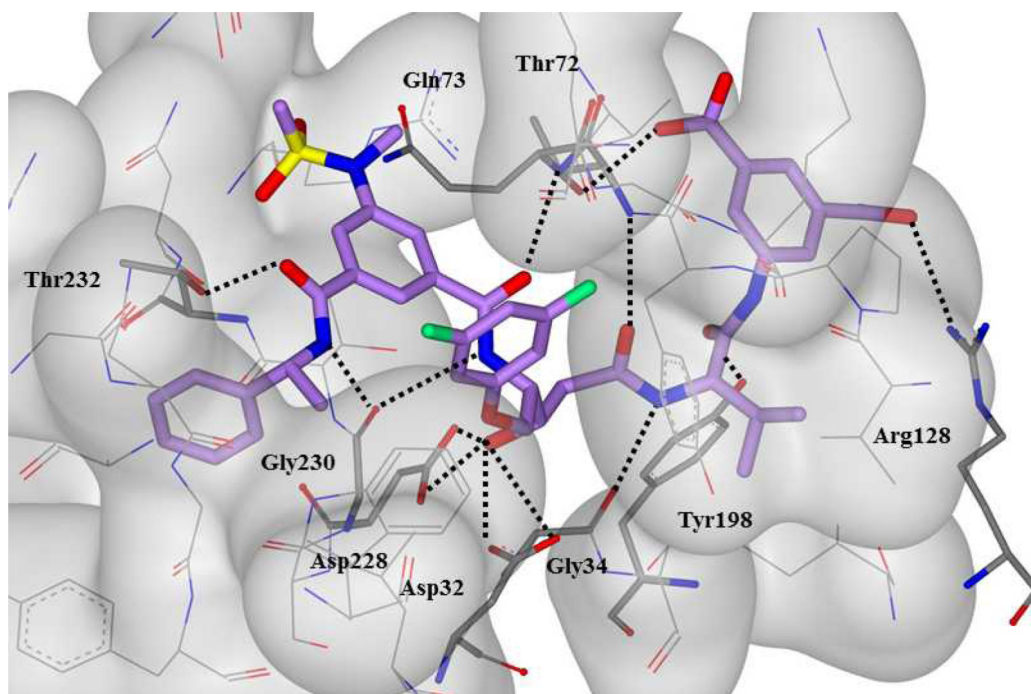


Figure 15.
The X-ray crystal structure of the **17** and BACE1 complex (PDB: 3DM6)

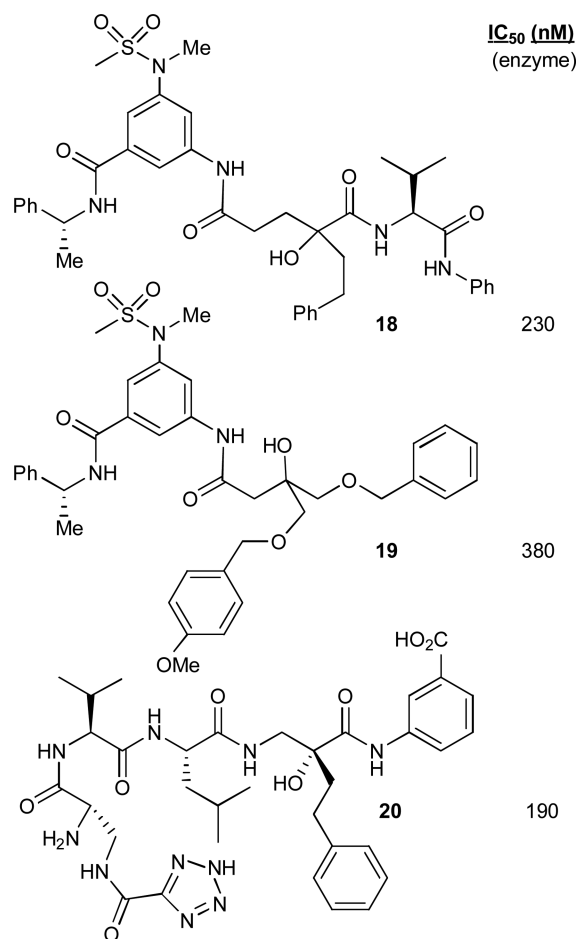


Figure 16.
Exploration of *tert*-hydroxyl isostere containing inhibitors **18-20**.

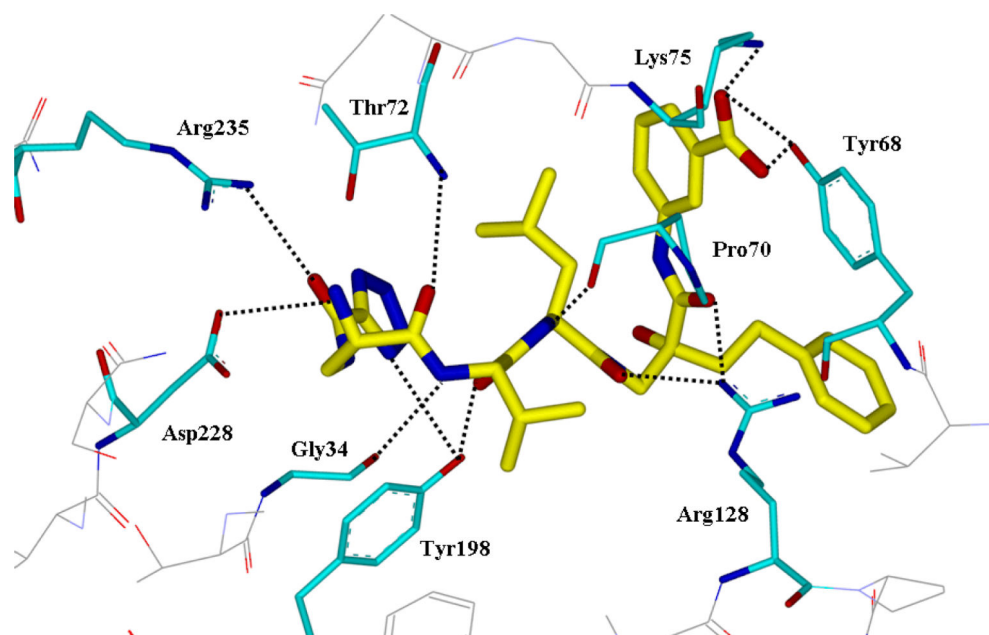


Figure 17.
X-ray crystal structure of inhibitor **20** and BACE1 complex. PDB code:3KYR

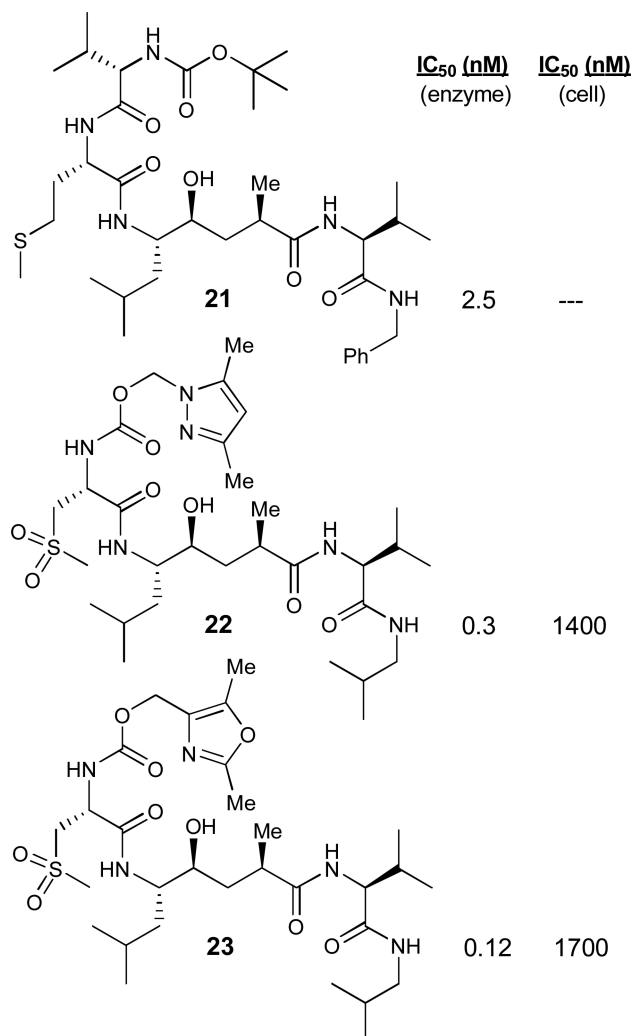


Figure 18. BACE1 inhibitors **21-23** containing Leu-Ala hydroxyethylene isosteres.

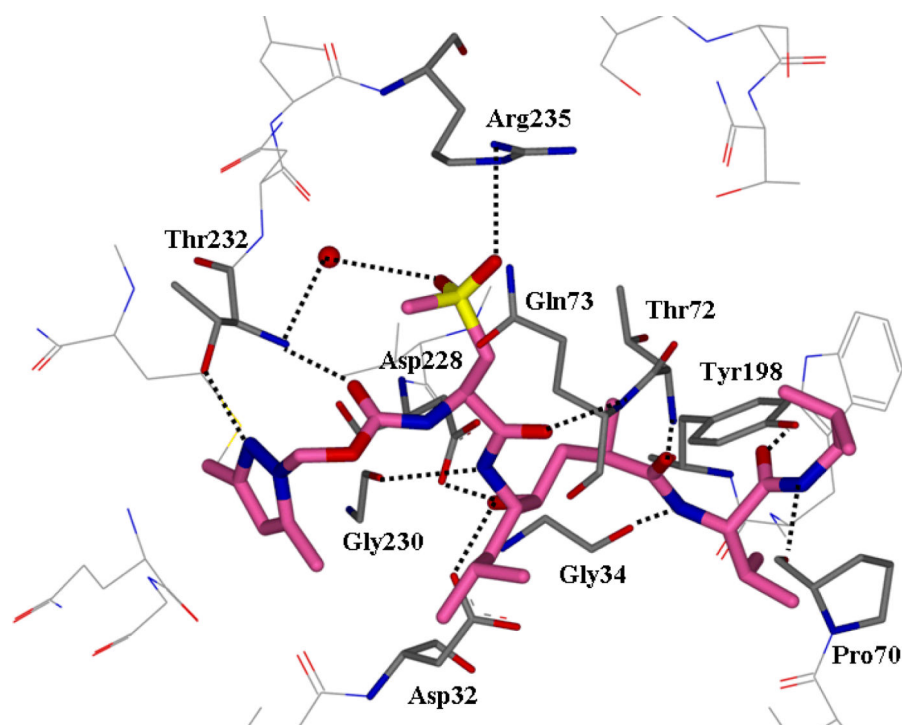


Figure 19.
An X-ray crystal structure of **22** in the BACE1 active site. (PDB: 2G94)

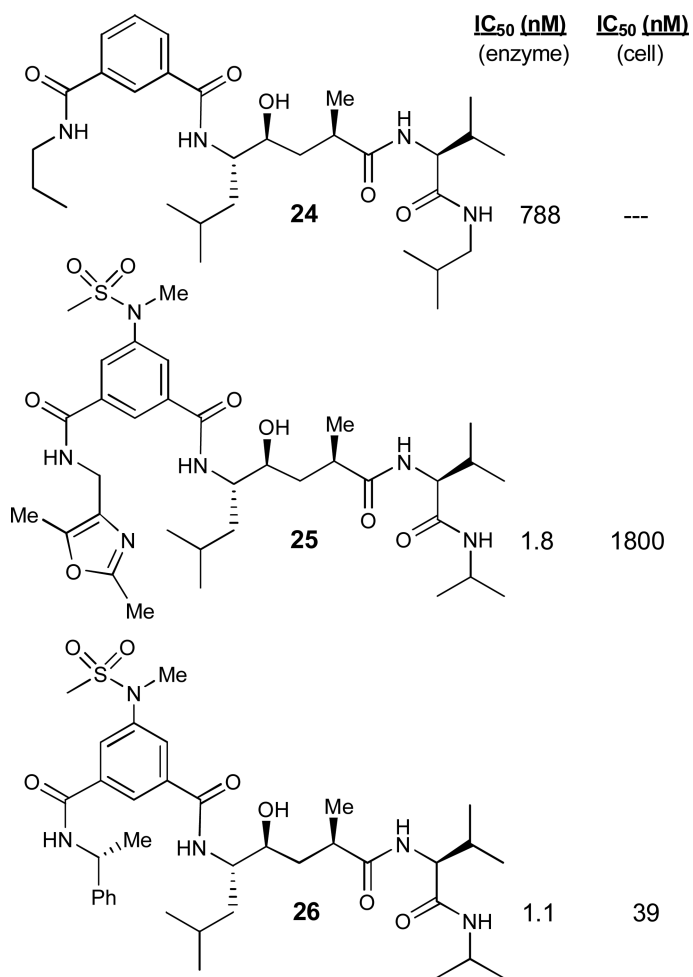


Figure 20.
BACE1 inhibitors **24-26** with Leu-Ala isosteres and P2-isophthalic amides

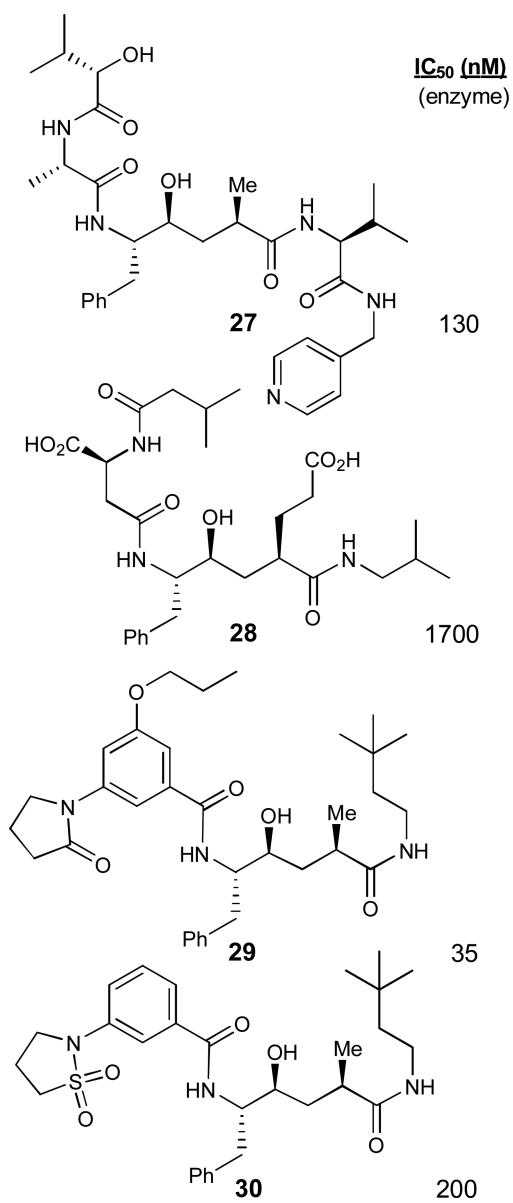


Figure 22.
BACE1 inhibitors **27-30** with other isosteres.

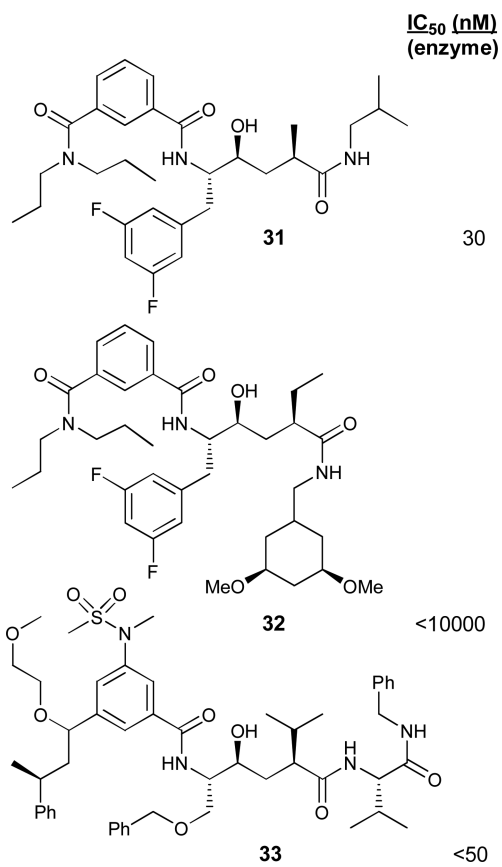


Figure 23.
Structures and activity of inhibitors **31-33**.

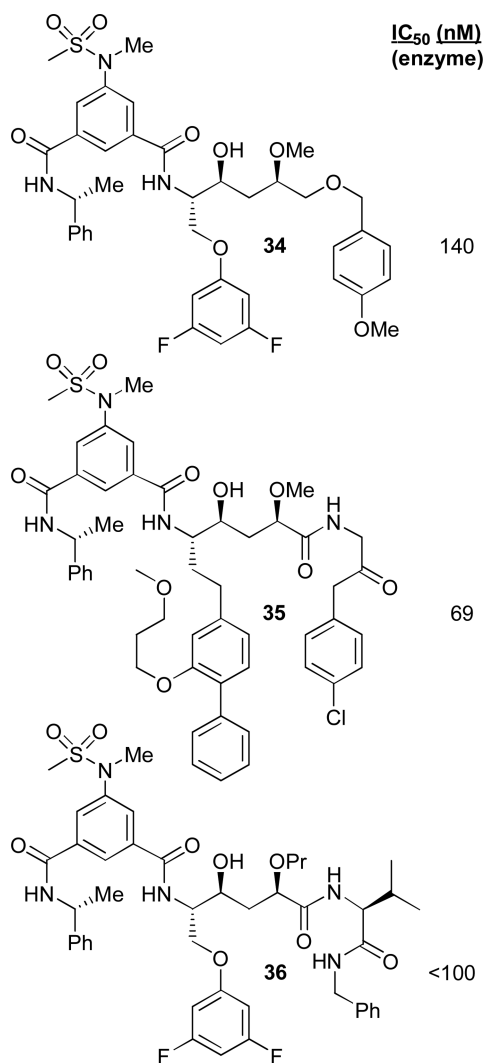


Figure 24. BACE1 inhibitors **34-36** with hydroxyethylene isosteres with designed P1-P1' ligands.

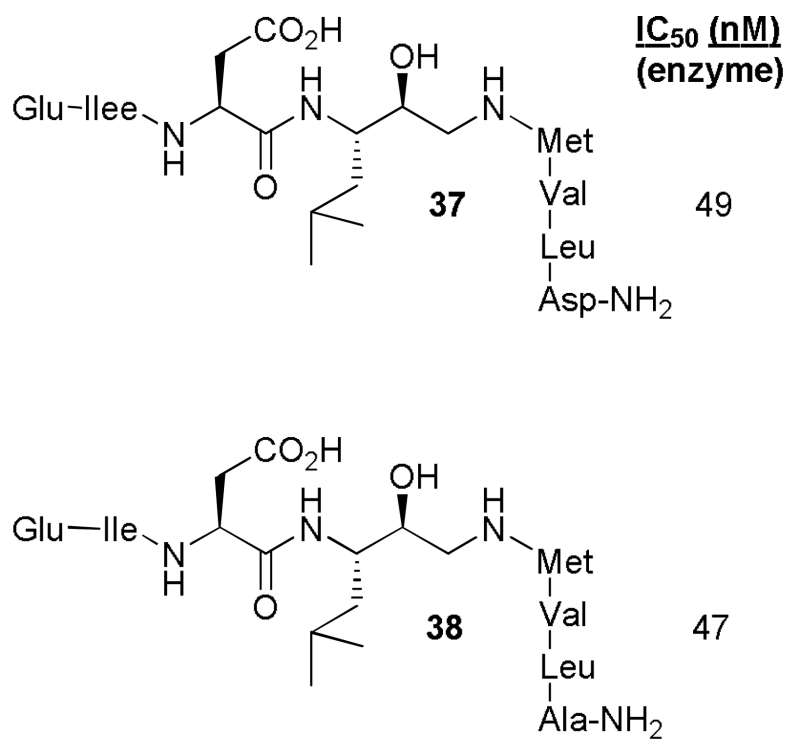


Figure 25.
Pseudo-peptide BACE1 inhibitors **37** and **38**.

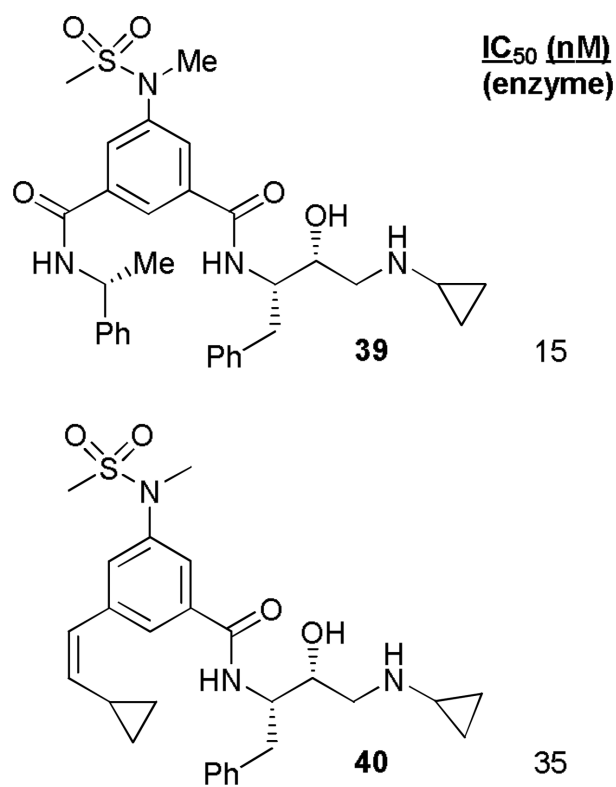


Figure 26.
Structures and activity of inhibitors **39** and **40**.

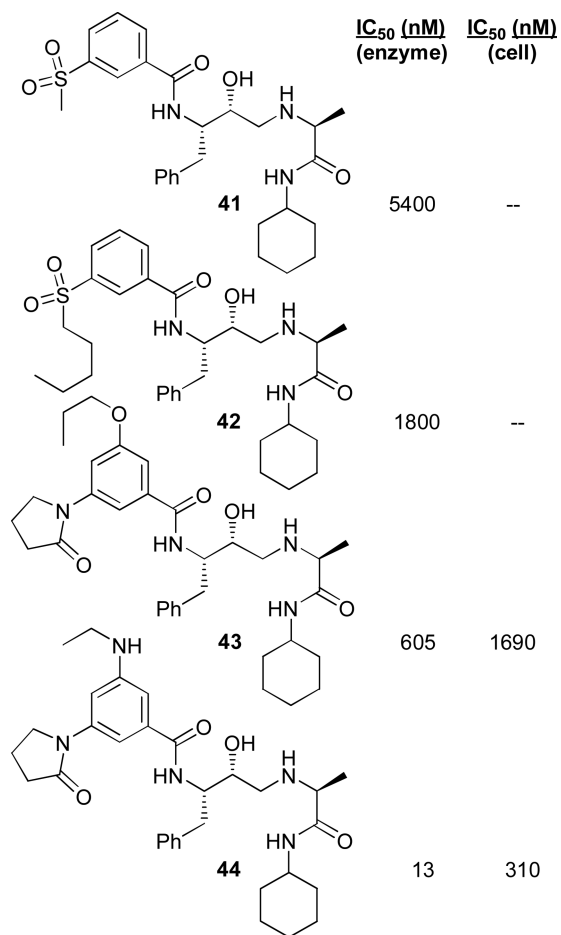


Figure 27.
BACE1 inhibitors **41-44** with P1' Ala derivatives

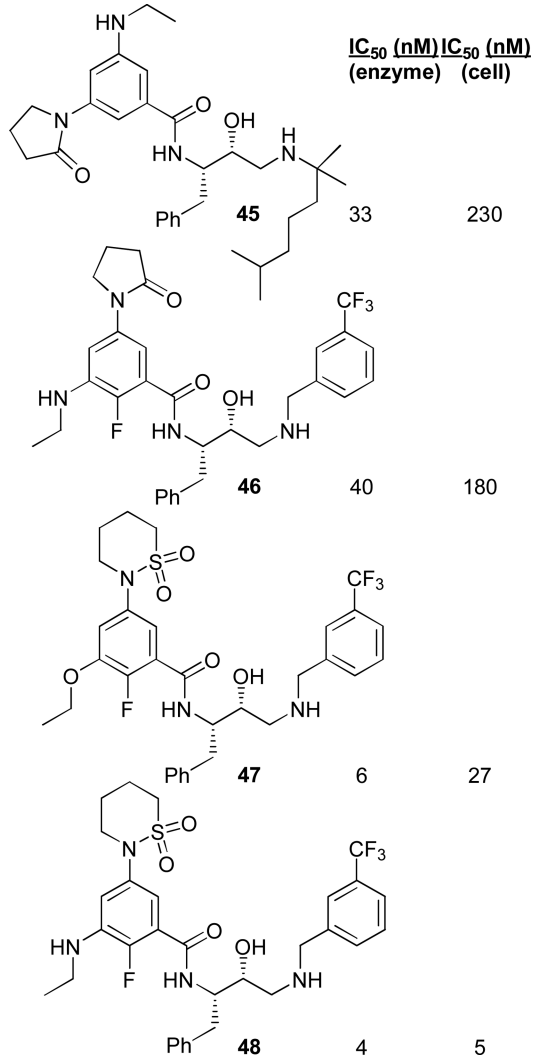


Figure 28.
BACE1 inhibitors **45-48** with P1' alkyl and benzyl derivatives

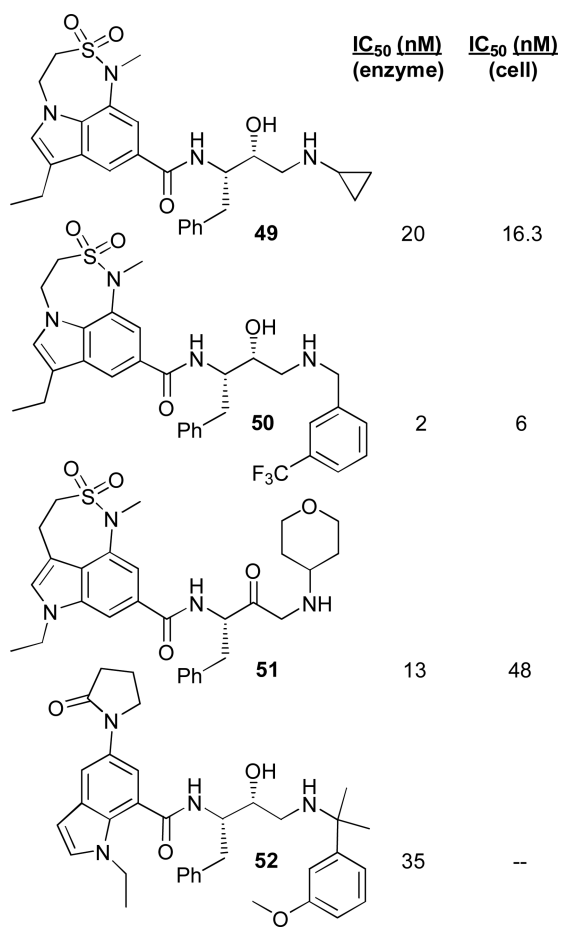


Figure 29.
BACE1 inhibitors **49-52** incorporating a tricyclic sultam and lactam moieties.

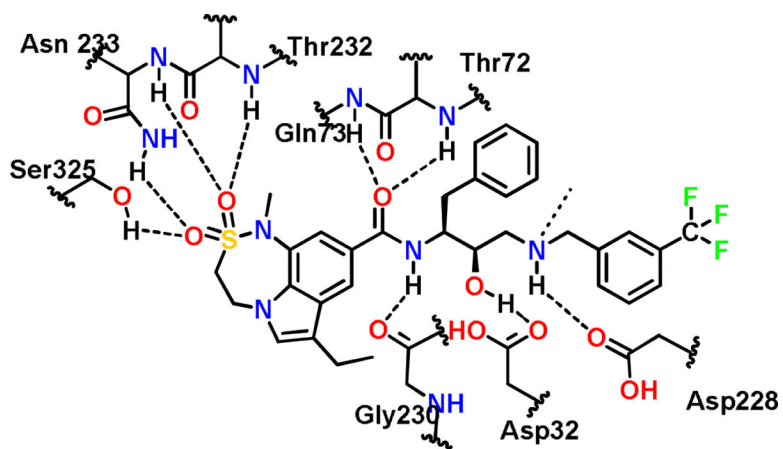


Figure 30.
Binding mode of BACE1 inhibitor 50.

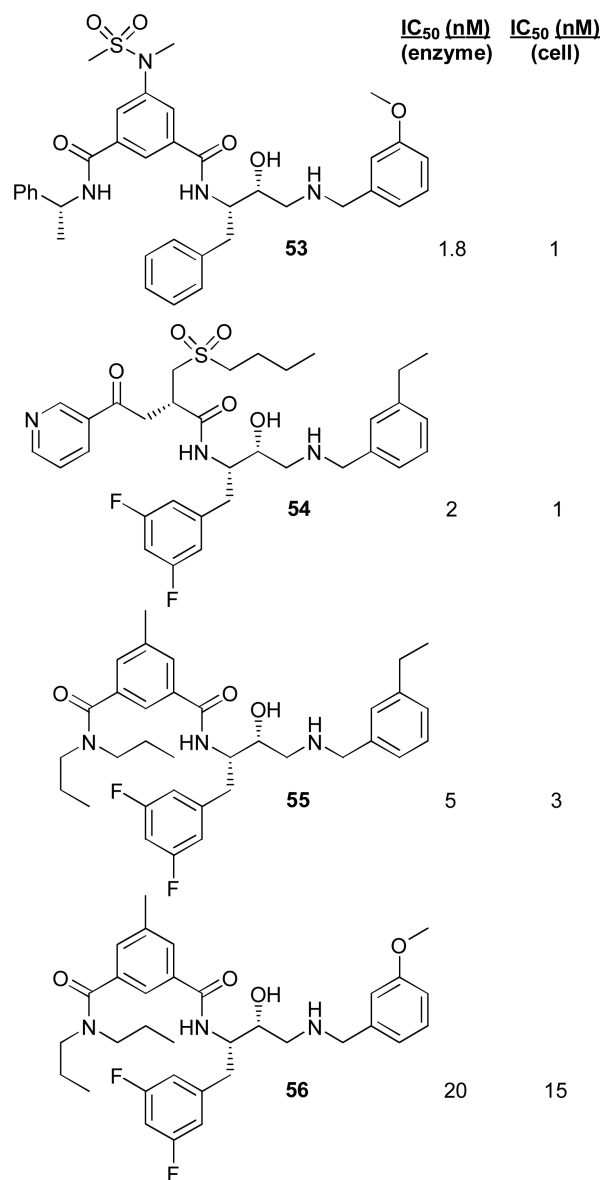


Figure 31.
BACE1 inhibitors **53-56** with a phenylalanine or fluorophenylalanine P1 ligand.

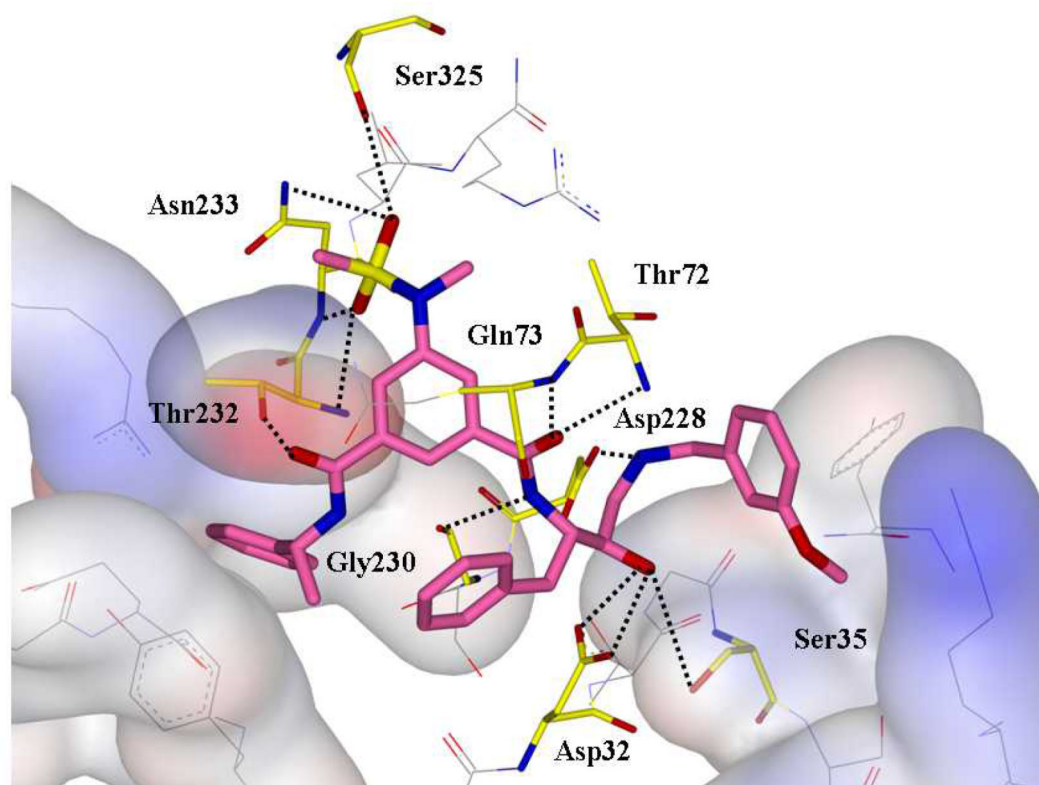


Figure 32.
An X-ray crystal structure of inhibitor **53** and BACE1 complex PDB: 2VKM.

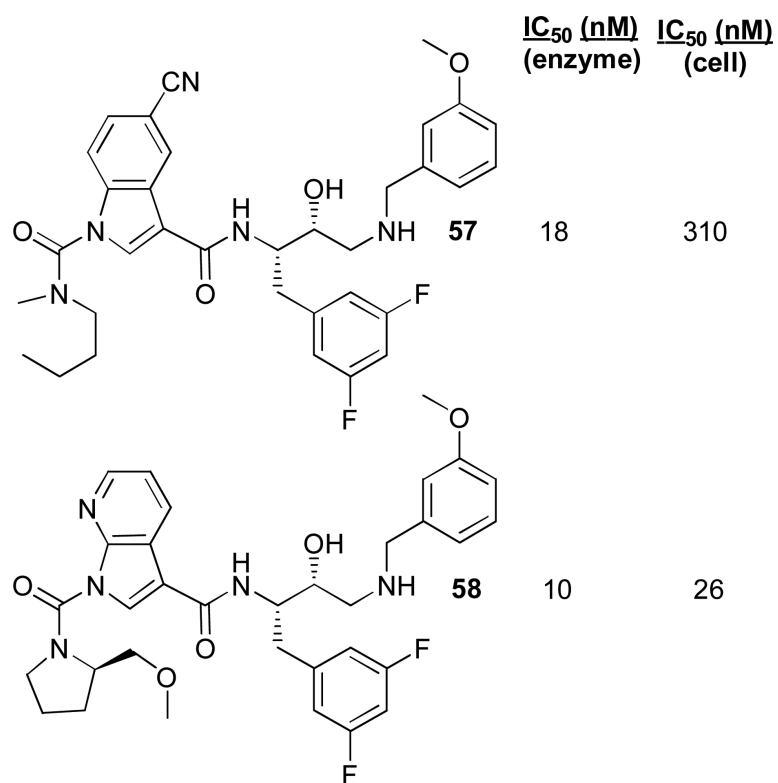


Figure 33.
Structures and activity of inhibitors **57** and **58**.

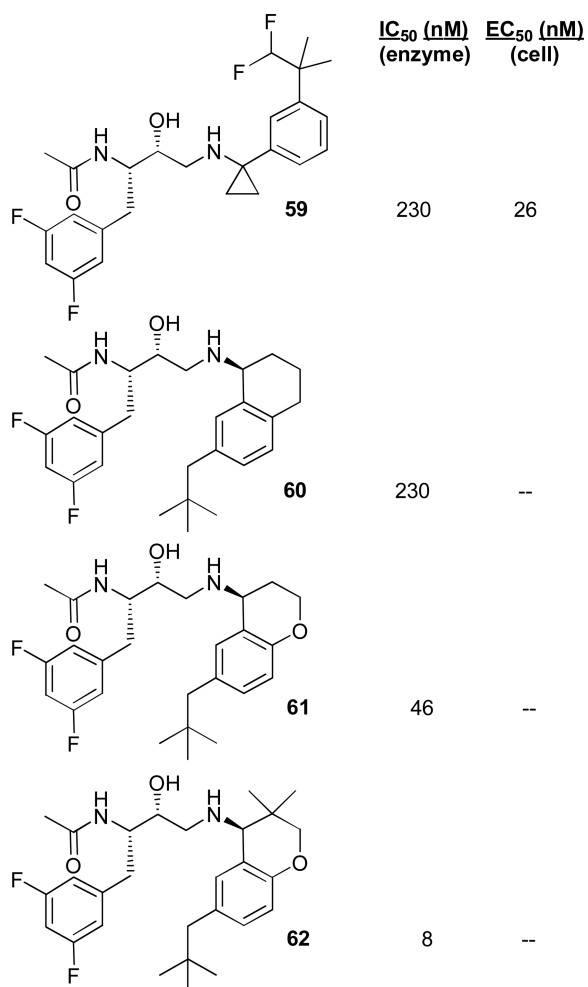


Figure 34.
Structures and activity of inhibitors **59-62**.

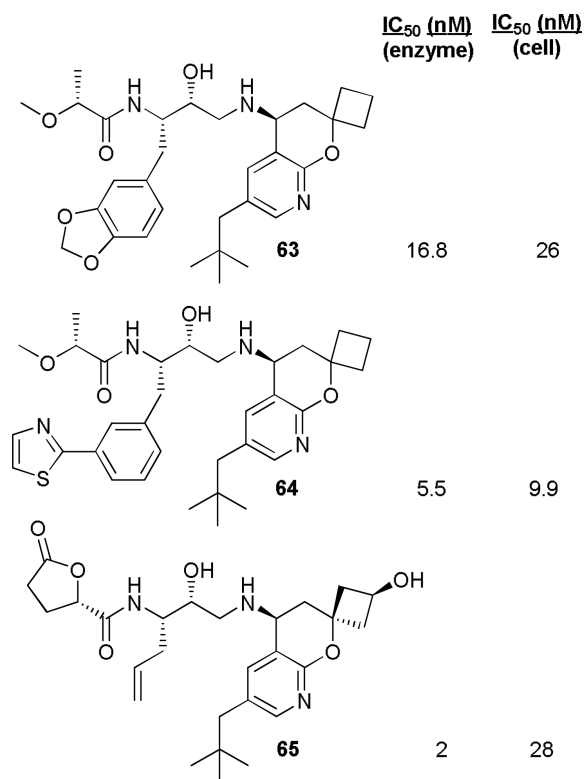


Figure 35.
Structures and activity of inhibitors **63-65**.

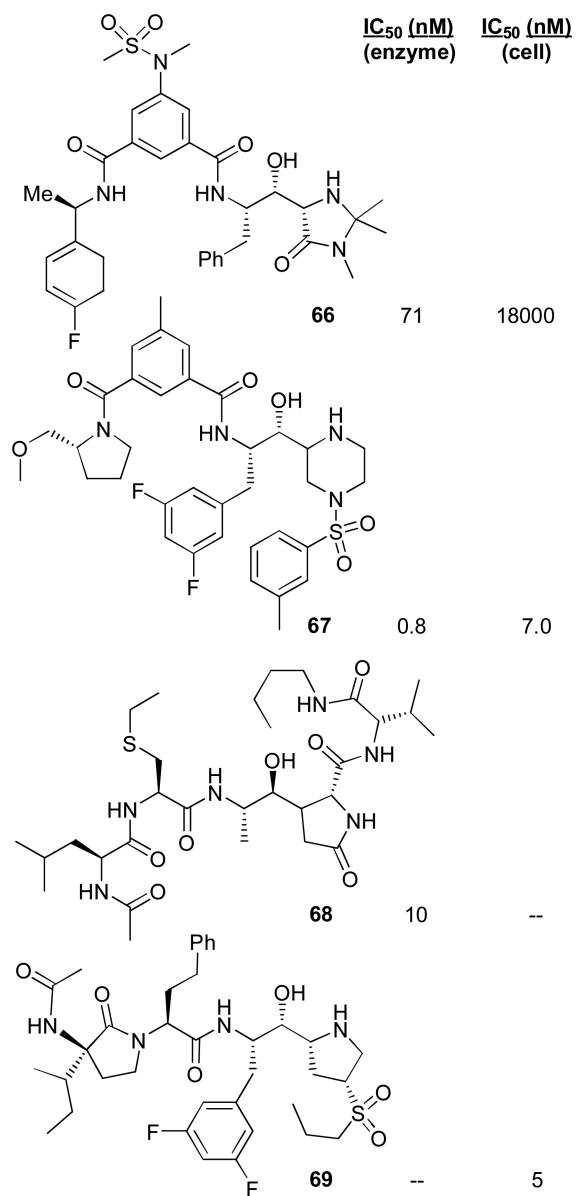


Figure 36.
Structures and activity of inhibitors **66-69**.

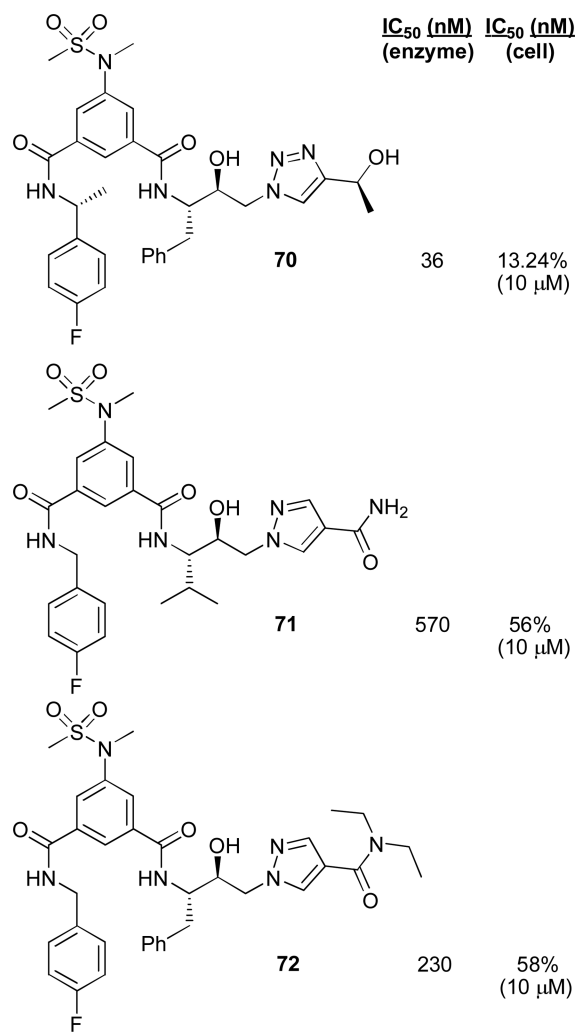


Figure 37.
Structures and activity of inhibitors **70-72**.

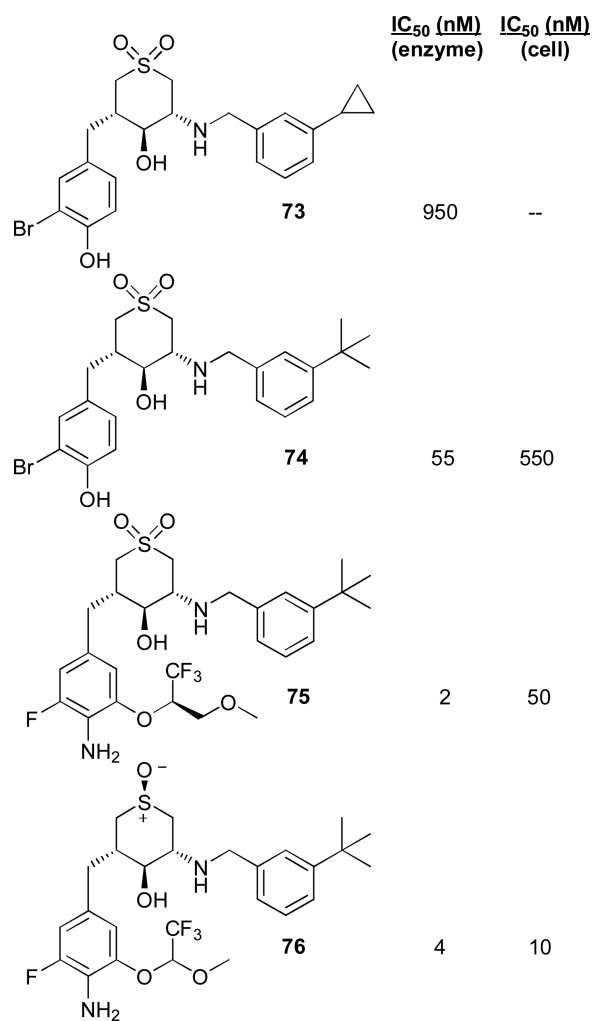


Figure 38.
Structures and activity of compounds **73-76**.

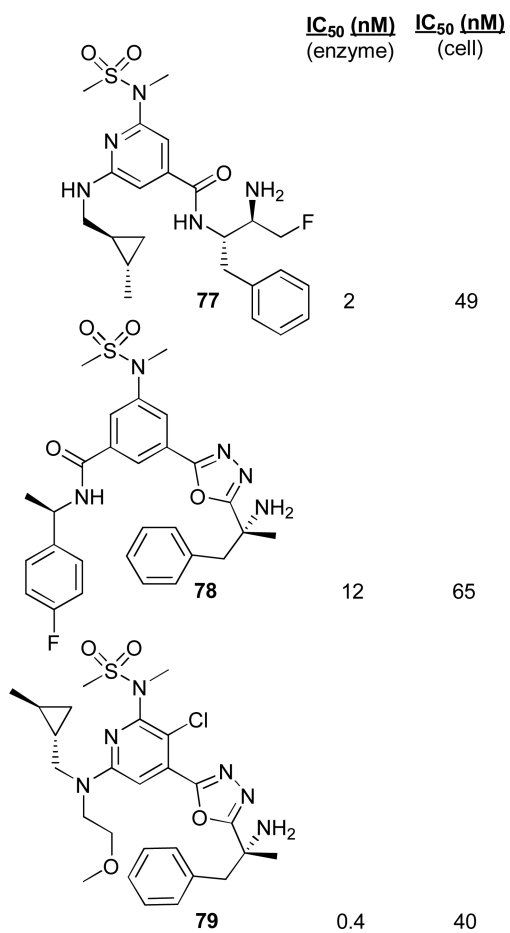


Figure 39.
Structures and activity of compounds **77-79**.

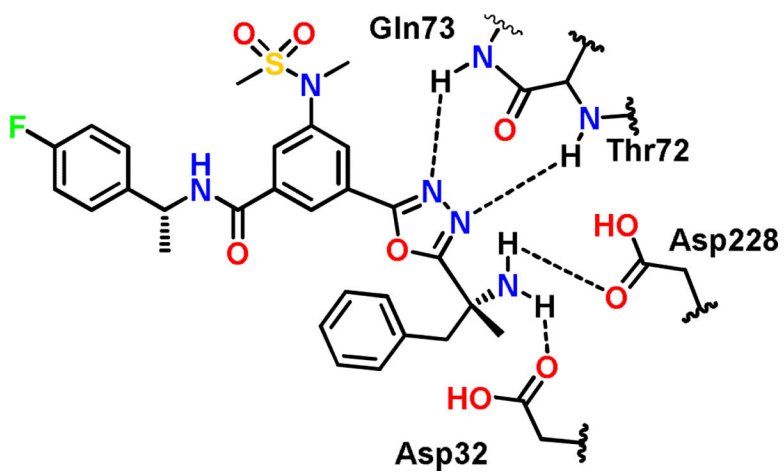


Figure 40.
Binding of compound 78

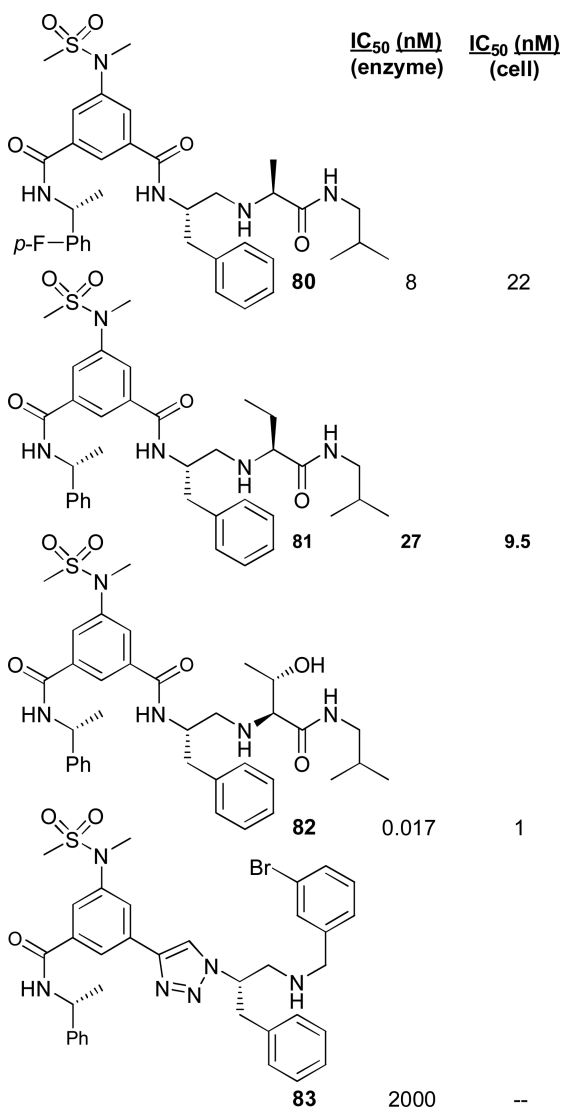


Figure 41.
Structures and activity of reduced amide-based inhibitors **80-83**.

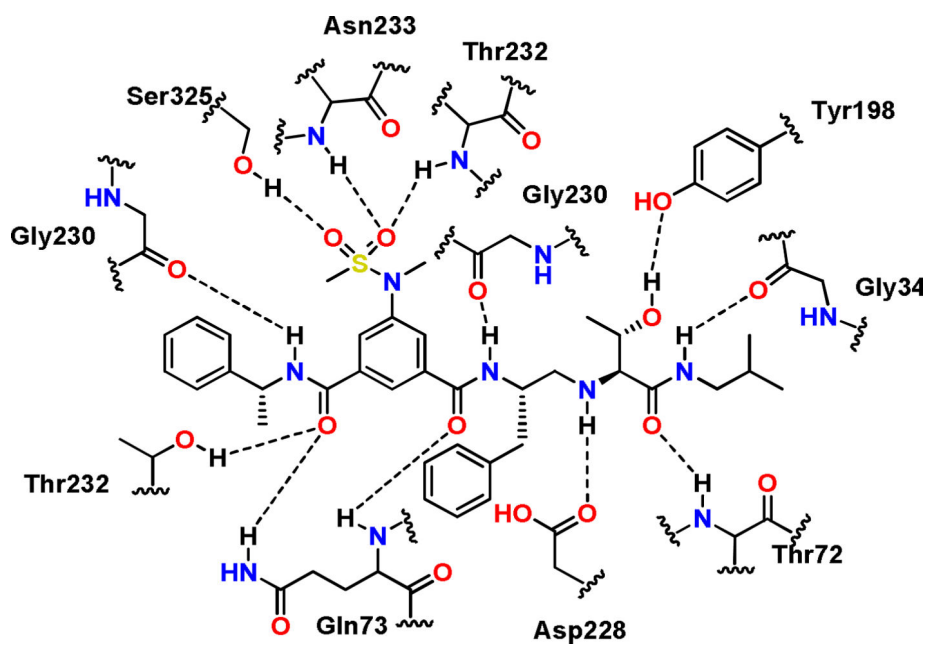
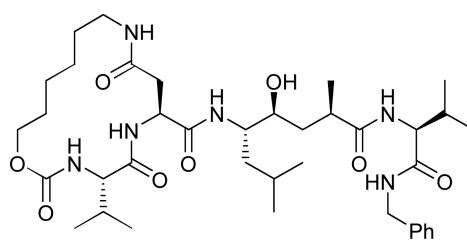
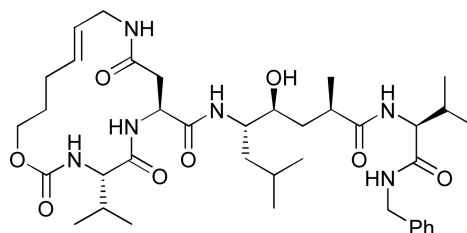


Figure 42.

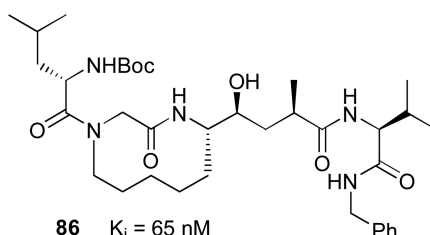
An X-ray structure of **82** and BACE1 complex. PDB code: 4GID



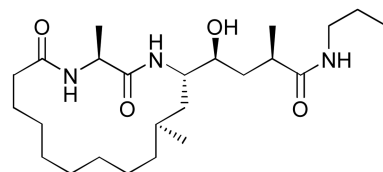
84 $K_i = 25.1 \text{ nM}$
 $IC_{50} (\text{cell}) = 3.9 \mu\text{M}$



85 $K_i = 14.2 \text{ nM}$



86 $K_i = 65 \text{ nM}$
 $IC_{50} (\text{cell}) = 880 \text{ nM}$



87 $K_i = 250 \text{ nM}$
% inhibition (cell) = 27% (10 μM)

Figure 43.
Structures and activity of macrocyclic inhibitors **84-87**.

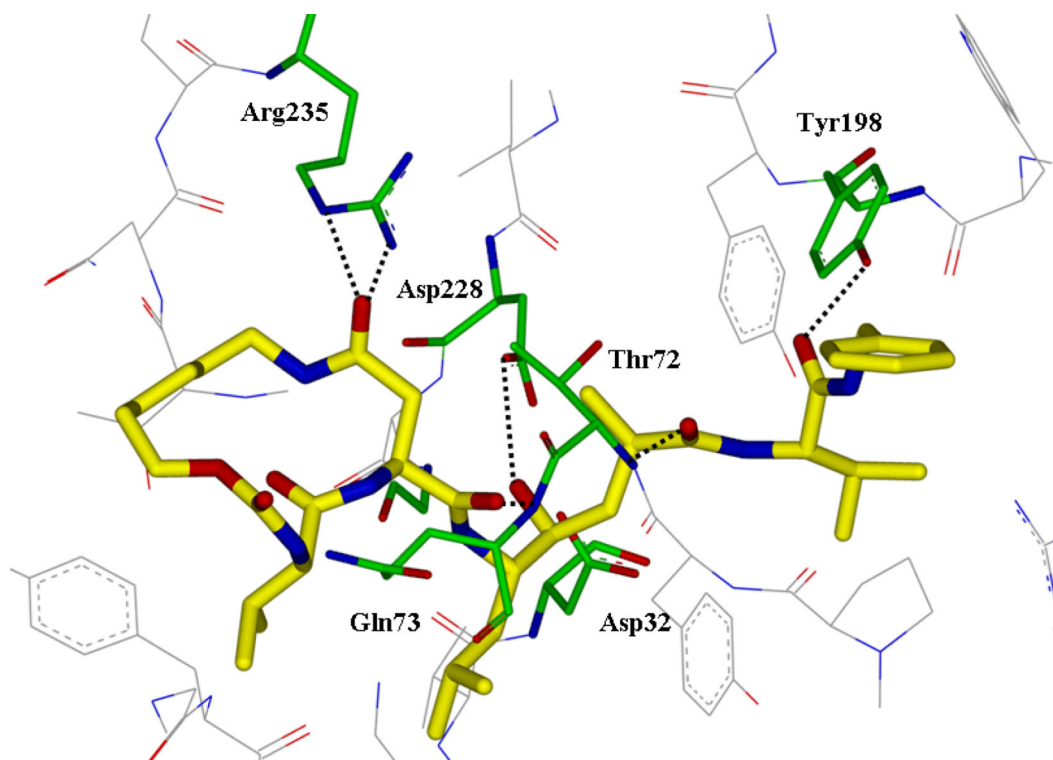


Figure 44.
An X-ray crystal structure of **84** and BACE1 complex. PDB: 1XS7.

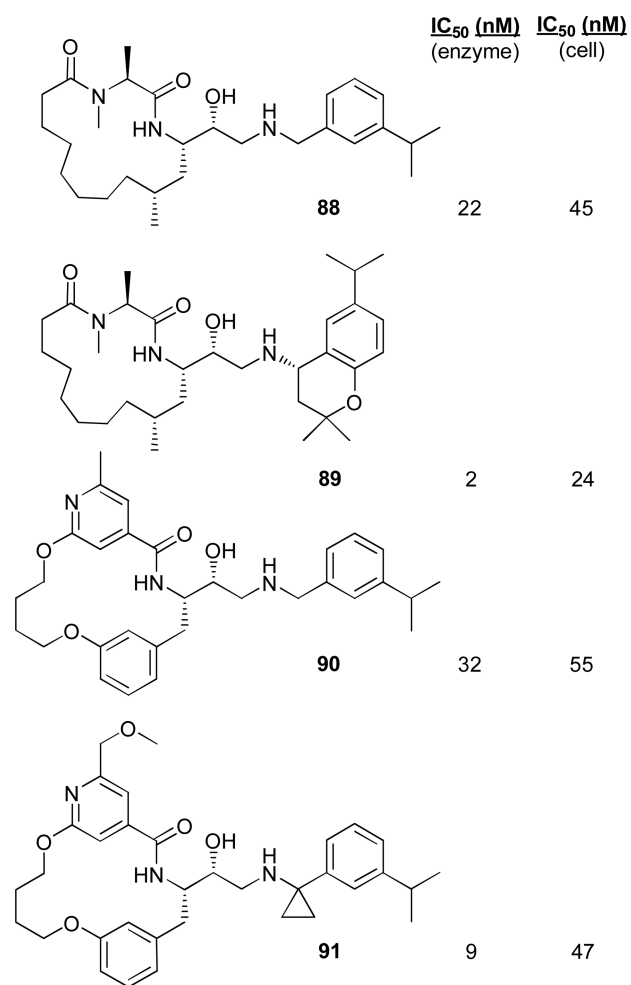


Figure 45.
Structures and activity of macrocyclic inhibitors **88-91**.

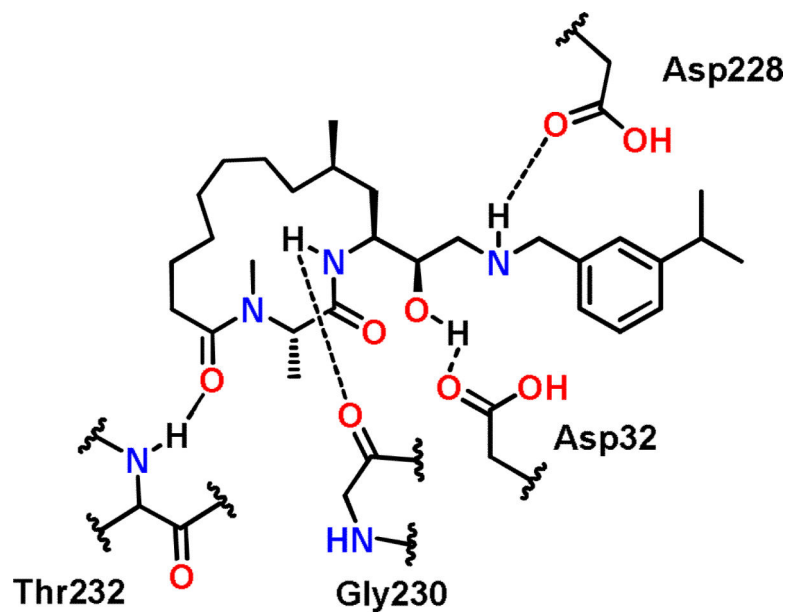


Figure 46.
A binding mode of inhibitor **88** in the BACE1 active site.

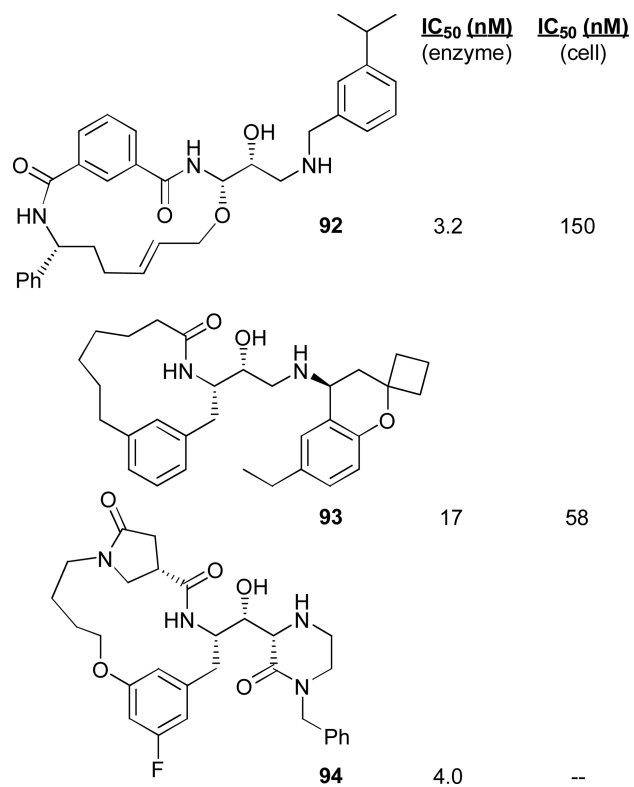


Figure 47.
Structures and activity of macrocyclic inhibitors **92-94**.

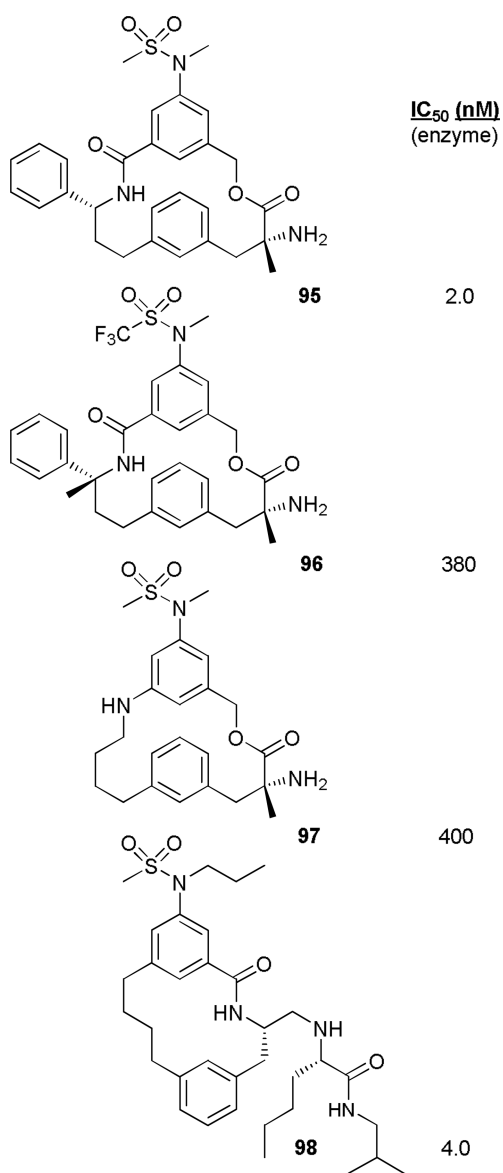


Figure 48.
Structures and activity of carbinamine and reduced amide-derived macrocyclic inhibitors **95-98**.

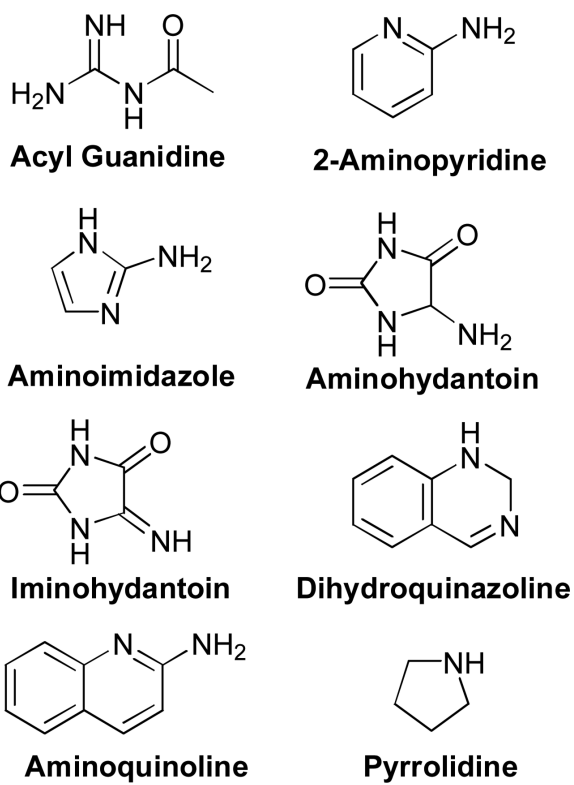


Figure 49.
Nonpeptide scaffolds

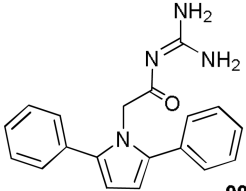
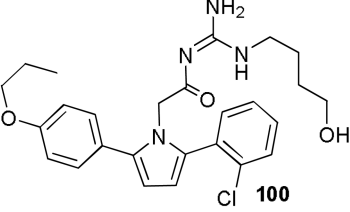
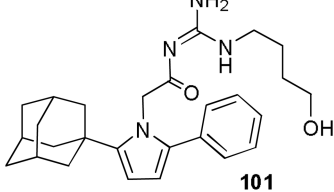
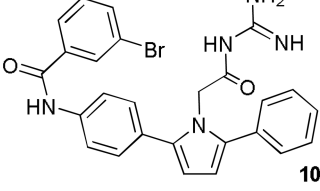
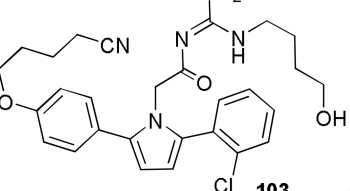
	IC₅₀ (nM) (enzyme)	EC₅₀ (nM) (cell)
 99	3700	--
 100	110	--
 101	239	1840
 102	600	5600
 103	<100	--

Figure 50.
Structures and activity of compounds **99-103**.

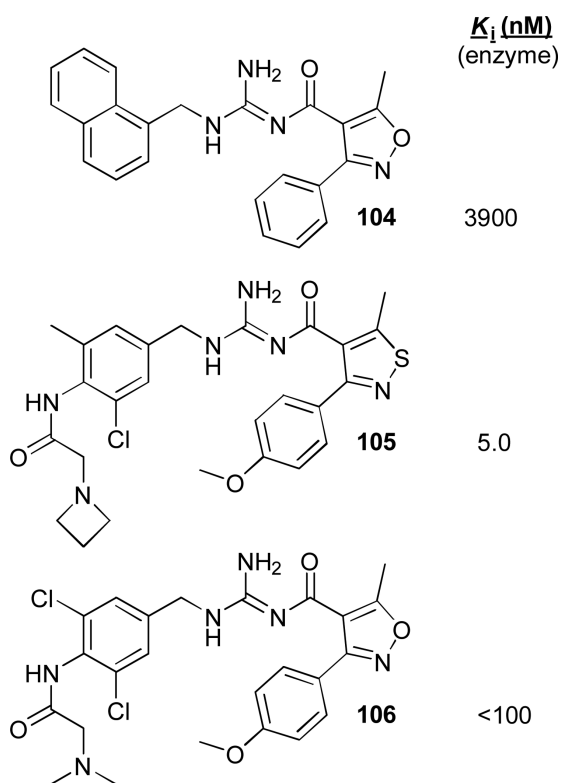


Figure 51.
Structures and activity of compounds **104-106**.

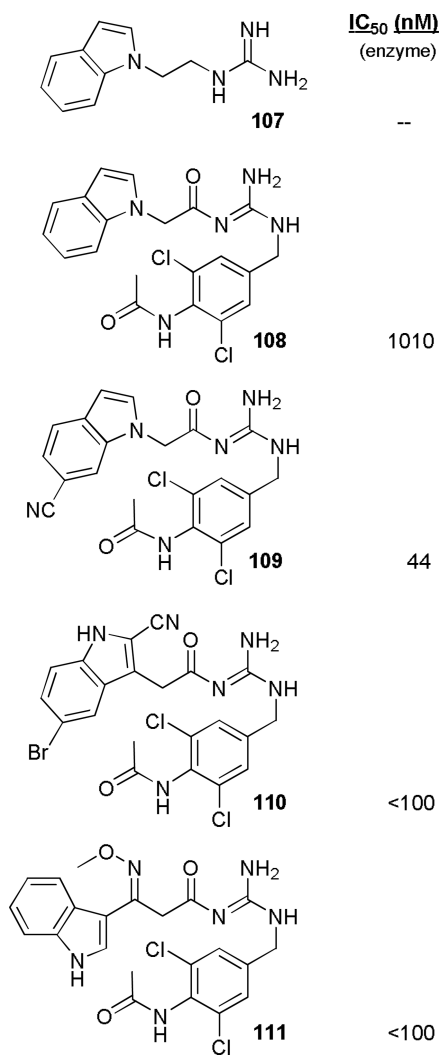


Figure 52.
Structures and activity of compounds **107-111**.

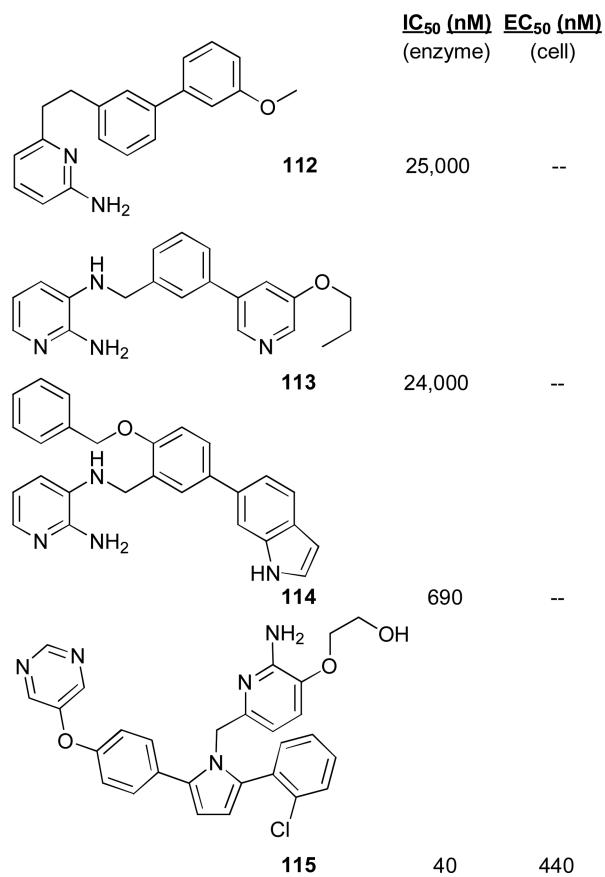


Figure 53.
Structures and activity of compounds **113-115**.

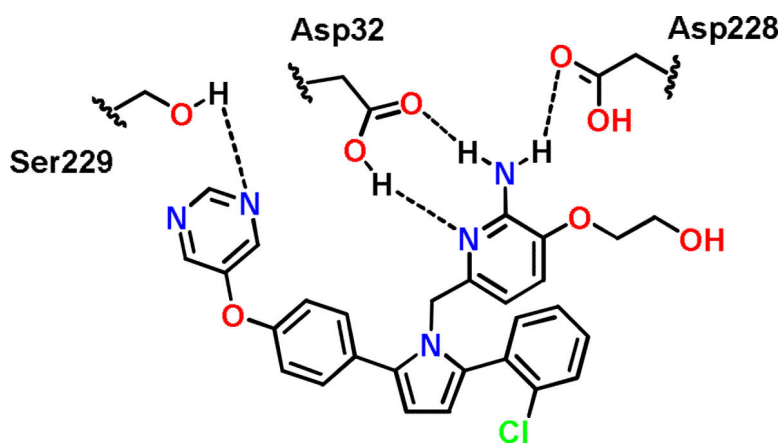


Figure 54.
Binding mode of compound **115** in the BACE1 active site.

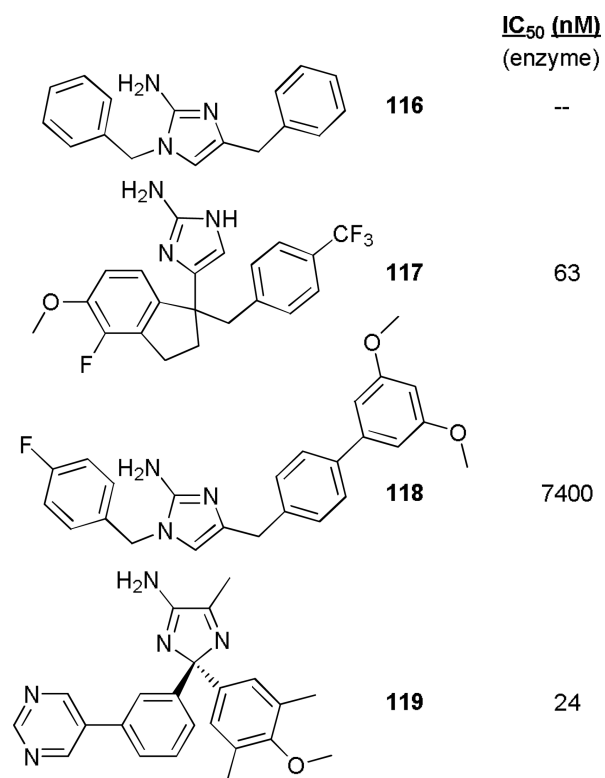


Figure 55.
Structures and activity of compounds **116-119**.

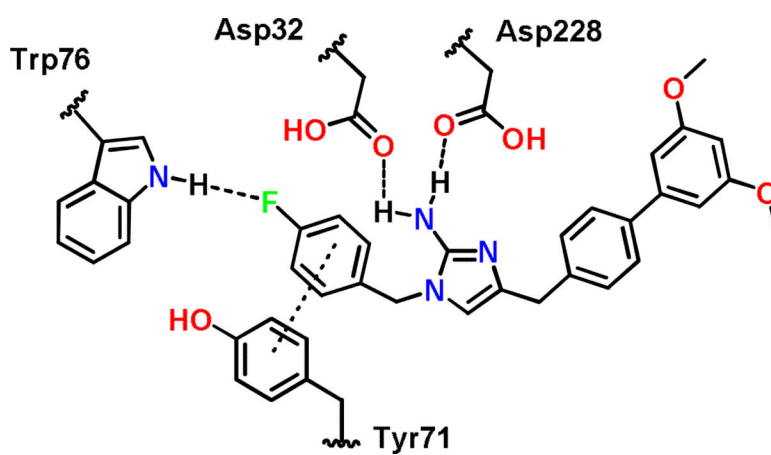


Figure 56.
Binding of compound **118** in the BACE1 active site.

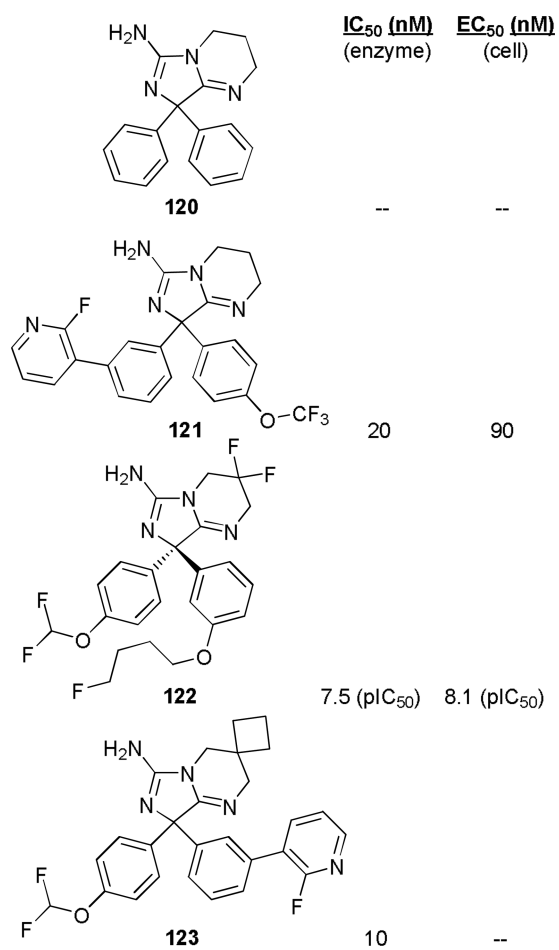


Figure 57.
Structures and activity of compounds **120-123**.

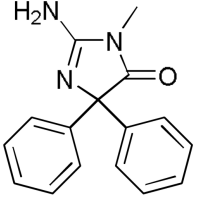
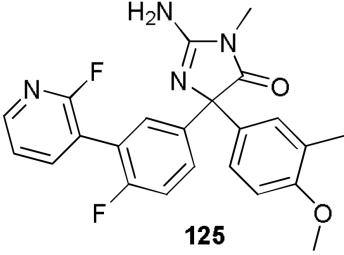
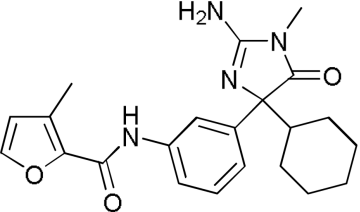
	<u>IC₅₀ (nM)</u> (enzyme)	<u>EC₅₀ (nM)</u> (cell)
 124	3400	--
 125	10	20
 126	40	180

Figure 58.
Structures and activity of inhibitors **124-126**.

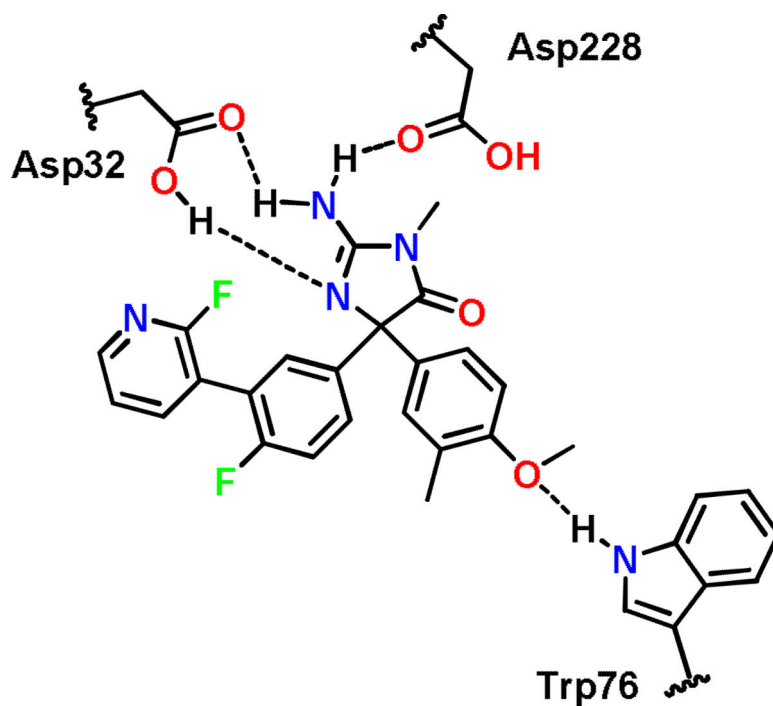


Figure 59.
Binding of compound **125** in BACE1 active site.

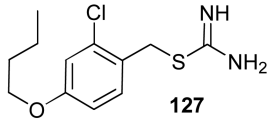
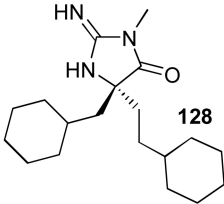
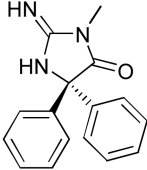
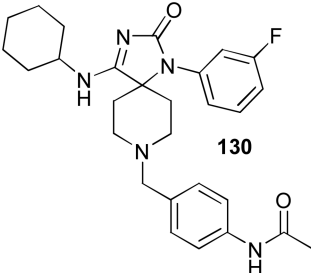
	<u>IC₅₀ (nM)</u> (enzyme)	<u>IC₅₀ (nM)</u> (cell)
 127	--	--
 128	605	2600
 129	7100	12000
 130	2800	8200

Figure 60.
Structures and activity of compounds **127-130**.

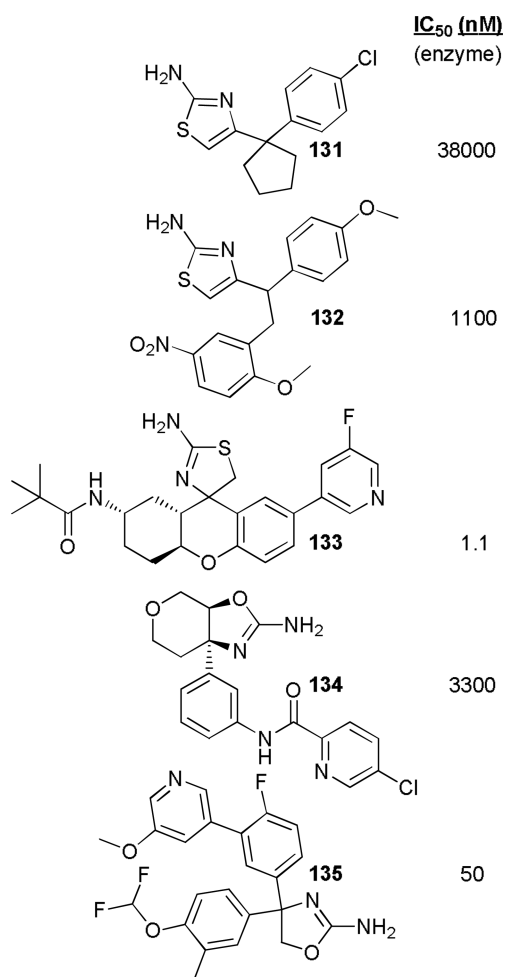


Figure 61.
Structures and activity of inhibitors **131-135**.

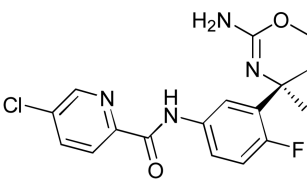
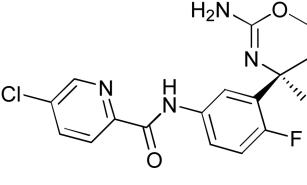
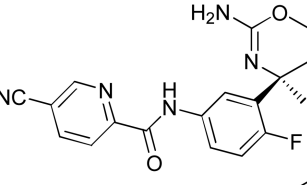
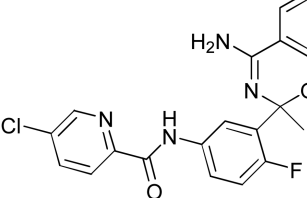
	IC₅₀ (nM) (enzyme)	IC₅₀ (nM) (cell)
	137	10
	26	17
	12	2
	120	67

Figure 62.
Structures and activity of aminooxazine inhibitors **136-139**.

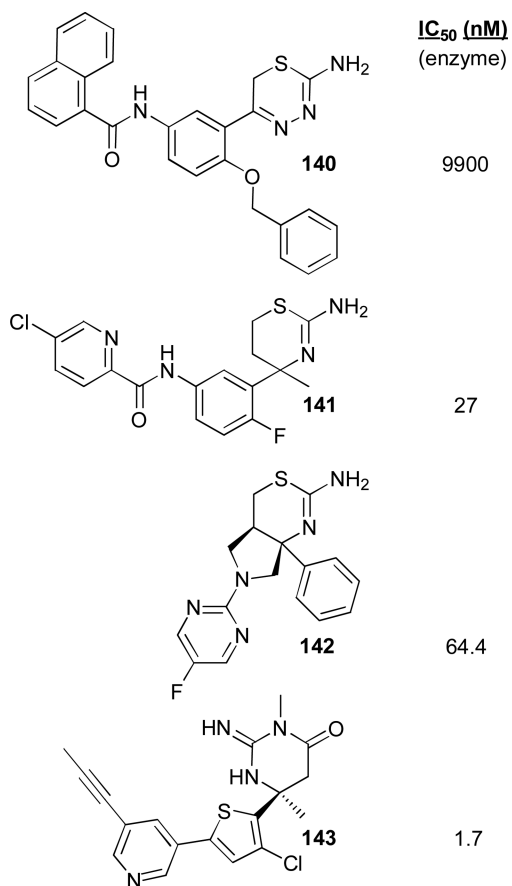


Figure 63.
Structures and activity of compounds **140-143**.

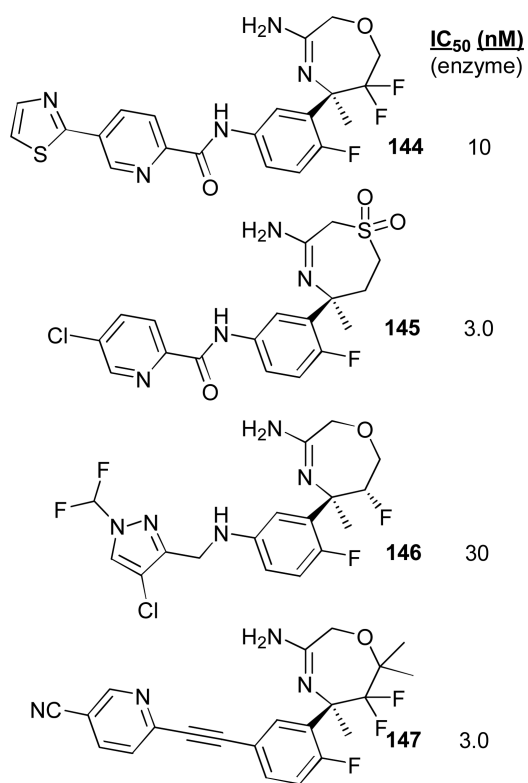


Figure 64.
Structures and activity of 7-membered heterocycles **144-147**.

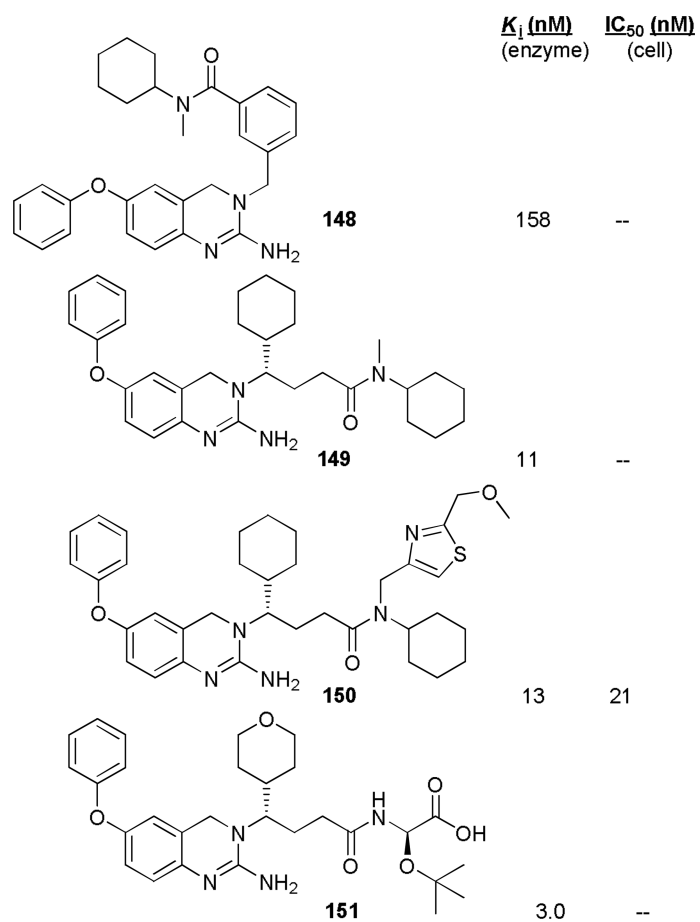


Figure 65.
Structures and activity of inhibitors **148-151**.

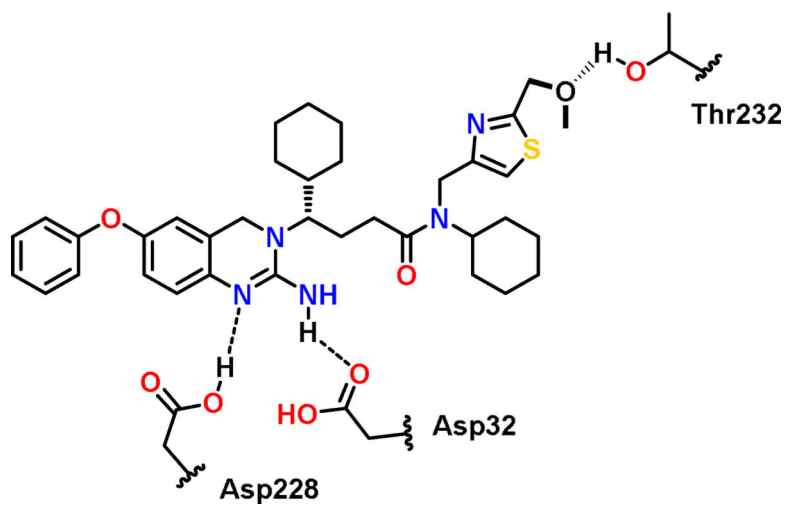


Figure 66.
Binding of compound **150** in the BACE1 active site.

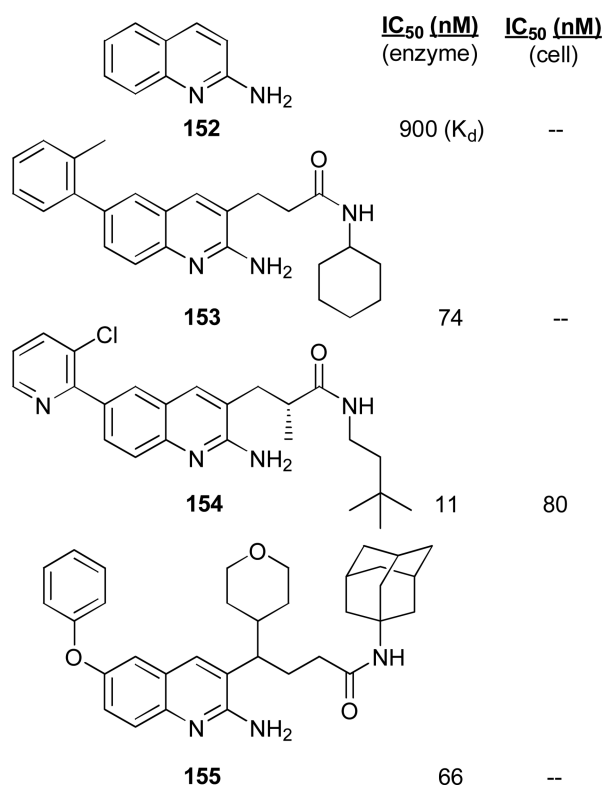


Figure 67.
Structures and activity of inhibitors **152-155**.

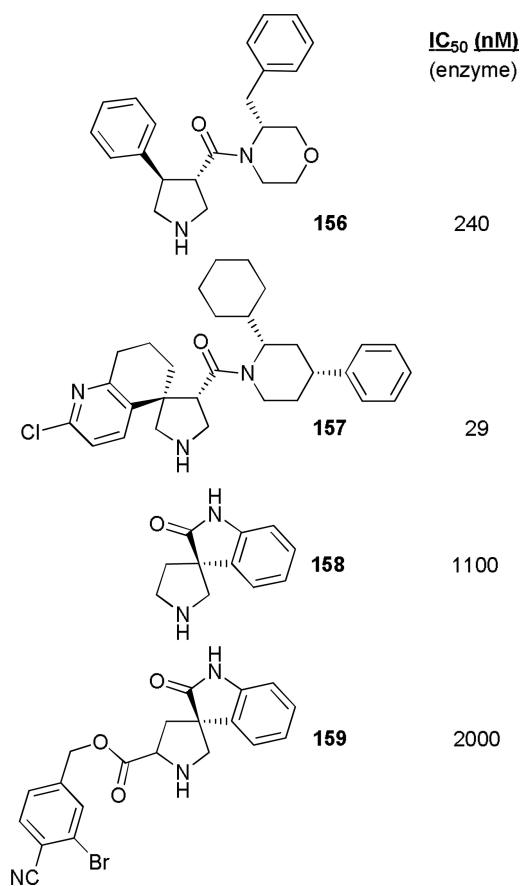


Figure 68.
Structures and activity of compounds **156-159**.

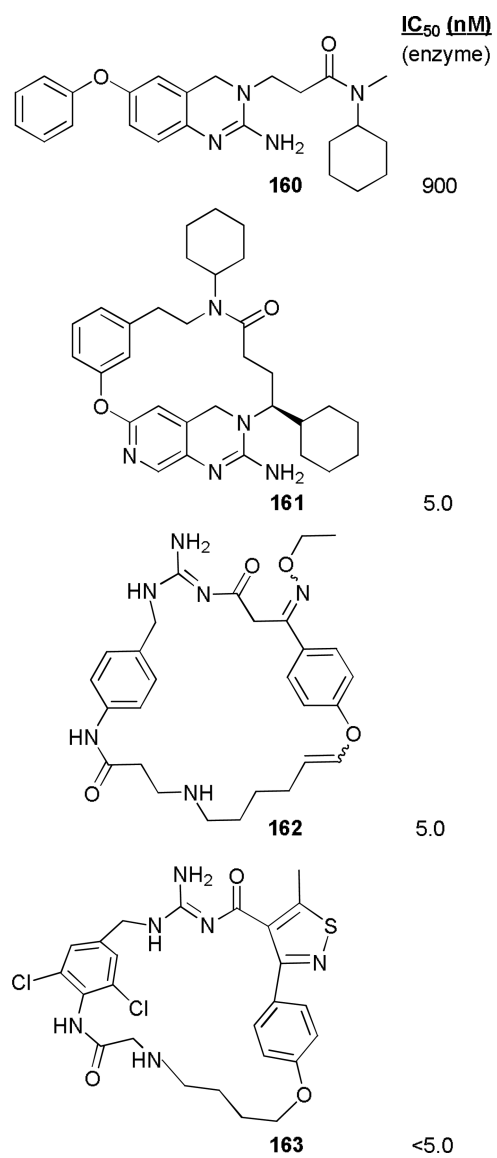


Figure 69.
Structures and activity of inhibitors **160-163**.

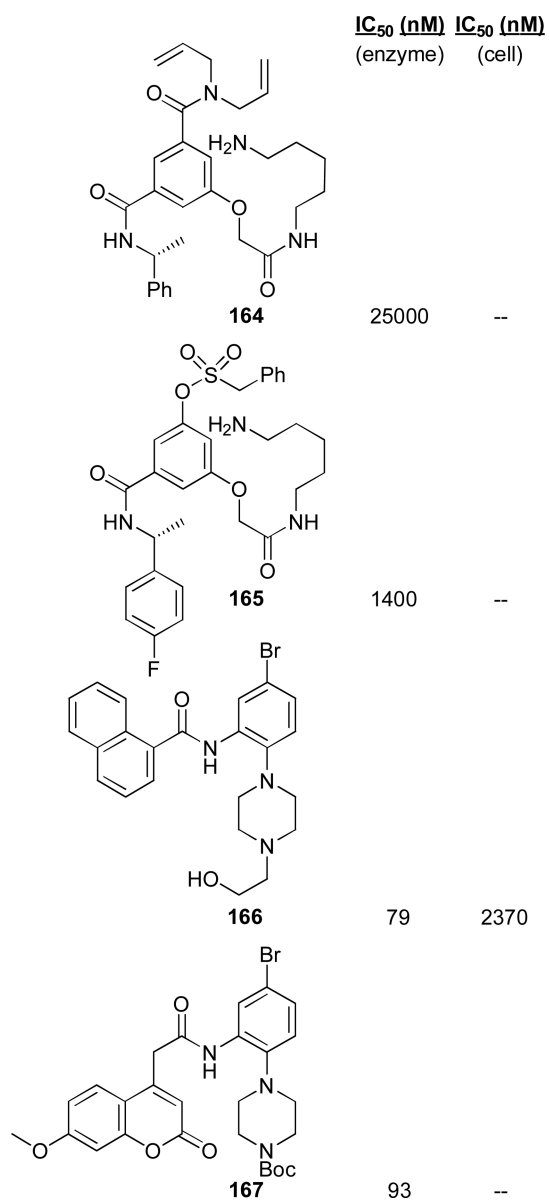


Figure 70.
Structures and activity of compounds **164-167**.

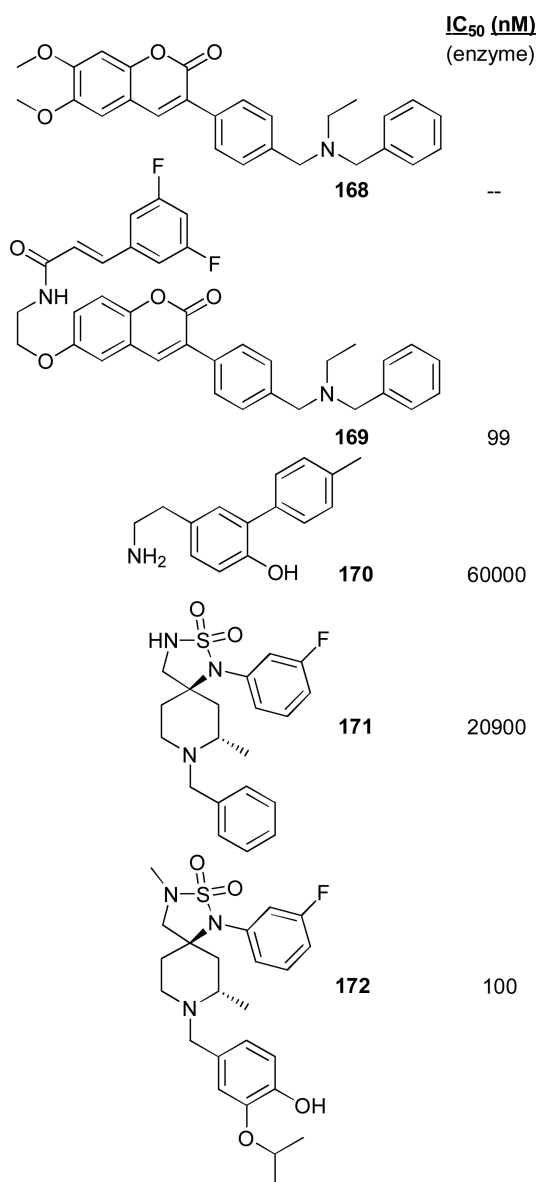


Figure 71.
Structures and activity of compounds **168-172**.

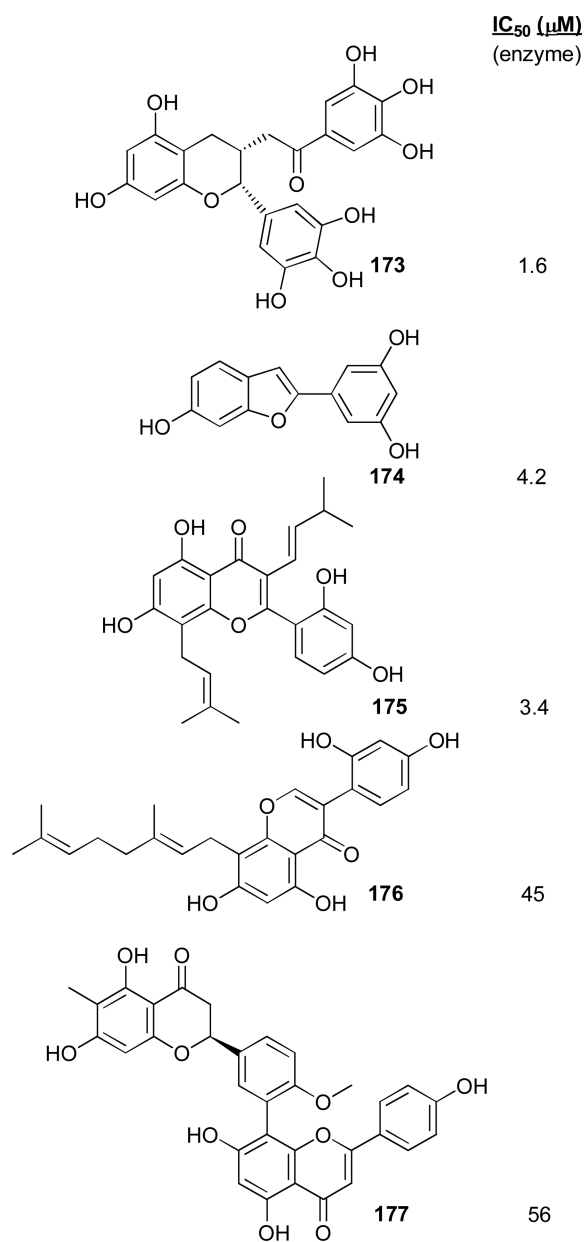


Figure 72.
Structures and activity of compounds **173-177**.

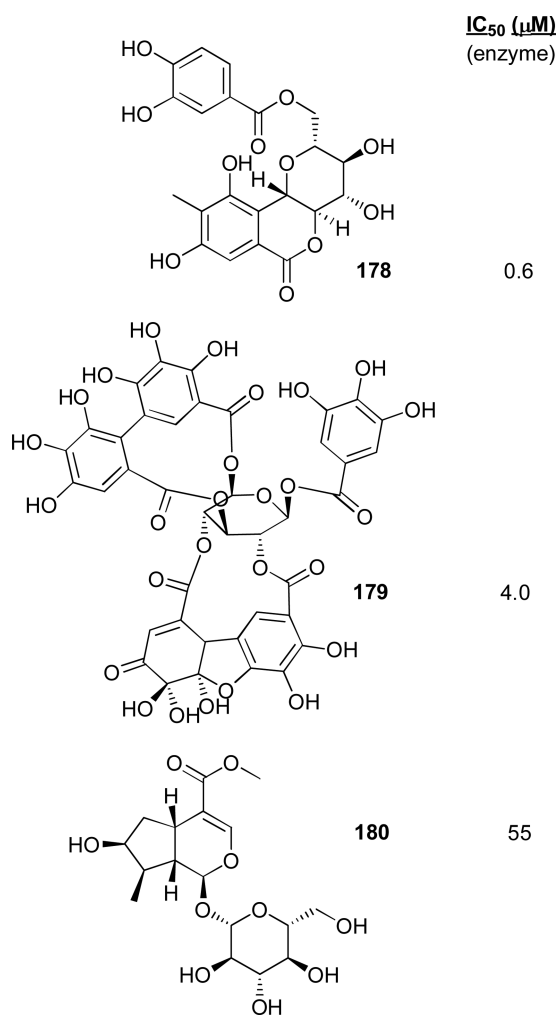


Figure 73.
Structures and activity of compounds **178-180**.

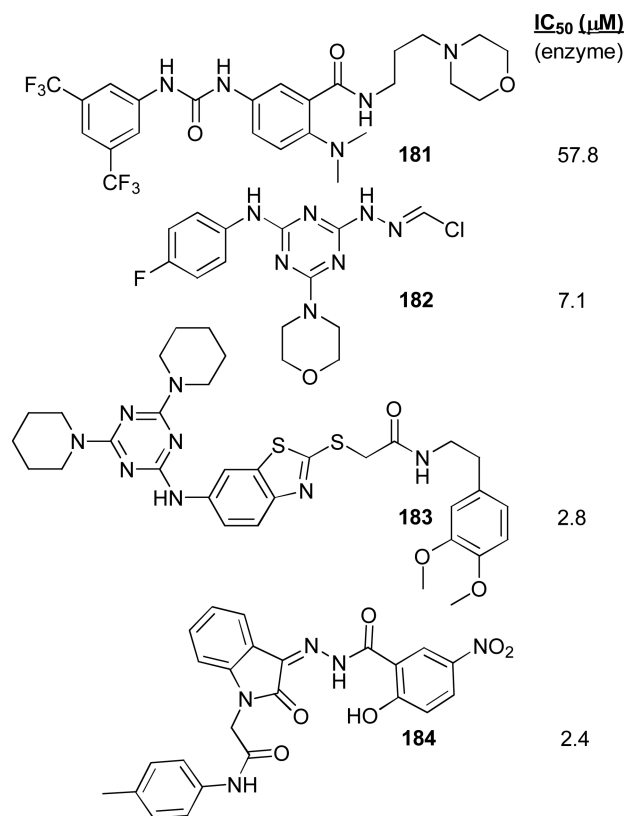


Figure 74.
Structures and activity of compounds **181-184**.

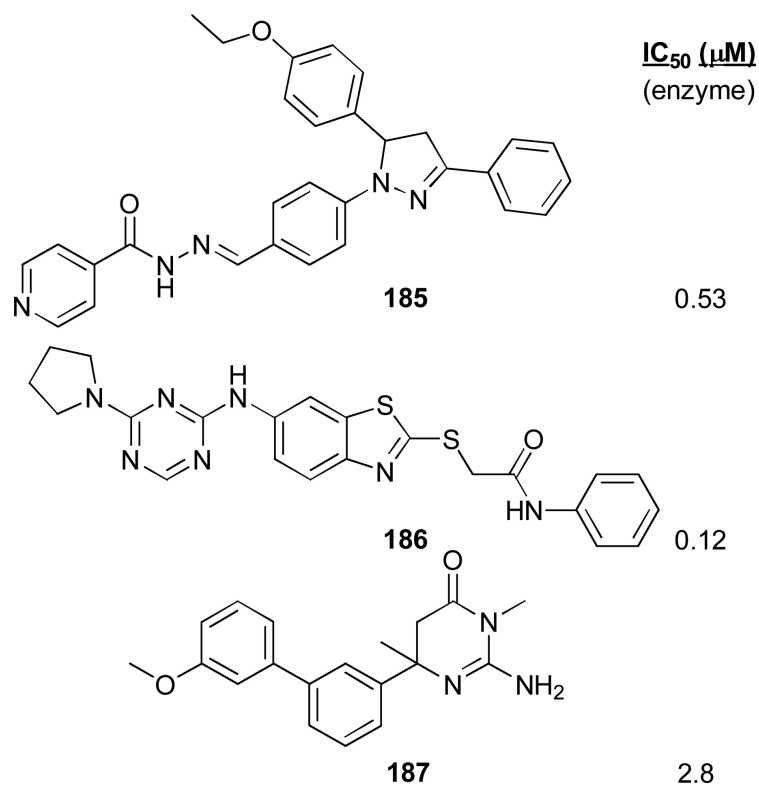


Figure 75.
Structures and activity of compounds **185-187**.

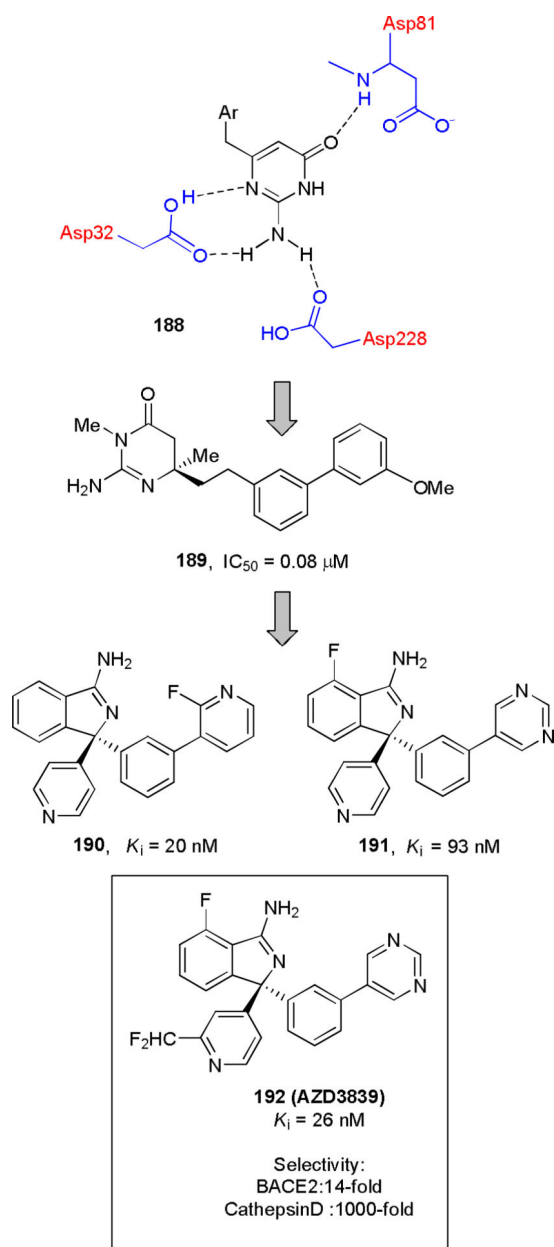


Figure 76.
Structures and activity of inhibitors **188-192**.

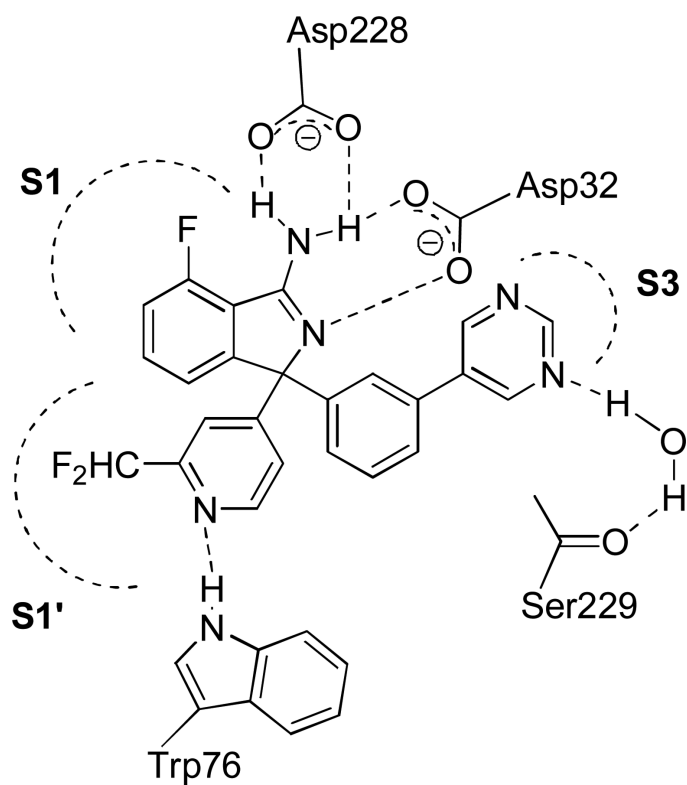


Figure 77.
Binding mode of compound **192** in the BACE1 active site.

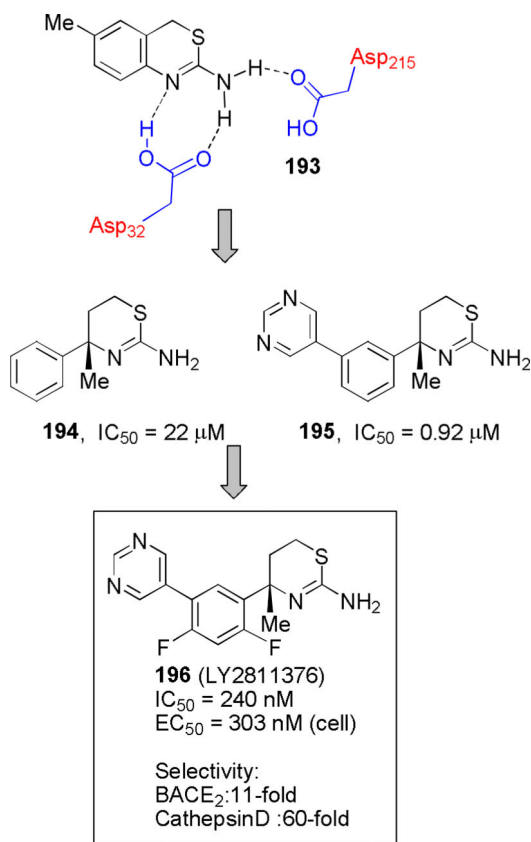


Figure 78.
Structures and activity of inhibitors **193-196**.

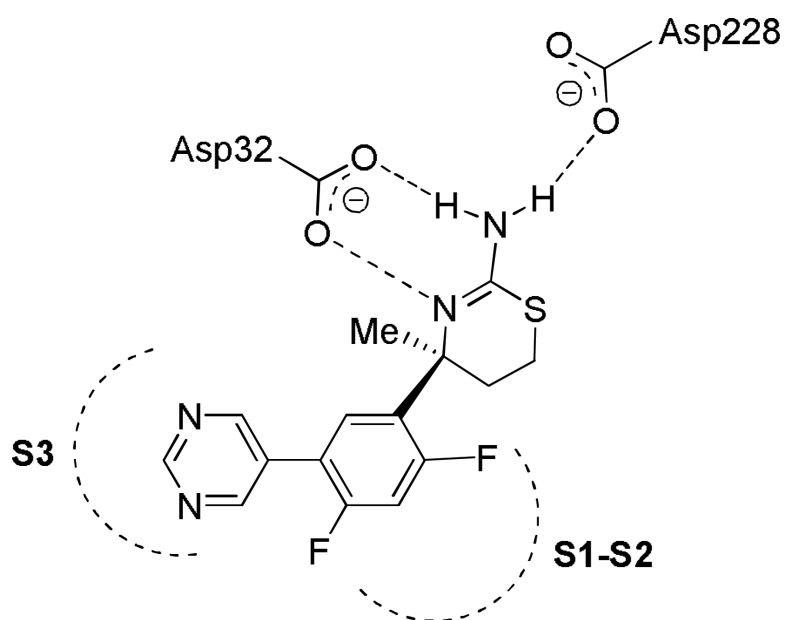


Figure 79.
Binding mode of compound **196** in the BACE1 active site.